2008

NEU

Alberto
Lecina
Laplana

PHASE-ONLY FILTERING FOR COMPARISON OF FUNCTIONAL NEUROIMAGING TIME SEQUENCES

From the image processing literature, we know that the phase information is often significantly more important than amplitude in preserving the features of a visual scene. A modified version of the traditional matched filter has been computer simulated and tested. The modification consists of using only the phase function and setting the amplitude function to unity; a so-called Phase-Only Matched Filter (POMF). This thesis presents a new method to match two different spatio-temporal movies using the POMF. The aim of this project is to implement a Phase-Only filter, which automatically give us the degree of similarity between two different functional neuroimaging time sequences. Practical results are presented for this application. All the properties of this filter have been tested. The results are compared in terms of correlation peak height, relation main-secondary peak and signal/noise ratio.

INDEX

1. Phase-Only Filter: Definition and Characteristics

1.1- Matched filtering

1.1.1 Introduction

Image Matching, defined as the problem of evaluating the similarity of objects in different images, is used to detect changes in a scene, estimate object motion, locate targets, indentify objects, or integrate information from different types of images, etc. A matching algorithm should be robust with respect to low signal to noise ratio (SNR), and should be accurate even when the same object has different intensities or different orientations and sizes in the two images to be matched, or when the object is partially truncated in one of the images. Furthermore, a matching algorithm must be efficient computationally.

The most common approach to image matching is based on the cross-correlation technique, also referred to as template matching [1]-[8]. This technique is not ideal, however, because the auto-correlation function of natural images has significant values even at rather large distances. This means that the maximum of the cross-correlation between two images is rather broad, and therefore difficult to locate in the presence of noise [4]. Several alternatives to the cross-correlation function have been proposed, such as Venot's sign change criterion [9],[10]. All these techniques require the calculation of some kind of generalized correlation for all possible values of the parameters that characterize the geometric transform relating the two images. Such an exhaustive calculation is extremely time consuming when the geometric transforms relating the two images include not only translation, but also a rotation angle and scaling. This is why few researchers have used cross-correlation techniques to match rotated and scaled (dilated) images. Another group of image matching techniques are based on moments or moment invariants [11]-[18]. Since moments are very sensitive to noise, most matching algorithms have been applied to binary images (e.g., in character recognition) or to binarized gray value images, using only lower order moments.

The important of the phase of the Fourier Transform (the spectral phase) in image reconstruction has systematically been demonstrated by Oppenhin and Lim [20]. Much effort has been made to use phase information for image matching, particularly in optical image processing systems where analogue Fourier transforms can be achieved efficiently. Some well know matching techniques are based on phase-only matched filters [21] and variants [22]-[25], such as the binary phase-only matched filter [23] and nonlinear matched filters [24],[25]. The advantages of these filters are their high discriminating power, computational efficiency, and robustness against noise. A major drawback, however, is that the spectral phase of an image is not invariant

to rotation and scaling. Hence, phase-only matched filtering is efficient only when the effects of the rotation and scaling are small and can be ignored [26].

The matched filter has well-known sensitivity to distortion of the input pattern from the reference pattern. For example, in-plane rotations of several degree, or scale changes of several percent, typically result in a 50- percent reduction in the correlation peak intensity.

1.1.2 Formulation

The aim of image matching is either to determine the presence of a known image $r(x',y')$ in a noisy scene $n(x,y)$,

$$s(x,y) = r(x',y') + n(x,y), \tag{1}$$

or to determine the paremeters p1,…,pn of a geometric transformation relating two images **s** and **r**:

$$s(x,y) = r(x'(x,y,p1,\dots,pn), y'(x,y,p1,\dots,pn)) + n(x,y), \tag{2}$$

where the functions $x'(x,y,p1,\dots,pn)$ and $y'(x,y,p1,\dots,pn)$ define a geometric transformation depending on *n* parameters *p1,...,pn.* In (1) and (2), $n(x,y)$ denotes a zero-mean stationary random noise field that is independent of the signal $r(x,y)$.

In this section, we consider a simple two-dimensional translation problem, with translation (x_o, y_o), thus $x' = x - x_o$, $y' = y - y_o$. The Fourier transforms of the two images are defined by: $R(u,v) = F\{r(x,y)\}$ and $S(u,v) = F\{s(x,y)\}$ with $F\{.\}$ denoting Fourier Transformation. In [AA] the authors claim that the classical matched filter which maximizes the detection signal-noise ratio, has a transfer function

$$H(u,v) = \frac{R^*(u,v)}{|N(u,v)|^2} \tag{3}$$

Where $R^*(u,v)$ is the complex conjugate of the Fourier spectrum $R(u,v)$ and $|N(u,v)|^2$ is the noise power-spectral density. If the noise has a flat spectrum with intensity n_w the transfer function of the matched filter reduces to

$$H(u,v) = \frac{1}{|n_w|} R^*(u,v) \tag{3'}$$

and the output of the filter is the convolution of $r^*(-x,-y)$ and $s(x,y)$:

$$q_o(x,y) = \frac{1}{|n_w|^2} \iint_{-\infty}^{\infty} s(a,b) r^*(a-x, b-y)\, da\, db \tag{4}$$

This function has a maximum at (x_o, y_o) that determines the parameters of the translation.

We will study in depth the effects of the translation in 2-d images and 3-d spatio-temporal movies later in the thesis, in chapters 2 and 3.

1.2-Phase-Only Matched Filter

1.2.1-Definition and properties

The authors in [27] state that "one limitation of the matched filter defined by (3) is that the output of the filter is primarily dependent on the energy of the images rather than on its spatial structures. This is why the matched filter provides a relatively poor discrimination between objects of different shapes but similar size of energy content. Furthermore, the filter output is proportional to the image auto-correlation, and the shape of the filter output around its maximum (x_o, y_o) is broad. Accurately locating this maximum is therefore difficult in the presence of noise. This problem can be solved using a phase-only matched filtering (POMF).

The transfer function of a phase-only filter is equal to the spectral phase of the image:

$$H(u,v) = Phase\left(R^*(u,v)\right) = exp\,[j(-\emptyset_r(u,v))] \tag{5}$$

where, $j^2 = -1$. Since the spectral phase preserves the location of objects but is insensitive to the image energy the application of the phase-only matched filter to a pair of identical images under the constraint of translation yields a much sharper peak than the classical matched filtering. The detection and location of the maximum is then easier, and the POMF allows a better discrimination between different objects than standard matched filtering".

As we can read in [19] the authors state that "the importance of phase in signals has been recognized for many applications in which a signal can be recovered completely or in part from knowledge of its phase alone. In a number of context, the Fourier Transform's phase data contain more of the "important" information than the Fourier Transform's magnitude data. In a sense, the phase reflects the location of "events" more than magnitude whereas the magnitude contains information more relevant to the size and shape of an object. The time shift property is an example: a translation in position (time or space) of a signal has no effect on the Fourier transform magnitude but only affects the phase by adding a liner phase term.

Ideally, a flat infinite spectrum produces a Dirac delta function in the time domain. By eliminating the shape information from the two input spectra, the phase-only filtering (attenuating the magnitude information and accentuating the phase information in the frequency domain) can sharpen the correlation peak in the time domain"

1.2.2 Phase information

As we have introduced before, in the Fourier representation of signals, spectral magnitude and phase tend to play different roles and in some situations, many of the important features of signals are preserved if only the phase is retained [20]. A corresponding statement cannot in general be made for the spectral magnitude. This observation about phase has been made in number of different contexts and applications and including one-dimensional, two-dimensional and three-dimensional signals.

Let $f(x)$ denote an n-dimensional signal and $F(\omega) = |F(\omega)|e^{j\varphi(\omega)}$ its n-dimensional Fourier Transform where $x = (x_1, x_2, \dots, x_n)$ is the vector of independent variables and $\omega = (\omega_1, \omega_2, \dots, \omega_n)$ is the vector of frequency variables, and $|F(\omega)|$ and $\varphi(\omega)$ are the magnitude and phase, respectively, of $F(\omega)$. The magnitude-only Fourier synthesis $f_m(x)$ is defined as the signal with Fourier Transform $|F(\omega)|$, i.e.,

$$F\{f_m(x)\} = |F(\omega)| \tag{6}$$

Correspondingly, the phase-only synthesis $f_p(x)$ is to have the Fourier transform

$$F\{f_p(x)\} = M(\omega)e^{j\varphi(\omega)} \tag{7}$$

where $M(\omega)$ is either unity or perhaps more generally a magnitude function which is in some way representative of the class of signals but not obtained from any knowledge of the specific signal f(x).

We illustrate how this transform behaves with a visual example:

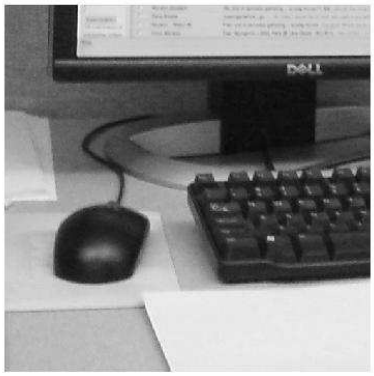

Figure 1: $I_1(x,y)$

Figure 2: $I_2(x,y)$

To visualize how important is the preservation of the magnitude and the phase when trying to recover an original image, we are going to show an example of what happen when we only preserve the magnitude of the original images.

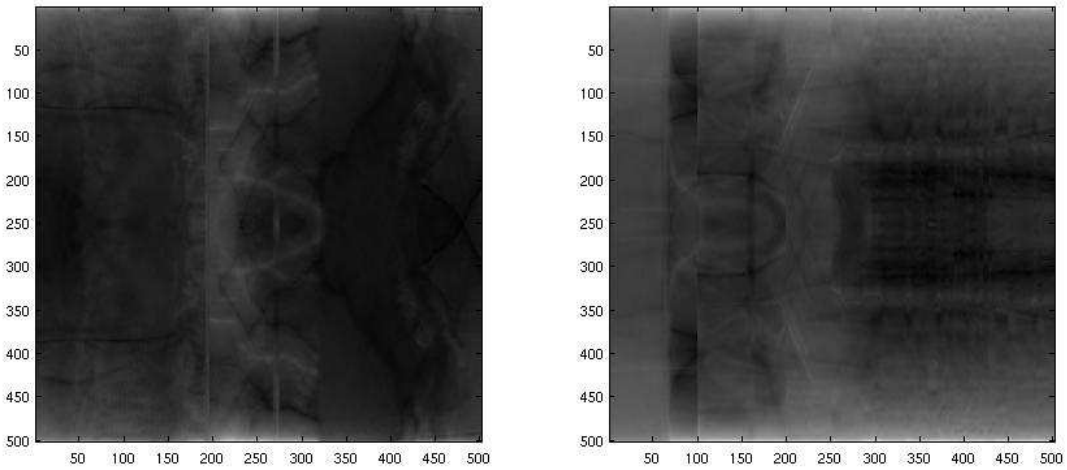

Figure 3 Both images are images synthesized from the Fourier transform magnitude of $I_1(x,y)$ *and* $I_2(x,y)$.

We can see that the identification of the original images is almost impossible if we only preserve the magnitude of them before the inverse of the Fourier Transform.

To see more specifically how important the phase is in one of these images, let's take the formula before written $F\{f_p(x)\} = M(\omega)e^{j\varphi(\omega)}$.

In this case we are going to try to recover the original image by preserving the phase of it, and to do it more complex the magnitude that we are going to introduce is going to be the magnitude of the other image.

$$F\{f_{p1}(x,y)\} = \sqrt{X_2^2 + Y_2^2} * e^{j\varphi 1(\omega)}$$
$$F\{f_{p2}(x,y)\} = \sqrt{X_1^2 + Y_1^2} * e^{j\varphi 2(\omega)} \quad (8)$$

We can see how to recover the image 1, we will preserve its phase and we will change its magnitude for the magnitude of the image 2.

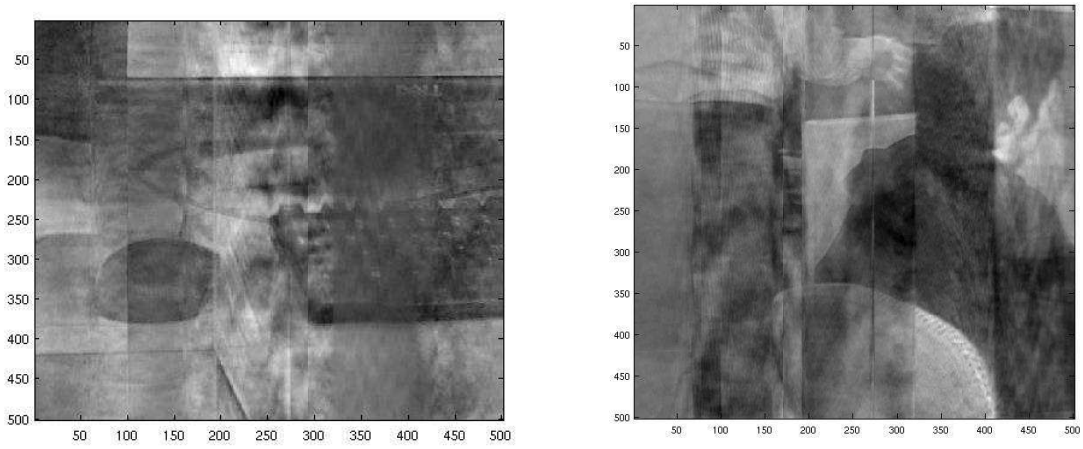

Figure 4. First image has been synthesized from the Fourier transform phase of image $I_1(x,y)$ and the Fourier Transform magnitude of the image $I_2(x,y)$ and vice versa.

We can see how taking the phase and adding another magnitude not related with the image that we want to reconstruct, we obtain a image more similar to the original one than only taking its Fourier transform magnitude.

The fact that phase-only reconstruction preserves much of the original information between signals would suggest that the "location" of events tends to be preserved. A related observation that can be made about the example of Fig 3 is that much of the intelligibility in the

original and reconstructed signals is related to the location of "events" such as lines, points, etc. It is generally plausible that the phase reflects the location of evens more than magnitude and, at least for simple examples this is exactly true.

Another similar informal justification for the intelligibility of the phase-only reconstructions derives from the interpretation of the generation of the phase-only signal when using unity magnitude as spectral whitening process. Specifically, with $M(\omega)$ chosen as unity in (7),

$$F[f_p(x)] = \frac{1}{|F(\omega)|} F[f(x)] \tag{9}$$

Since the spectral magnitude of speech and pictures tends to fall off at high frequencies, the phase-only signal $f_p(x)$ will, among other effects, experience a high-frequency emphasis which accentuates lines, edges and other narrow events without modifying their position.

1.3. Symmetric Phase-Only filter

In [27] the authors claim that a further improvement of the phase-only matched filtering can be achieved by extracting and correlating the phases of both $r(x, y)$ and $s(x, y)$ defined in **1.1.2**. This is done by defining a nonlinear filter with an output given by the inverse of the Fourier transform of the function:

$$Q(u,v) = \frac{S(u,v)}{|S(u,v)|} * \frac{R^*(u,v)}{|R^*(u,v)|} = exp\,[j(\emptyset_s(u,v) - \emptyset_r(u,v))] \tag{10}$$

where, $\emptyset_s(u,v)$ and $\emptyset_r(u,v)$ are the spectral phases of $s(x,y)$ and $r(x,y)$. In the absence of noise, this function reduces to

$$Q(u,v) = exp\,[-j2\pi(ux_o + vy_o)] \tag{11}$$

The inverse Fourier transform of (11) is a Dirac δ −function centered at (x_o, y_o), yielding an even sharper maximum than the phase-only filter. This technique, referred to as a symmetric phase-only matched filtering (SPOMF), can be seen as a nonlinear two step process, the first step being the extraction of the phases of the input images and the second the phase-only matched filter [30]. Some further improvements of the symmetric phase-only matching can be achieved

by preprocessing the spectral phases [22],[24],[29],[30]. This is the filter that we will implement in the next subsection and that has been the base of this project.

1.3.1 Phase-Only filter: implementation

To quantify the similarity between images and spatiotemporal movies in this project we have used implementation of the Symmetric Phase-Only filter defined before as:

Given two images $I_1(x,y)$ and $I_2(x,y)$, the Fourier transform $F\{\}$ of these images can be written as:

$$\begin{cases} Z_1(u,v) = F\{I_1(x,y)\} = X_1(u,v) + jY_1(u,v) \\ Z_2(u,v) = F\{I_2(x,y)\} = X_2(u,v) + jY_2(u,v) \end{cases} \tag{12}$$

If one uses the symbol $F^{-1}\{\}$ for the inverse Fourier Transform, the phase-only filter is given by:

$$F(x,y) = F^{-1}\{exp\,[j * arctan\,(\frac{X_1Y_2 - X_2Y_1}{X_1X_2 + Y_1Y_2})]\} \tag{13}$$

2. Phase-Only Filter: 2-D

2.1 Matched Filtering

2.1.1 Autocorrelation by using traditional cross-correlation filter and Phase-Only filter

As I have demonstrated in the section 1.2.1, there are a lot of differences between the traditional cross-correlation filter and the Phase-Only filter. The importance of the phase in a signal (1.2.2) is really important when we are trying to determinate if two images are similar or not.

We are going to study now how different is the analysis of the output of the filter when we use the traditional cross-correlation filter or the Phase-Only filter. In this section I will analyze it by showing easy examples.

2.1.1.1 Cross-correlation filter and Phase-Only filter: Autocorrelation

Given one image $I_1(x,y)$, if one uses the symbol F^{-1} for the inverse Fourier Transform, F{} for the Fourier Transform and the operator * for the complex conjugate, the autocorrelation of this image by using the traditional cross-correlation filter is defined by:

$$\mathbf{I}(x,y) = \mathbf{F}^{-1}\{\mathbf{F}\{\mathbf{I}_1(x,y)\} * \mathbf{F}\{\mathbf{I}_1(x,y)\}^*\}$$

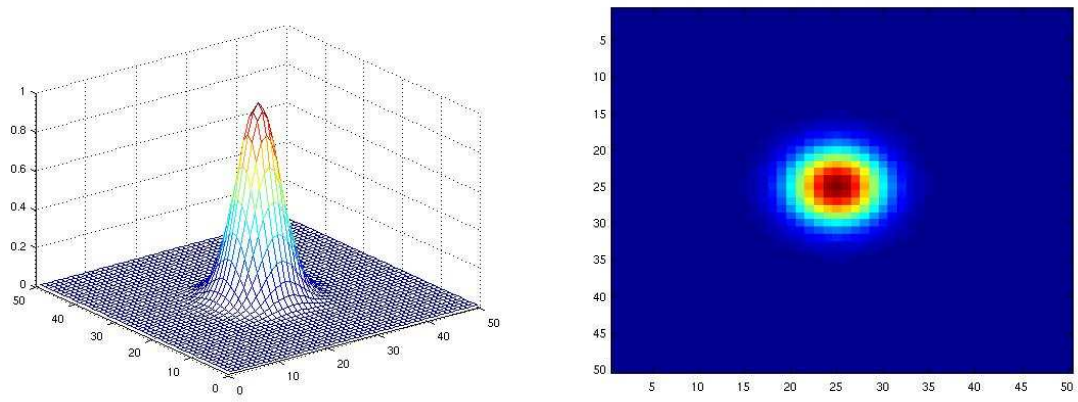

Figure 5. $I_1(x,y)$

If $I_1(x,y)$ is a Gaussian placed in the center of an image, the output of the traditional cross-correlation filter is:

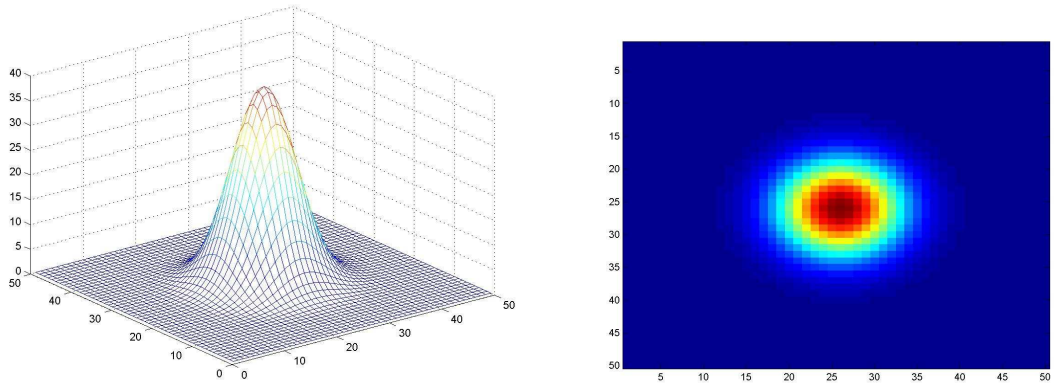

Figure 6. Output of the cross-correlation filter

Given the same image $I_1(x, y)$ as before, this time the output of the Phase-Only filter, defined in **2.1.2** is:

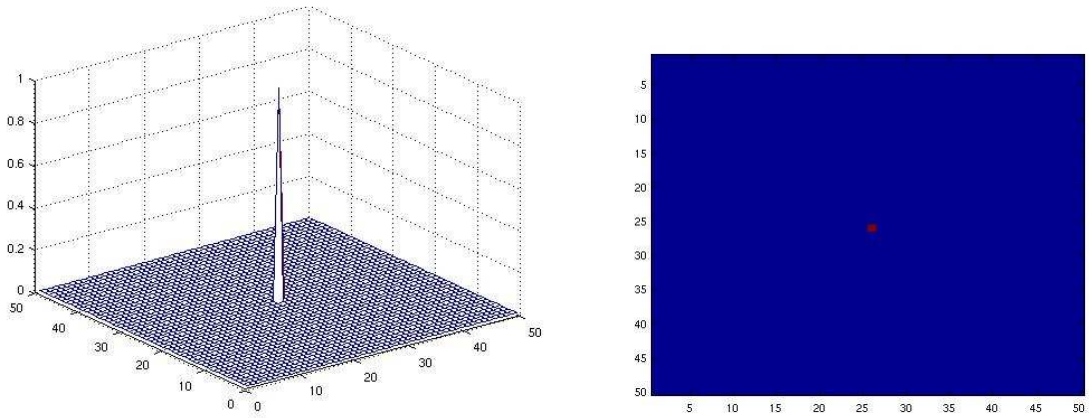

Figure 7. Output of the Phase-Only filter

We can see here several differences between the behavior of the cross-correlation filter and the Phase-Only filter when the inputs are the same image..

The Phase-Only filter by eliminating the shape information from the two inputs (attenuating the magnitude information and accentuating the phase information in the frequency domain) can sharpen the autocorrelation peak in space domain.

The detection and location of the maximum is easier then when we use the Phase-Only filter rather than the cross-correlation filter. As we can see, the maximum of the output when the inputs are totally equal, is a narrow peak centered in the center of the image (due to the zero lag is there) with amplitude equal to 1. So from now on, this will be the ideal situation when we try to compare two different images.

2.1.1.2 Cross-correlation filter and Phase-Only filter: Cross-correlation

We are studying now what happens when the inputs are not equal. From this experiment we will see more advantages of using the Phase-Only filter instead of the traditional Cross-correlation filter while working with 2-D images.

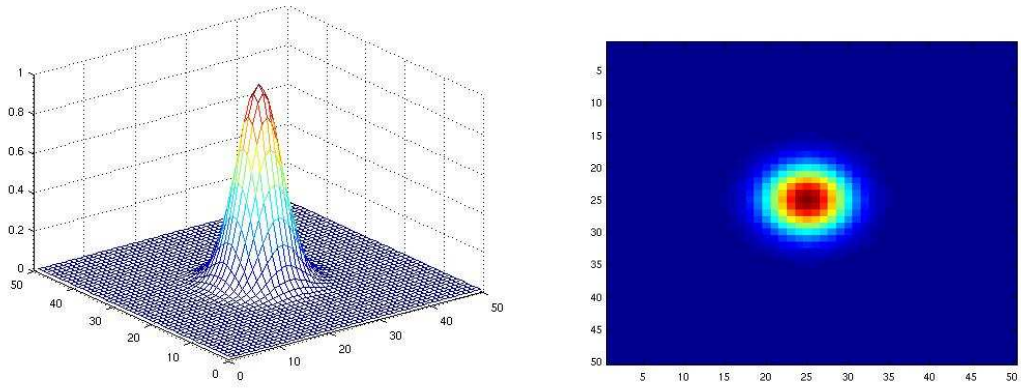

Figure 8. Input $I_1(x, y)$

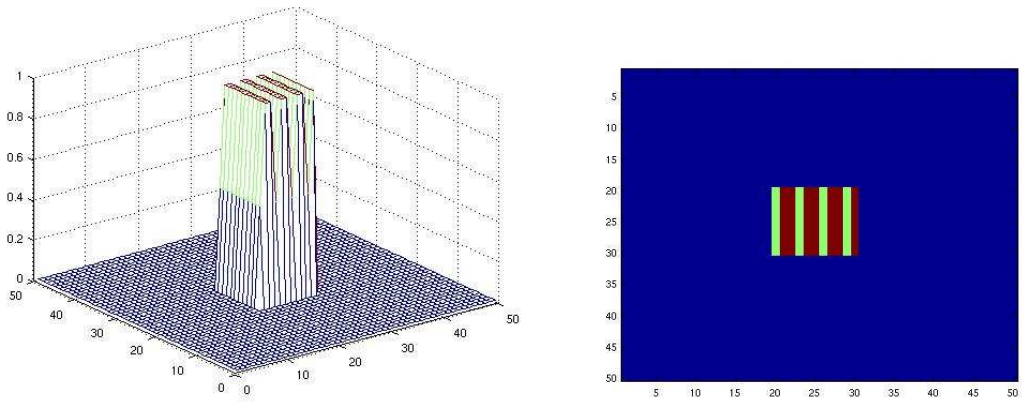

Figure 9. Input $I_2(x,y)$

Cross-correlation filter

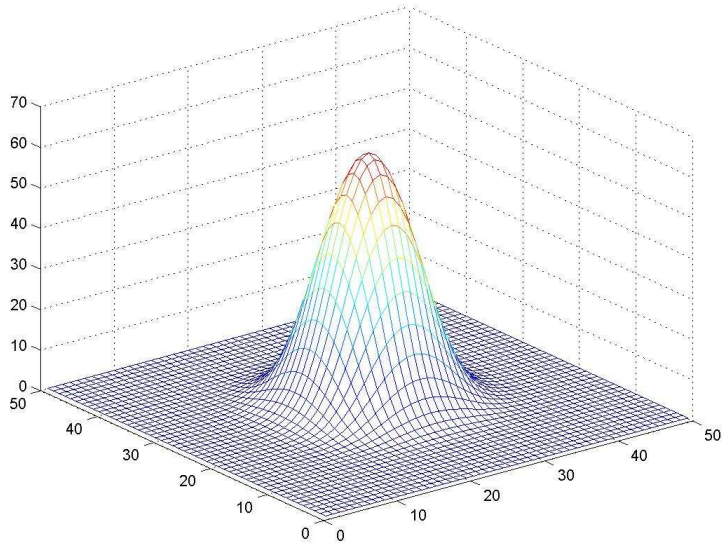

Figure 10. Output of the cross-correlation filter

We see in the figure above, the behavior of the cross-correlation filter when the inputs are clearly different. If we take a look at the figure 6 we realize that although the outputs are different it is really difficult to take any conclusion about the similarity between the inputs if we don't know a priori the shape of them. We cannot the similarities between the inputs only by taking a look at the output of the filter when the inputs are equal (Figure 6) and when they are

different (Figure 10). This is not the behavior we were expecting from a matched filter where its unique function is telling us if two images are similar or not.

Phase-Only filter

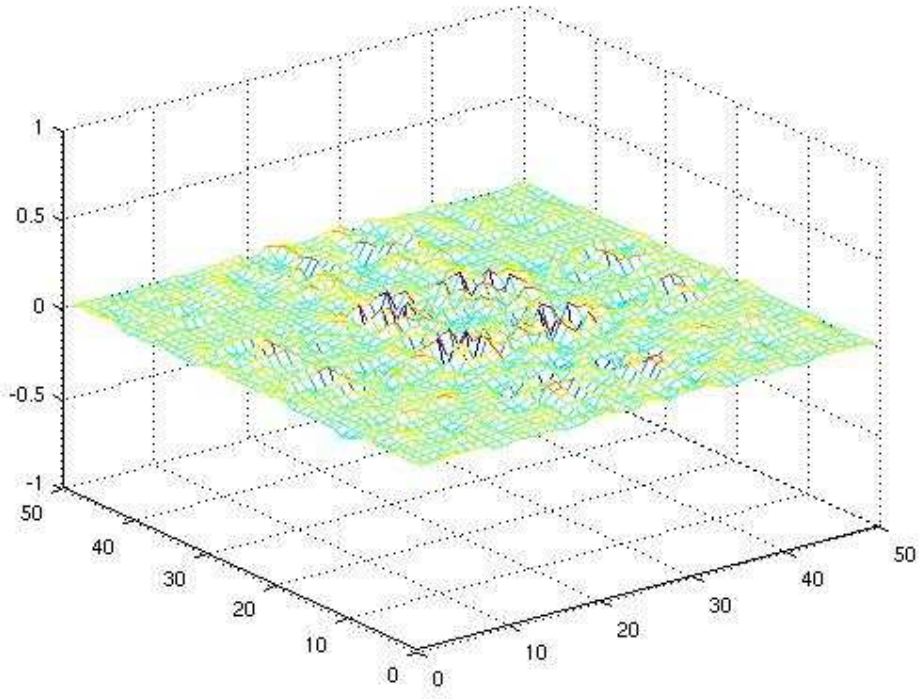

Figure 11. Output Phase-Only filter

We can see the differences between the figure 11 and the figure 7. There is no peak in the output and noise appears all over the image. This behavior is similar to what we were expecting to see. The Phase-Only filter shows us that the two inputs are different, and in this case, due to the high sensitivity of the filter we can appreciate it better.

Then, in summary, the Phase-Only filter can give us a better way to identify if two images are the same or not. Obviously this is very easy for us, and in this case is easier because for the human eye is easy to see how different two images are, but we will see how this is going to get more difficult when we have to deal with more dimensions. But this is a good introduction to see the behavior and a couple of peculiarities of this kind of filter.

2.2. Property: shift in space

2.2.1 Cross-correlation filter

We are going to analyze this property, the possibility of designing a filter that could tell us if two images are the same one, and moreover, if two images are the same one but one of them has undergone a translation. Such a property is very important and very useful in order to identify different objects.

This property is a result of the Fourier Transform properties and also the convolution properties, let's see now how it affects in this filter.

Given two images $I_1(x,y)$ and $I_2(x,y)$, I consider a two-dimensional translation problem with translation (x_0,y_0). So I can write $I_2(x,y) = I_1(x-x_0,y-y_0)$, applying the Fourier transformation: $F\{I_2(x,y)\} = e^{-ikx_0}e^{-ihy_0}If_2(k,h)$

$$OutputF(x,y) = F^{-1}\{F\{I_2(x,y)\}\,F\{I_1(x,y)\}^*\} = F^{-1}\{If_1(u,v)e^{-iux_0}e^{-ivy_0}If_1(u,v)^*\} =$$

$$= F^{-1}\{If_1(u,v)If_1(u,v)e^{-iux_0}e^{-ivy_0}\} = I_1(x,y) * I_1(x,y)F\{e^{-iux_0}e^{-ivy_0}\} =$$

$$= Autocorrelation\ I_1(x-x_0,y-y_0)$$

Defining (*) the symbol of the convolution

Seeing this, we can expect that the output of the cross-correlation filter when the inputs are the same image, but one has been translated, will be the same as the output of the autocorrelation but also translated to the same point (x_0,y_0).

We will see this in the next two examples,

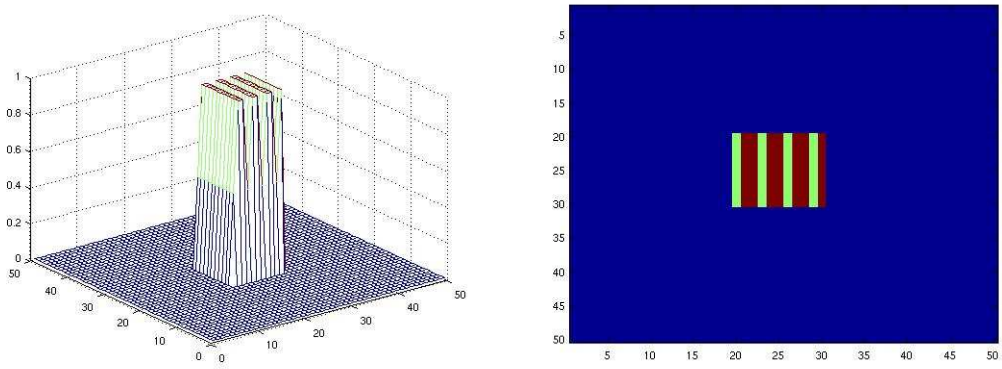

Figure 12. Image $I_1(x, y)$

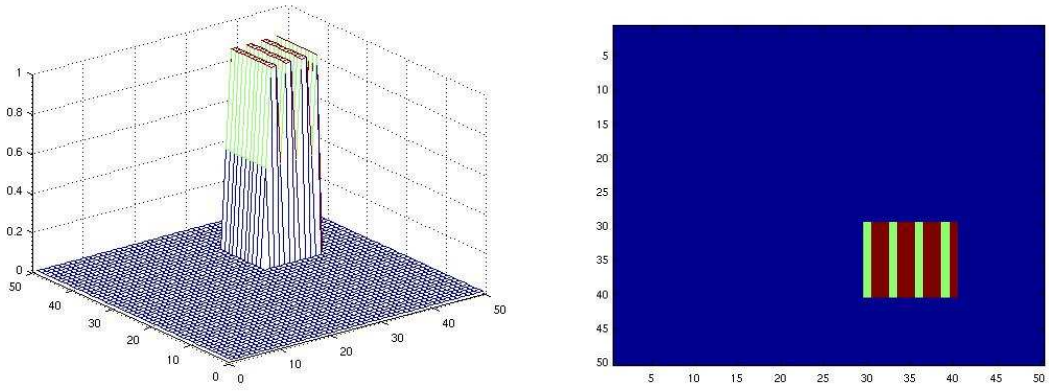

Figure 13. Image $I_2(x, y)$ with a shifted $(10,10)$

The output of the cross-correlation filter is:

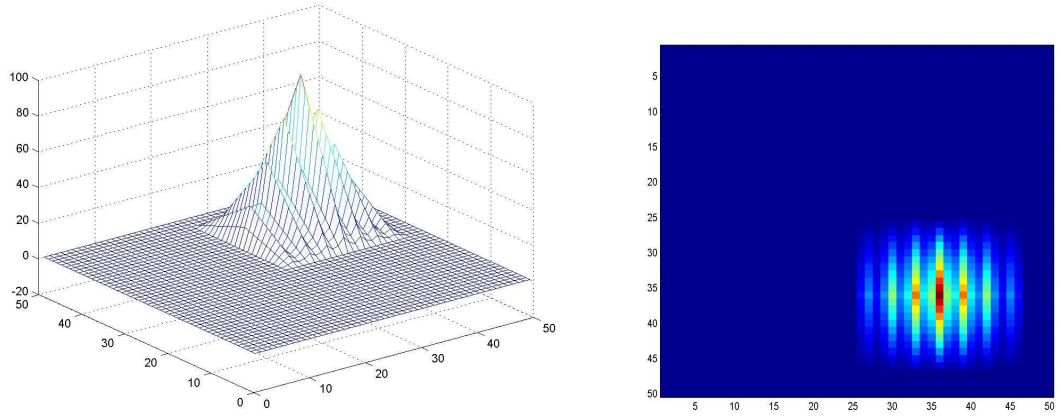

Figure 14. Output of the cross-correlation filter

We can see how the output is placed in the point $(x-10, y-10)$, where x and y mark the center of the image in the figure 12. We appreciate how the cross-correlation filter tells us the shift between the two images, but we still have the same problem while identifying if the two inputs are similar or not.

2.2.2 Phase-Only filter

Applying the same translation (x_0, y_0) to one of the inputs, by using the Phase-only filter we extract the phase of both $I_1(x,y)$ and $I_2(x,y)$ images and the output of the filter will be the inverse of Fourier transform of the function:

$$F(u,v) = \frac{I_1(u,v)}{|I_1(u,v)|} * \frac{I_2^*(u,v)}{|I_2^*(u,v)|} = exp\,[j(\emptyset_{I_1}(u,v) - \emptyset_{I_2}(u,v))]$$

where, $\emptyset_{I_1}(u,v)$ and $\emptyset_{I_2}(u,v)$ are the spectral phases of $I_1(x,y)$ and $I_2(x,y)$. In the absence of noise, this function reduces to

$$F(u,v) = exp\,[-j2\pi(ux_o + vy_o)]$$

The inverse Fourier transform of the function above will be a Dirac δ-function centered at (x_o, y_o), yielding a narrow peak at that point.

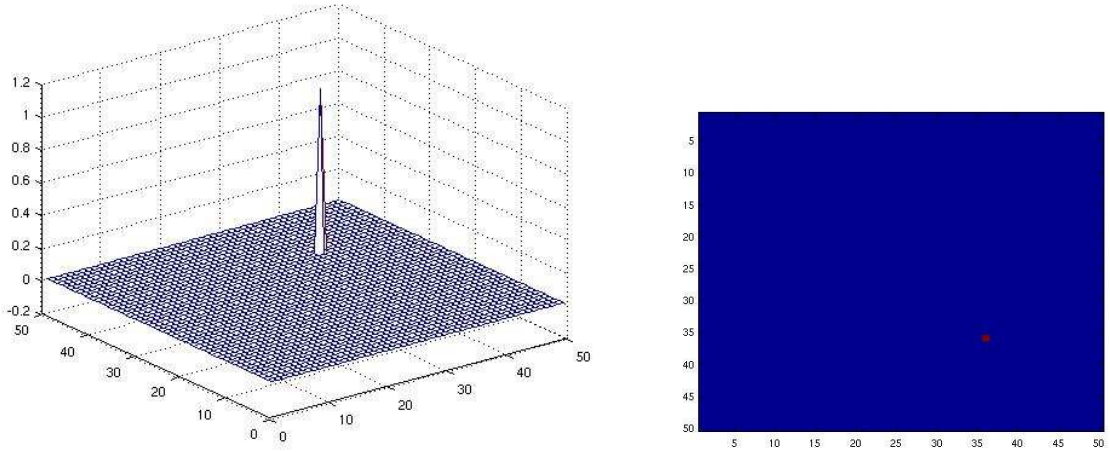

Figure 15. Output of the Phase-Only Filter

We see the POMF peak placed at the point $(x-10, y-10)$, so the POMF is able to locate the translation undergone by the inputs perfectly. We will see later how this property can also be applied when we work with more dimensions.

2.3 Rotation angle in 2-D images by using the POMF

In order to assess the sensitivity of the Phase-Only filter, the experiment of rotating an image gives us a very good idea of how sensitive is the filter if we introduce a rotation in one of the inputs.

By doing this experiment we will see if the Phase-Only filter is very sensitive or not

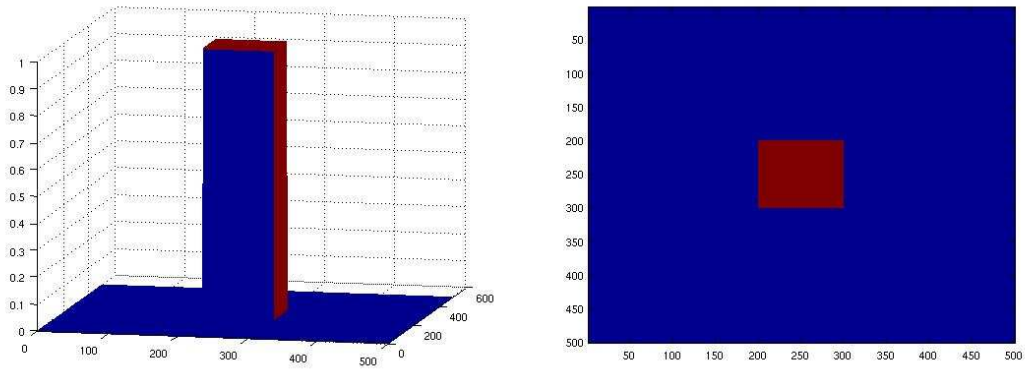

Figure 16. Image $I_1(x, y)$

In this test I will rotate the image $I_1(x, y)$ and I will check the maximum amplitude of the output of the Phase-Only filter. We have to remember the ideal scenario when the two inputs are the same image; we obtained a marrow peak placed in the center (zero-shift) with amplitude equal to 1.

The result of this easy test can be seen in the next graphic

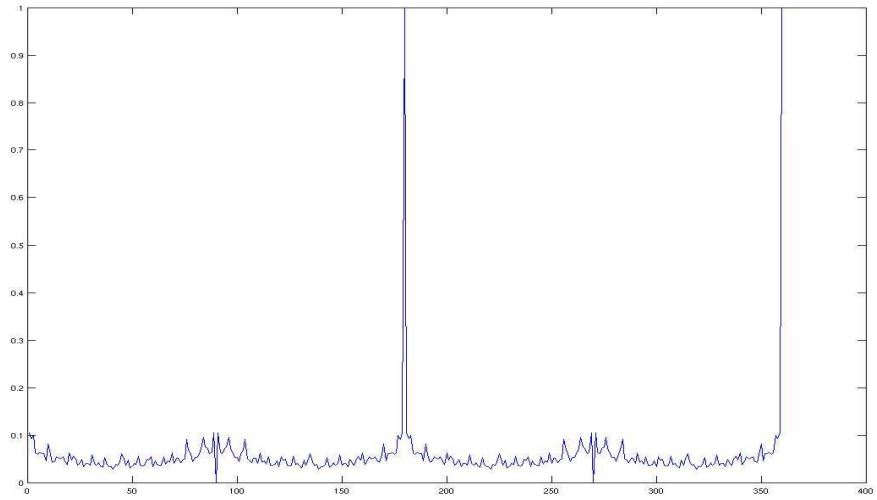

Figure 17. rotation experiment, amplitude of the output of the POMF when we rotate the Fig. 16 n degrees, from 1 to 360.

We can see how we obtain a maximum when we rotate the image 180 degrees and 360 degrees because both inputs are totally equal, but for any degree of rotation the output show us that the two inputs are not the same. Seeing this we can assure that the Phase-Only filter is very sensitive to changes in the inputs what give us an idea of how much difficult is going to be to obtain a clear peak when we deal with real images, where they barely are going to be identical.

While working with real data, we expect our POMF to be variant to rotation, to be able to discriminate between different activation in the brain as we will see later in the thesis. When we have to recognize an object like for example a key, the fact that the key has undergone a rotation doesn´t affect to the fact that both keys are the same one. But talking about brains, if one activation in the brain is the same as another one but it has suffered a rotation, they obviously will not be the same one, and it is very probable that those activation won´t come from the same stimulation.

2.4 Circular convolution and zero-padding

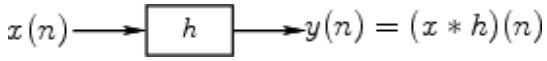

Figure 18. System diagram for filtering an input signal x (n) by filter h(n) to produce output y(n) as the convolution of x and h.

Figure 18 illustrates the conceptual operation of filtering an input signal x(n) by a filter with impulse-response h(n) to produce an output signal y(n). By the convolution theorem for DTFTs

$$(h * x) \leftrightarrow H \cdot X$$

or,

$$\mathrm{DTFT}_\omega(h * x) = H(\omega)X(\omega)$$

where h and x are arbitrary real or complex sequences, and H and X are the DTFTs of h and x, respectively. The convolution of x and h is defined by

$$y(n) = (x * h)(n) \triangleq \sum_{m=-\infty}^{\infty} x(m)h(n-m).$$

In practice, we always use the DFT (preferably the FFT) in place of the DTFT, in which case we may write

$$\mathrm{DFT}_k(h * x) = H(\omega_k)X(\omega_k)$$

where now h, x, H, X $\epsilon\, \mathbb{C}^N$ (length N complex sequences). It is important to remember that the specific form of convolution implied in the DFT case is cyclic (also called circular) convolution:

$$y(n) = (x * h)(n) \triangleq \sum_{m=0}^{N-1} x(m)h(n-m)_N$$

The convolution theorem states that convolution of time-domain functions is equivalent to multiplication of their Fourier transforms. If they are discrete-time functions (sequences), the

Fourier transforms are continuous in frequency and periodic. An inverse DFT evaluated over one frequency period produces the desired discrete-time convolution. But the continuous nature of the DTFT makes it computationally cumbersome. Instead, a common practice is to substitute the discrete Fourier transform, which is just a discrete sampling of the DTFT.

But since that is an approximation, the inverse DFT also produces only an approximation to the desired convolution. In particular, when the DFT of each sequence is substituted for its DTFT, the equivalent effect in the time-domain is periodicity -- the original time-domain sequence is replicated at periodic offsets and summed. When the two periodic sequences are convolved (by the inverse DFT), the result is also periodic, or **circular**.

This is important when we want to use either the cross-correlation filter or the Phase-Only filter because all the convolutions made with Matlab are going to be circular convolution instead of linear convolution. What means that Matlab will always overlap the samples closer to the edges of the image.

Since we will apply our methods to neuroimaging later in thesis, in the example we use here, all the frames in the spatio-temporal movies are going to show a brain with some kind of activation.

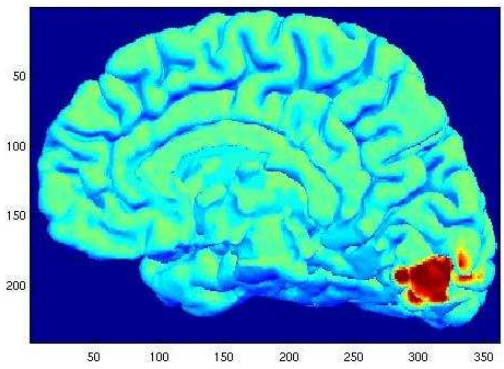

Figure 19. typical image of the brain with some activation

Seeing this, the application of the circular convolution to a brain image could be totally erroneous and could bring us to a wrong result in the output of the filters. Thus we have to apply some kind of transformation to change the circular convolution to lineal convolution.

I have done this by zero-padding the images in the space domain. By using zero-padding I am trying to avoid the aliasing and to convert the cyclic convolution to lineal convolution.

Notice that when we work with spatiotemporal movies the zero-padding is only applied to the space domain and not to the temporal domain. This is because of the nature of the spatio-temporal movies that we worked with and the way they were obtained (see 5.3.2) .

I will talk about that in depth in other sections in this thesis, but as introduction, the movies I have worked with are periodic in time but not in space. This is due to the definition of the evoked potential that I will explain below.

This is an example of zero-padding image:

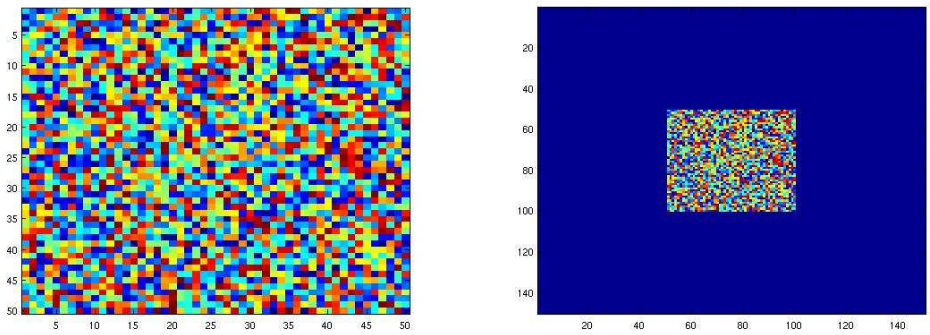

Figure 20. Initial image and the same image after zero-padding transformation

The zero-padding transformation multiplies the size of the original image by 3, and place the original image in the center of this new image, so if the size of the original image is 50x50, the size of the new image will be 150x150, with the original image surrounded by zeros.

3. Phase-Only filter: 3-D

3.1 Introduction

The two preceding sections are an introduction to the basic knowledge we need to deal with more complicated scenarios, such as spatio-temporal movies.

Many papers have studied and analyzed the use and applications of the Phase-Only filter to match 2-D images [21],[30],[48],[49],[50], but the use of the Phase-Only filter to match spatio-temporal movies is quite new. I have introduced before the concept of matched filter, Phase-Only filter and some properties of this kind of filter when we use it with traditional images, but what will happen if we try to use this filter with images in movement?.

In this section I will explain some properties of the Phase-Only filter if it is used with movies. We have to have in mind the aim of this project, "phase-only filtering for comparison of functional **time sequences**" , what means that the last part of this thesis will be the use of the Phase-Only filter to compare MEG (Magnetoencephalografy) movies in order to see if two different movies have a good match or not. I will introduce later in the thesis the concept of neuroimaging and the applications of the Phase-Only filter in this particular field of research.

Having this in mind, it is important to identify the properties of this filter in a 3-D scenario with basic examples, in order to be able to understand what will happen when we try to apply this filter to complex spatio-temporal movies.

3.2. Autocorrelation in spatiotemporal movies

3.2.1. Introduction to the spatiotemporal visualization

To visualize the spatio-temporal movies I have had to create a new way of visualization to be able to see all the point into the spatio-temporal movie with only one image, instead to create a plot for every frame of the movie.

In this visualization what is shown is the value of the peaks of the output of the Phase-Only filter as spheres whom radio is the amplitude of the peak before mentioned. In this way is easier to see the value of this amplitude in a 3-D representation. In order to improve the visualization, prior to show the spheres the output undergoes a thresholded where we pick the minimum value of the peak we want to see. By doing this the visualization is faster and more

precise. In all the example that we will show in this thesis the value picked is that which give us a number of spheres between 700 and 1000, which is a very good discrimination between high and low peaks.

Let's see one visual example to explain the advantages of this visualization,

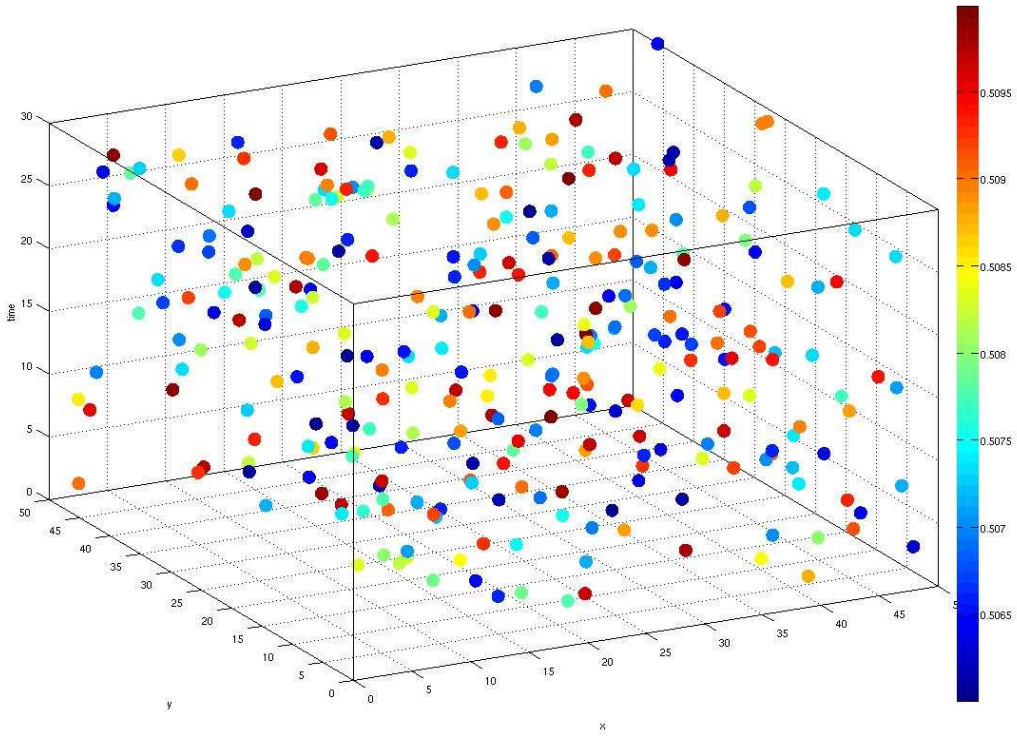

Figure 21. example of visualization of the matrix A; A=rand([50 50 30]), and here I am showing all the values in the 3-D matrix A, between 0.506 and 0.51.

In the example, we can see the advantages of this visualization. We have seen that the output of the Phase-Only filter should be narrow peaks placed in different locations inside the spatio-temporal output. With this visualization we can easily locate the peak and the **mapcolor** is also related with the radius of the sphere and consequently with the value of the peak. The axis will be space(x,y) and time (t).

3.2.2 Implementation of the Phase-Only filter

Given two movies $I_1(x,y,t)$ and ,$I_2(x,y,t)$ the Fourier transform $F\{\}$ of these movies can be written as:

$$Z_1(h,k,f) = F\{I_1^{sz}(x,y,t)\} = X_1(h,k,f) + jY_1(h,k,f)$$
$$Z_2(h,k,f) = F\{I_2^{sz}(x,y,t)\} = X_2(h,k,f) + jY_2(h,k,f)$$

If one uses the symbol $F^{-1}\{\}$ for the inverse Fourier Transform

and $I_1^{sz}(x,y,t)$ *and* $I_2^{sz}(x,y,t)$ are the functions zero padded in space, the phase only filter is given by:

$$POF(x,y,t) = F^{-1}\left[j \arctan\left(\frac{X_1Y_2 - X_2Y_1}{X_1X_2 - Y_1Y_2} \right) \right]$$

3.2.3 Autocorrelation in spatio-temporal movies

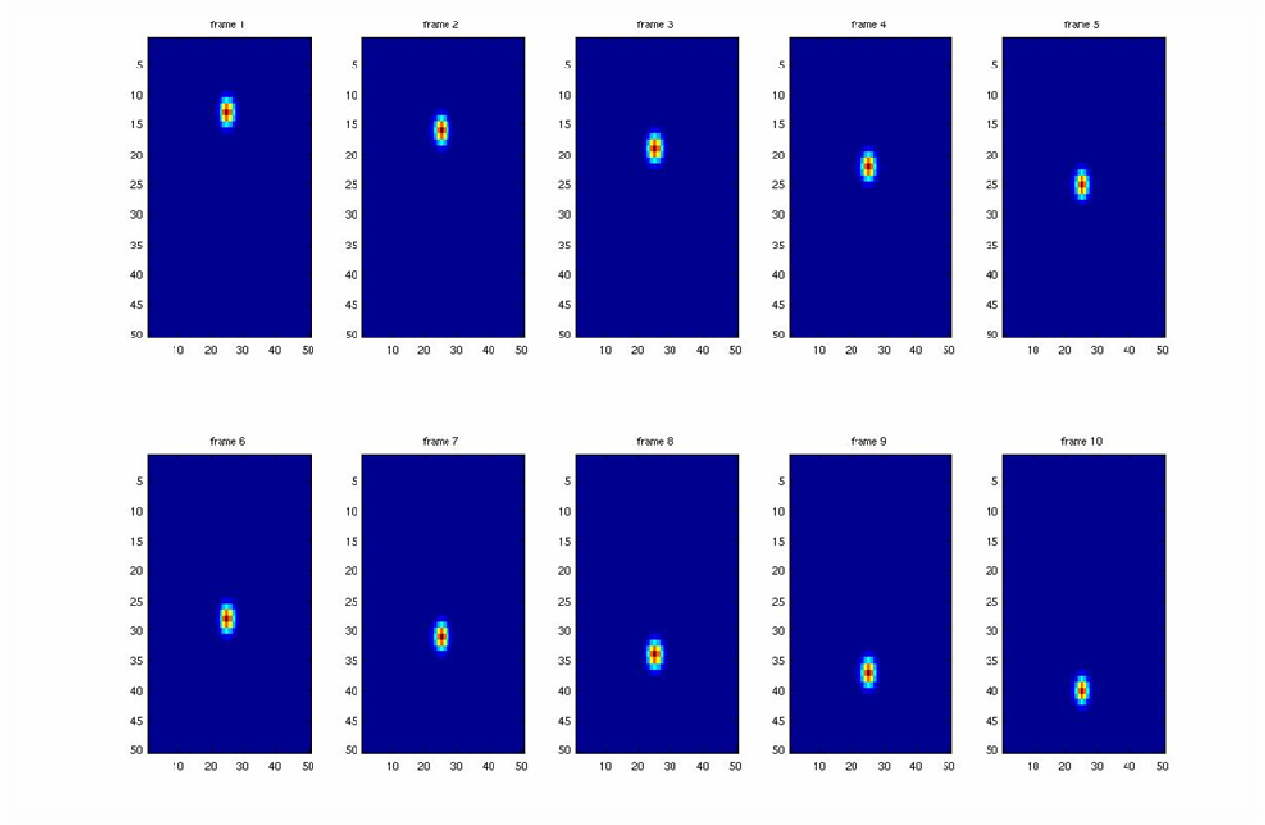

Figure 22. Movie $M_1(x, y, t)$ [50x50x30] shows a Gaussian moving in the x-axis

Given a spatio-temporal movie $M_1(x, y, t)$, we are going to see the autocorrelation of this movie by using the Phase-Only filter. We have analyzed the behavior of the POMF in 2-D images. We have to remember that we obtained a narrow peak with amplitude equal to 1, and placed in the center of the image (zero lag). This first experiment was done to study if the properties of the POMF for images could be extrapolated to movies. The autocorrelation of the movie $M_1(x, y, t)$ can be shown like this,

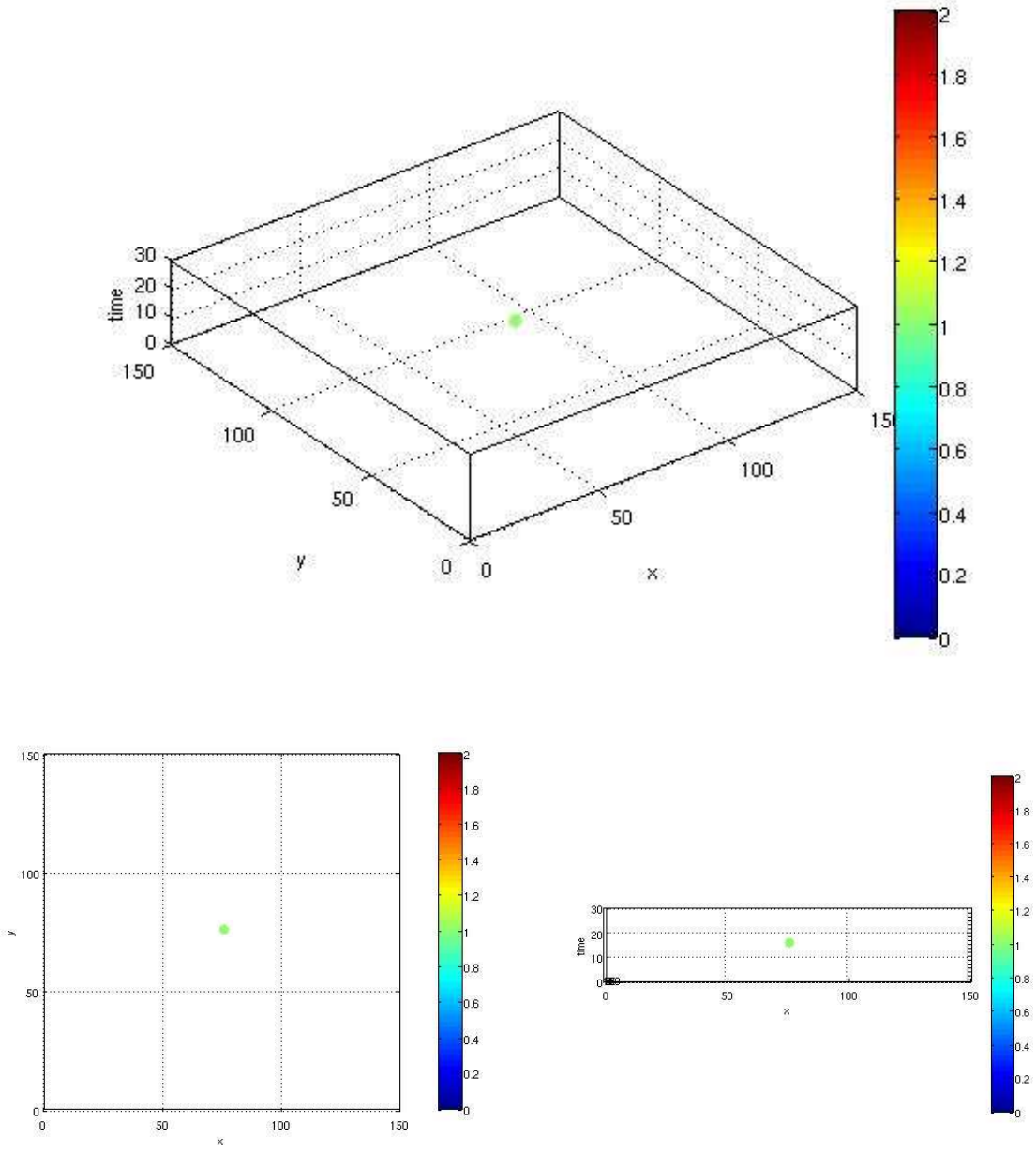

Figure 23. Output autocorrelation of $M_1(x, y, t)$ by using Phase-Only filter

We can see in the figure 24 how the autocorrelation of two movies by using the Phase-Only filter is a peak with value equal to 1, placed in the center of the output (zero lag).

In this example of a Gaussian moving around the x-axis in a movie composed of 30 frames of 50x50 pixels each one, the output of the filter is another movie composed of the same frames as the original but with a size of 150x150 pixels, due to the zero-padding applied to the original movie.

This first experiment is really positive because we can see how the results obtained in the 2-D experiments are completely valid for a 3-D scenario.

In all of the rest of the experiments this will be the ideal output for equal inputs. This is a very good point of reference in order to check how similar two movies are.

Now, the example below is just to see why the traditional cross-correlation filter doesn't work at all if we are expecting to give a grade of similarity.

As we can see in this figure the output of the filter doesn't give us information about the similarity of the inputs, which is the aim of this project.

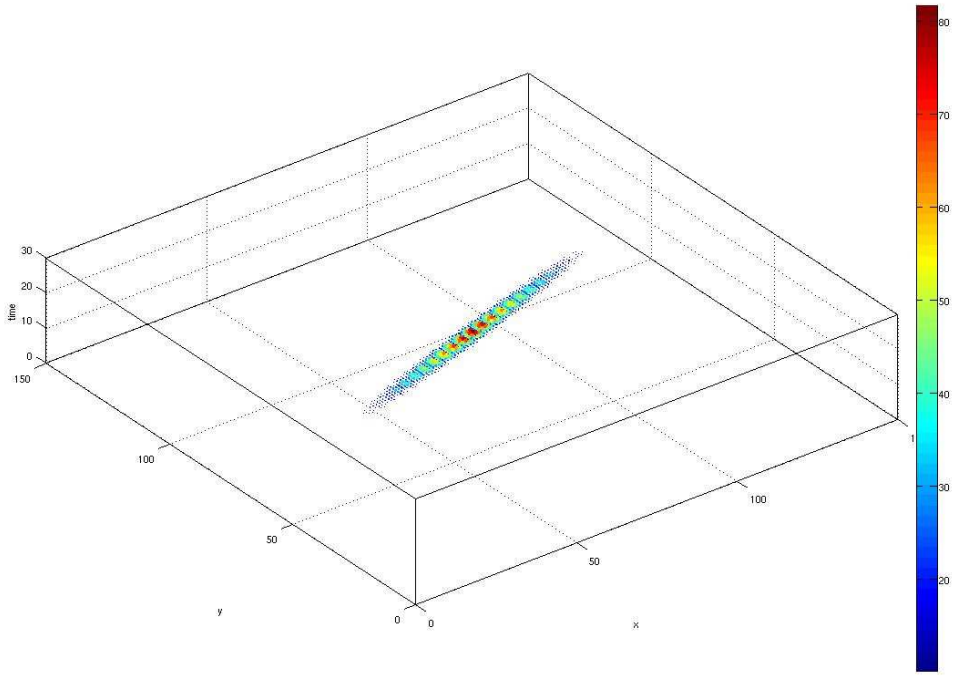

Figure 24. Output of the cross-correlation filter when the inputs are equal

3.3 Cross-correlation in Spatio-temporal movies

Given two movies $M_1(x,y,t)$ and $M_2(x,y,t)$ as inputs of the Phase-Only Filter we are going to analyze the output of this operation. If the filter works as we expect it to, we shouldn't

see any clear peak and that will mean that the cross-correlation of the inputs is very small showing us a poor grade of similarity between them .

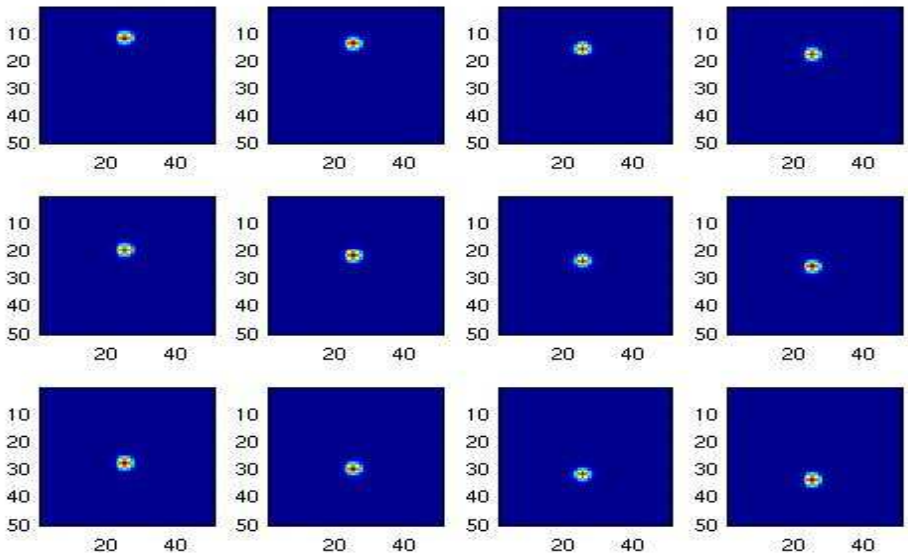

Figure 25. $M_1(x, y, t)$: Gaussian moving in the x-axis. Every frame shows a time sample different from time equal to 1 to 23.

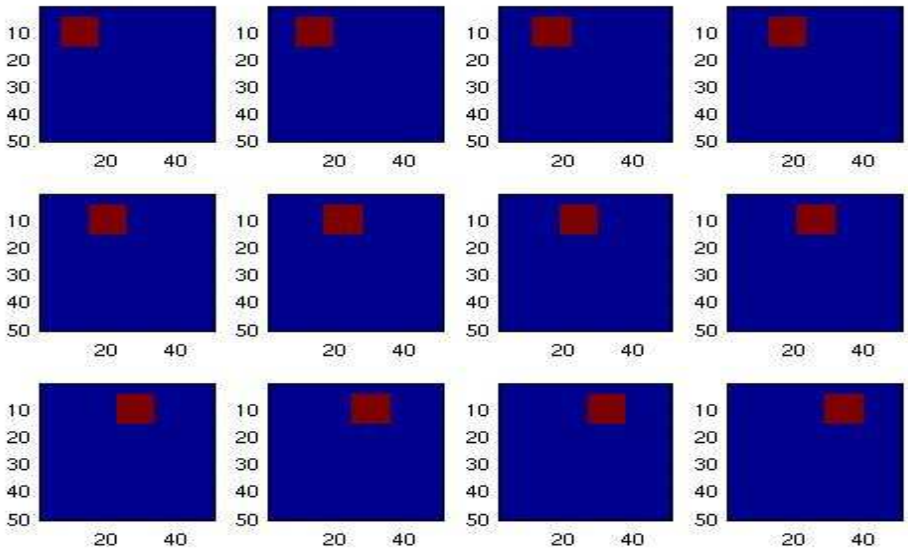

Figure 26. Cube moving in the y-axis. . Every frame shows a time sample different from time equal to 1 to 23.

Both movies are totally different in terms of shape of the object and its movement, so we will see if the Phase-Only filter tells us the same,

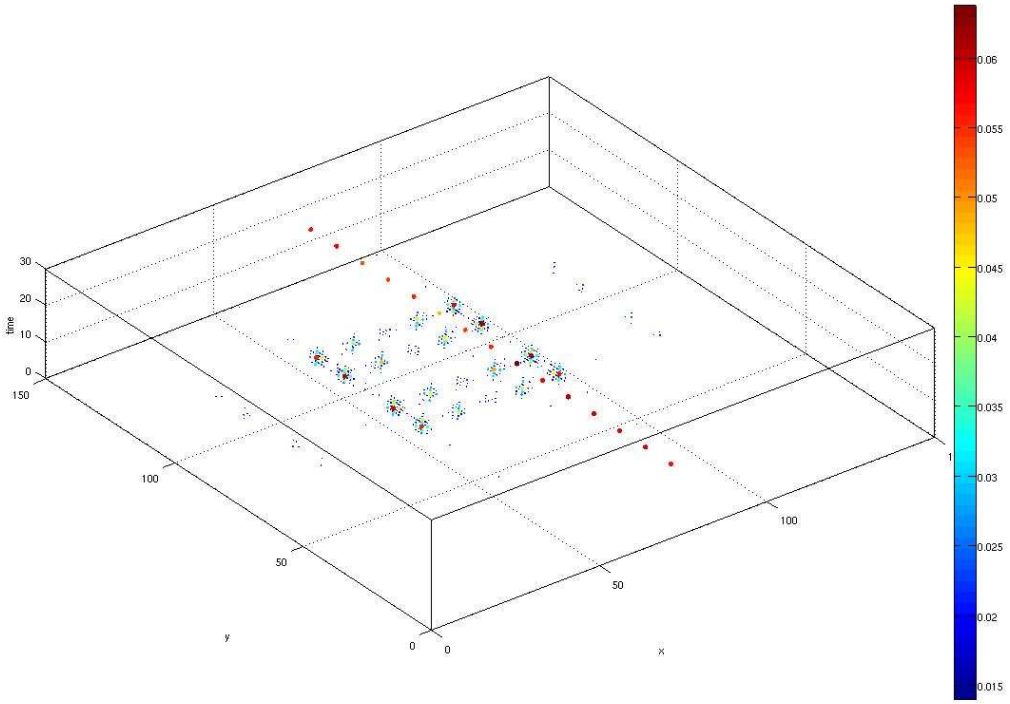

Figure 27. Visualization 3-D of the output of the Phase-Only filter

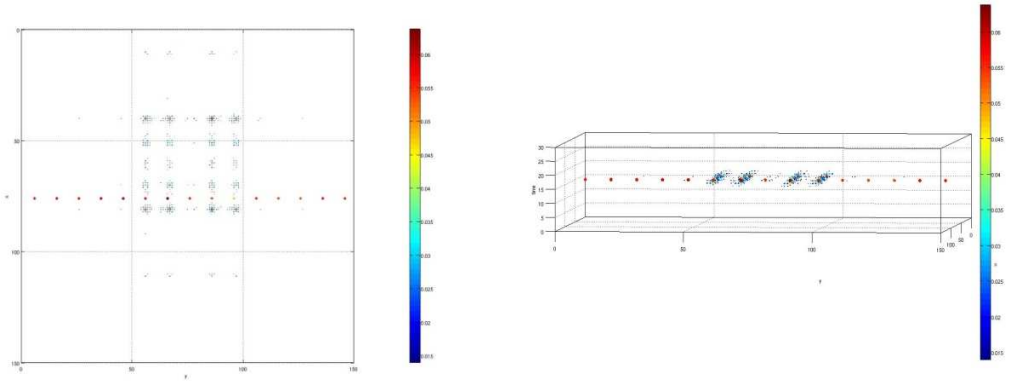

Figure 28. Visualization of the x-y view and the temporal view

We can see clearly the presence of a lot of sparse peaks in the output of the filter. We are unable to find a narrow peak, because the maximum amplitude of the output is equal to 0.06. So if we compare this data with the data obtained with the test of the POMF autocorrelation where the maximum amplitude was 1, clearly we can see a poor match between movies.

The output of the Phase-Only filter shows that the similarity between the two inputs is very small and we can take that conclusion by comparing this result obtained with the perfect situation of similarity showed in the figure 24.

We are going to check in the next section if the shift properties of the Phase-Only filter when we work with 2-D images could be extrapolated to 3-D and I will introduce the concept of shifted in time, very useful when one input doesn't start at the same time as the other one, but are both the same movie.

3.4 Property: Shift

3.4.1 Defining the space

The first step is to define the space we are going to work in. Since we will work with real data that comes from evoked responses tests, its appropriate if we define the space according the properties of that experiment in particular.

In the section (5.3.2) we will talk in depth about this kind of experiment but in order to define the space and the characteristics of the shift property study is correct to explain them at this point.

When working with spatio-temporal movies there will be one important difference between space and time. **While space is linear, time is cyclic.**

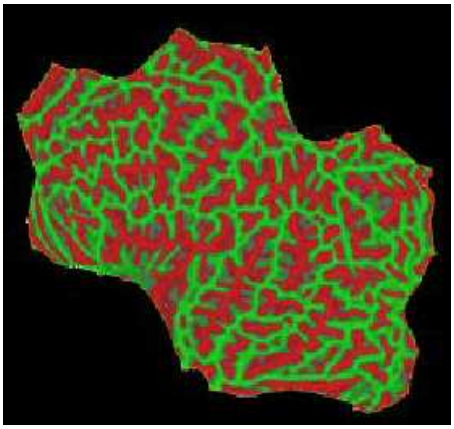

Figure 29. representation of a flattered brain

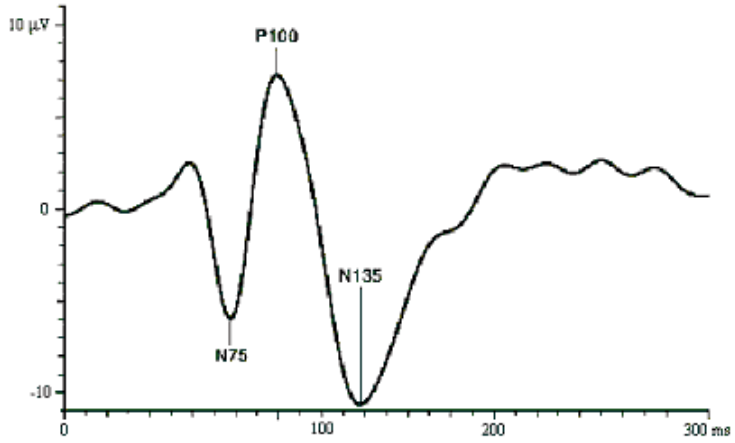

Figure 30. example of wave obtained from a evoked responses test

We can see in the figure 30 the relation between what is happening at time 1ms and 300ms. The cyclic nature of the time in this case comes from the way this data is obtained, section (5.3.2). Once we have defined the space we will study how this is important in terms of shifts.

3.4.2 Shift in space and time

The theoretical explanation of the translation property in space has been introduced in 2.2. Based on that property, the increase of dimensions doesn´t have to affect on the behavior of the filter.

Given two movies $M_1(x,y,t)$ and $M_2(x,y,t) = M_1(x - x_0, y - y_0, t - t_0)$, we are going to run the Phase-Only filter when the second movie has undergone a translation in space and time with respect to the first one. This time the movies are both a Gaussian that is getting bigger and bigger. There are two differences between the inputs, one of them is the translation

underwent in terms of space, and the other one is the translation underwent in terms of time. In this example the second movie stars 10 frames later than the first one.

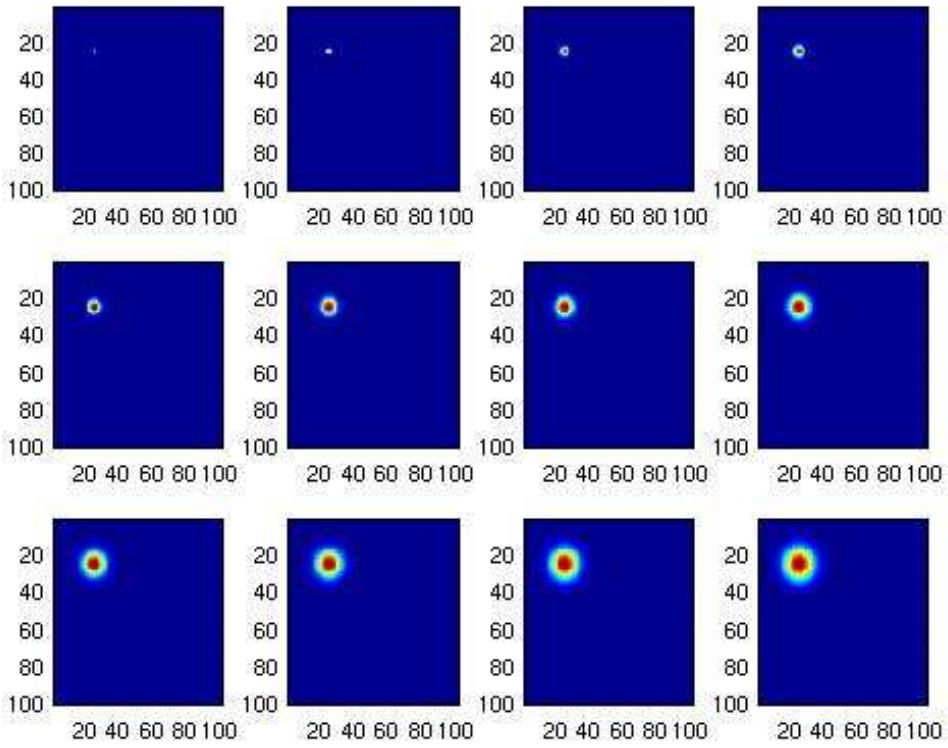

Figure 31. Movie $M_1(x, y, t)$

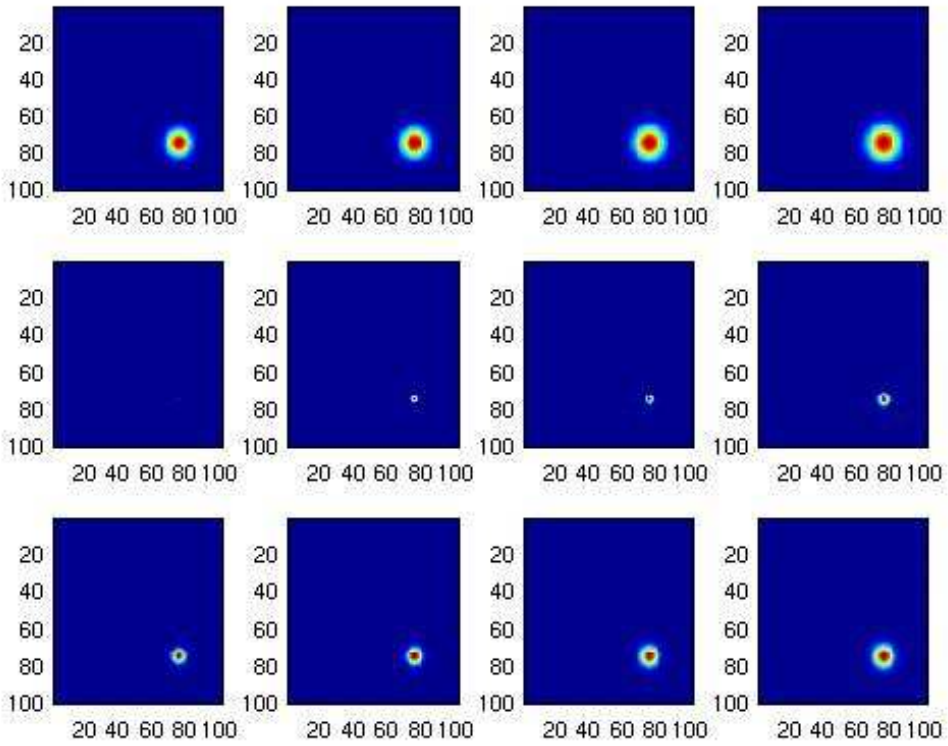

Figure 32. $M_2(x,y,t) = M_1(x-50, y-50, t-10)$

The output of the Phase-Only filter will show us exactly the translation of the second movie respecting to the first one.

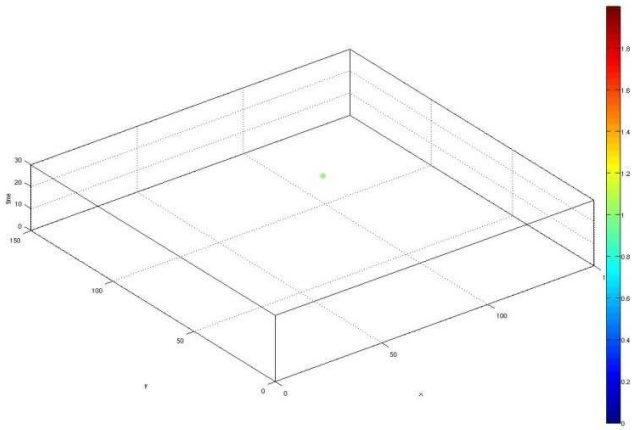

Figure 33. Output of the Phase-Only filter. 3-D view

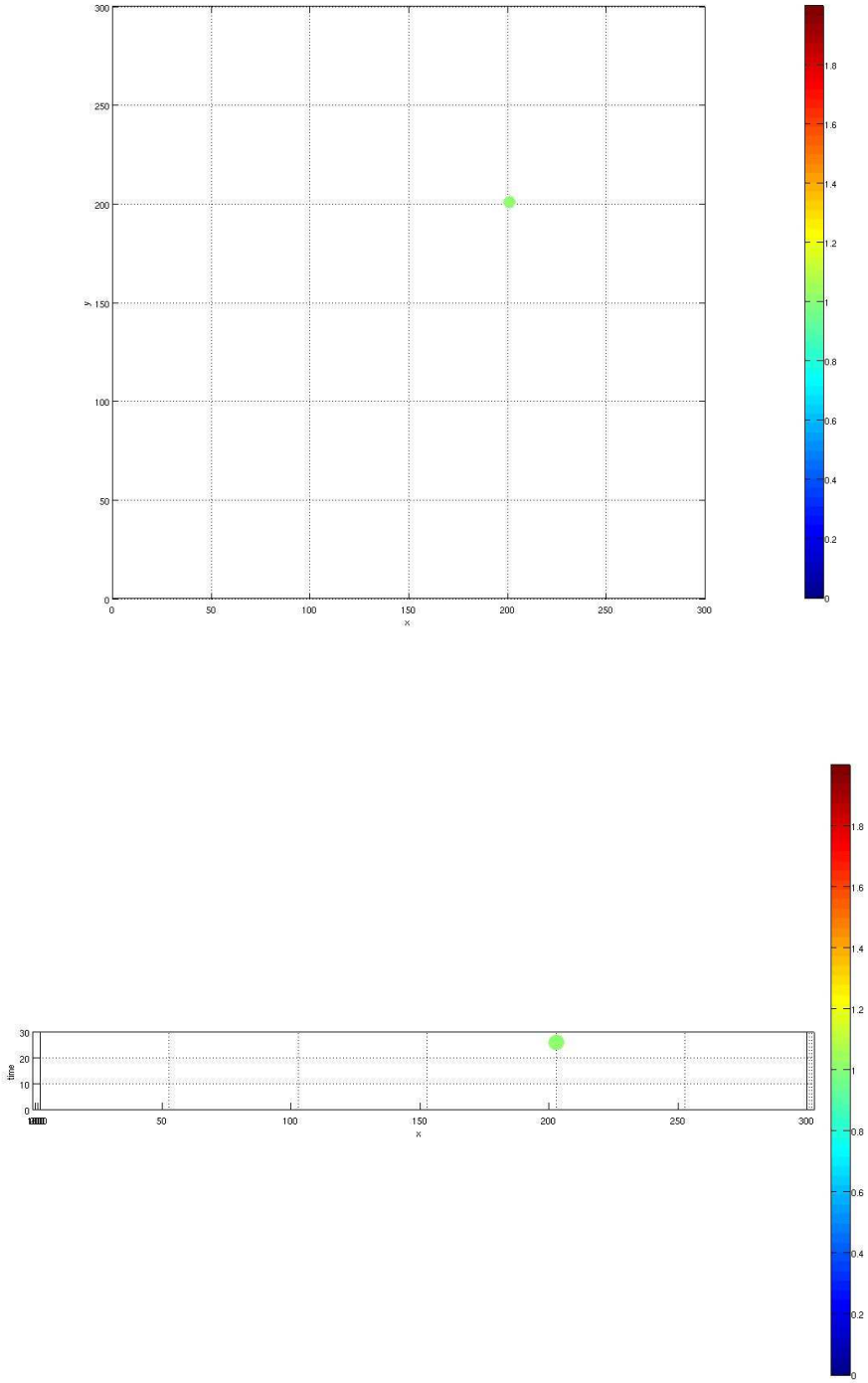

Figure 34. 2-D views of the output of the Phase-Only filter

We can see in the 2-D views how the Phase-Only filter perfectly locate the translation at the same time that shows us that the two movies are the same one due to the peak of amplitude equal to 1.

In this test, the zero-frequency is located in the center of the output (150 , 150 , 16), so.after the translation the peak appears in (200 , 200 , 26). So far, the Phase-Only filter perfectly locate translations in all the dimensions shown.

After this test we can see **the linear behavior** of the Phase-Only filter as long as the shift doesn't effect the shape of the movie nor the edges of the movie, otherwise artifacts will appear in the output.

3.5 "Movie vs. Static Movie" Fact

As I have shown in all the examples before explained, if the inputs of the Phase-Only filter are two images, we obtained as output another image. If the inputs of the Phase-Only filter are two movies, we obtained another movie. But one question of interest is what happens if one of the input movies is constant in time?.

Thus we have the following situation for the constant movie:

$$M(x,y,t_1) = M(x,y,t_2) = \cdots = M(x,y,t_n)$$

with n the number of frames of the movie M. So we can say that $M(x,y,t) = M(x,y)$ because this movie doesn't depend on time.

In this test we will have as inputs a Movie $M_1(x,y,t)$ and another movie $M_2(x,y)$. We treat time as continuous although the same result can be derived for discrete time.

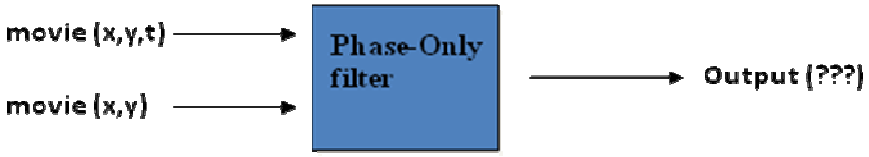

$$R_{M_1M_2}(x,y,t) = M_1(-x,-y,-t) * M_2(x,y)$$

$$F\{R_{M_1M_2}(x,y,t)\} = \iiint_{-\infty}^{\infty} M_1(-x,-y,-t)M_2(x,y)e^{-j2\pi xu}\, e^{-j2\pi yu}\, e^{-j2\pi tw}\, dx\, dy\, dt =$$

$$= \int_{-\infty}^{\infty} M_1(-u,-v,-t)M_2(u,v)e^{-j2\pi tw} = M_1(-u,-v,-w)M_2(u,v)\delta(w) =$$

$$= R_{M_1M_2}(u,v,w)$$

where $(*)$ denotes the operator convolution and $M_1(-x,-y,-t)\ and\ M_2(x,y)$ are real-valued movies.

The inverse Fourier transform of $R_{M_1M_2}(u,v,w)$

$$\iiint_{-\infty}^{\infty} M_1(-u,-v,-w)M_2(u,v)e^{j2\pi xu}e^{j2\pi yv}\, e^{j2\pi tw}\, du\, dv\, dw$$
$$= \int_{-\infty}^{\infty} M_1(-x,-y,-w)M_2(x,y)e^{j2\pi wt}\, dw = M_1(-x,-y,0) * M_2(x,y)$$
$$= R_{M_1M_2}(x,y)$$

Thus we see that the cross-correlation of a movie and a "static movie" is as also static

We thought that it was important to remark this fact because while working with spatio-temporal movies some basic assumptions a priori are not true once we have analyzed them. In this particular case we were convinced that the output had to be another movie, but the theory shows us the real behavior of the filter.

4. Identification of patterns present in different scenarios

4.1 Introduction

All the explanations until now have been illustrated with simple synthetic examples, in which either the inputs were equal to each other or they presented some differences in terms of shape and movement from each other, here we consider more complex examples as one might expect to find in an application scenario.

Thus, in this chapter we examine the performance of the POMF when the inputs are not equal, but rather are similar. We will see the difference between the autocorrelation of one input and the cross-correlation of the inputs and how the energy of the frames is a very important outcome in this operation.

We consider this work in the framework of **Template Matching**

First of all I will introduce the Phase-Only filter as an approach to Template Matching in 2-D.

In the template matching the inputs of the filter are two images, one of them will be the pattern we want to recognize and the other one will be the image where we hypothesize that the pattern may be present. By doing this, we are looking for a result that shows us that the pattern (the first input) is present in the second input.

After illustrating the performance of the Phase-Only filter works in this 2-D scenario, we will try the filter with movies. In those movies the filter will have to recognize objects in movement, where the shift property in space will be very useful, and also the shift property in time applied to objects in movement but starting their movement either before or after that the pattern.

This use of the Phase-Only filter to recognize different patterns in spatio-temporal movie will be very useful to interpret the results obtained when the inputs present some short of similarity between them in terms of shape and movement (pattern).,

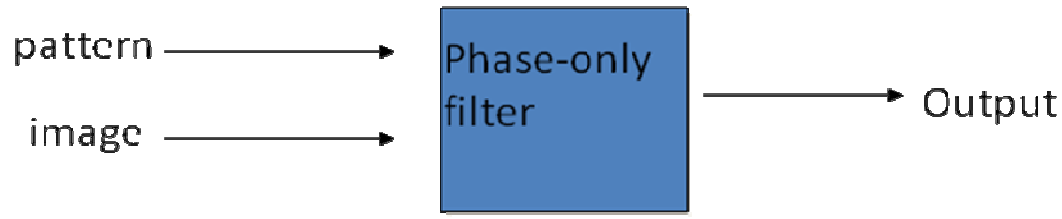

This is the diagram of the use of the Phase-Only filter used to recognize patterns in 2-D images.

There will be two important questions that the filter has to be able to answer,

1. Is the pattern present in the image?
2. Where is the pattern present in the image?

To evaluate the correct working of the Phase-Only filter it will have to answer these two questions.

4.2 Identification of patterns in 2-D

In this subsection we present several examples of increasing complexity of the pattern to recognize.

In this case we will have two inputs, where in both of them there will be present the same pattern.

Due to the distributive property of convolution,

$$f * (a + b) = f * a + f * b$$

we can see how this is applied to the correlation.

$$R_{ab_n}(x,y) = F\{a(-x,-y) * [a(x,y) + b_1(x,y) + b_2(x,y) + \cdots + b_n(x.y)]\} = R_{aa}(x,y) + R_{ab_1}(x,y) + R_{ab_2}(x,y) + \cdots + R_{ab_n}(x,y)$$

Then, if the filter was the traditional cross-correlation filter we would expect to see one autocorrelation peak, and then as many cross-correlation peaks as objects are in the image. We are going to analyze if this behavior is similar to the POMF behavior in this conditions.

Given 2 images, $I_1(x,y)$, $I_2(x,y)$ and the addition of these images,

$$I_{12}(x,y) = I_1(x,y) + I_2(x,y)$$

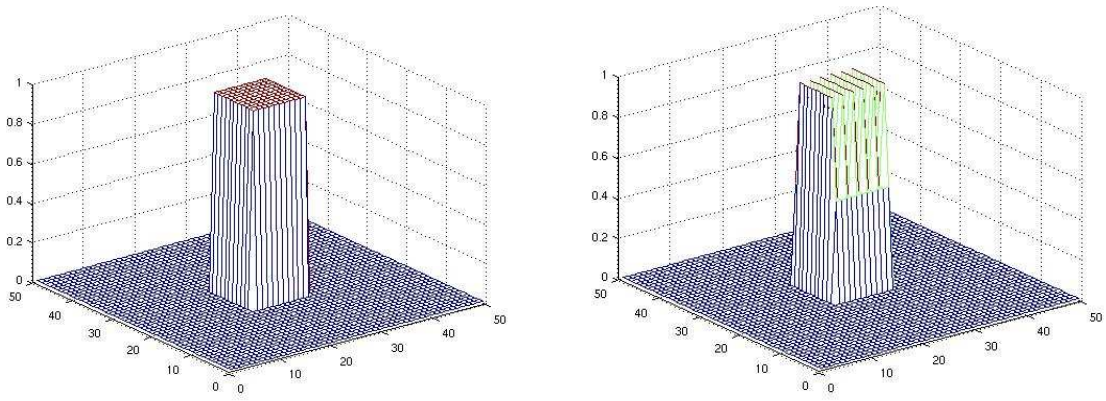

Figure 35. Images I_1 and I_2

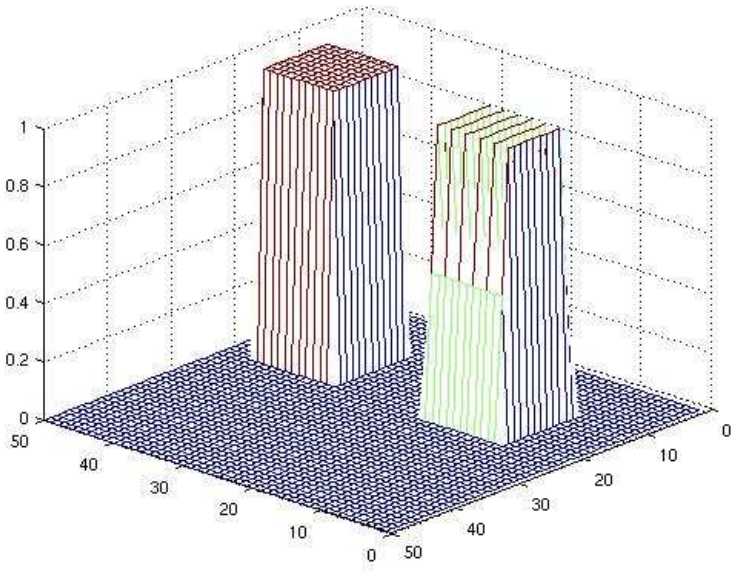

Figure 36. I_{12} is composed by the two patterns I_1 and I_2

I am going to explain the two possible tests we can do with this images. The inputs of the first experiment will be I_1 and I_{12}, and the inputs of the second one will be I_2 and I_{12}.

The pattern to recognize will be the first input, and the second input will be the image where the filter has to recognize the first input.

The output of the Phase-Only filter when the inputs are I_1 and I_{12} is:

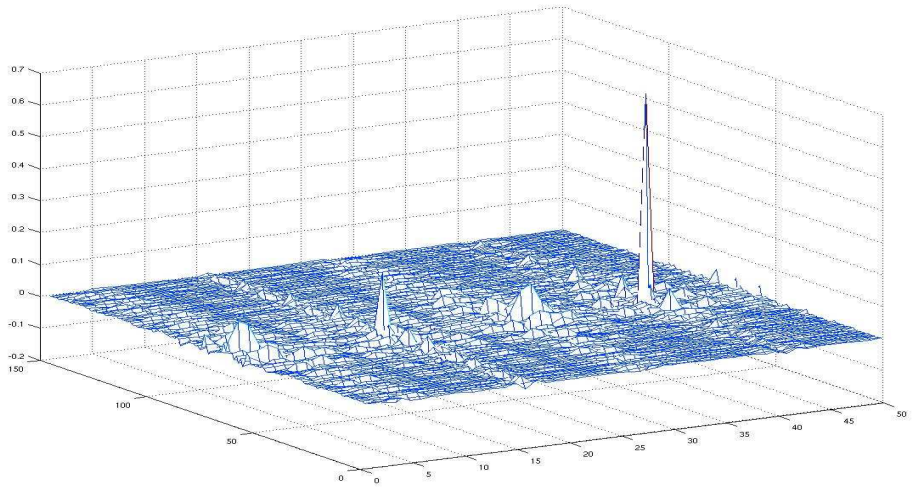

Figure 37. Output of the Phase-Only filter

We can see in the Figure 37 how the Phase-Only filter recognizes the presence of two inputs.

The main peak is showing us the presence of an object very similar in the two inputs and it is located at the location of the shift between them. And we can also see the presence of another narrow peak which is the cross-correlation peak between the pattern and an alien object in the image.

This behavior could seem similar to the traditional cross-correlation filter, but of course while working with POMF the concepts of "autocorrelation" and "cross-correlation" are not true in the traditional meaning. In the outputs we won´t see these real values, but it is a way to point out what is happening at the output. The location of those peaks would be the same as if we were working with the traditional cross-correlation filter, but the value of these points are not related to the real correlation points of those images.

What we wanted to study in this chapter was if the POMF was able to locate those areas where the two inputs could have a similarity between them. And as we will see, the POMF perfectly locates those points.

Now, the pattern to recognize will be the image I_2 in the image I_{12}.

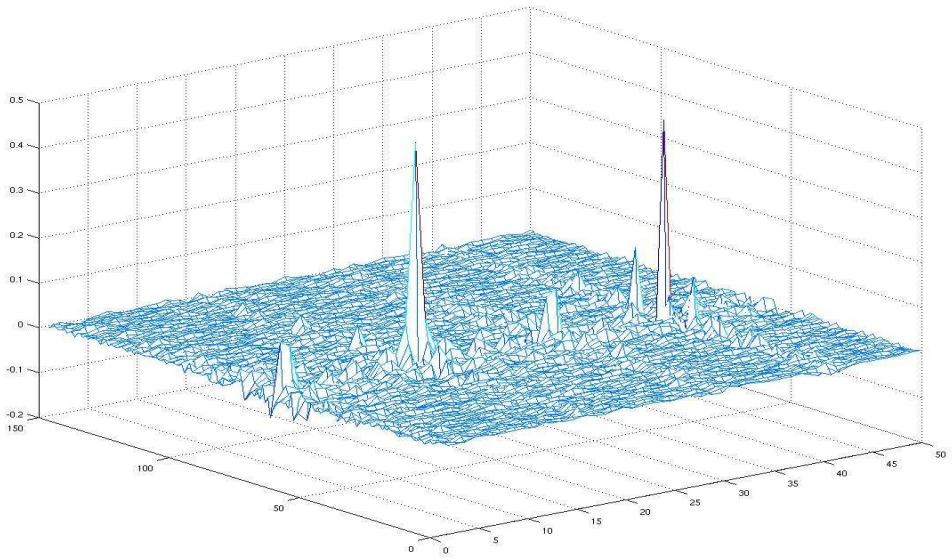

Figure 38. Output of the Phase-Only filter

In this output we can see what I have introduced before. The POMF locates two points where it could be a similarity between the inputs. We can see how the values of these peaks are different to the values of the peaks in Figure 38, but what it is important here is the location of those peaks rather than the values. We can´t predict how those values are going to be due to the non linearity of the POMF, what we can predict is where those peaks are going to show up.

4.3 Identification of patterns in 3-D

Now that I have introduced the aim of this chapter about identification of patterns, understanding pattern how common objects in both inputs, it is time to see how this could affect when we are working with spatiotemporal movies. The examples before commented were a 2-D examples, where the only thing that could affect to the output of the filter was either a different shape of the object under study or a different location of that object in the input.

In this case, I introduce movement to the examples. So from now on, it is going to be important the fact that the objects have some kind of movement, and some kind of translation, that could be in terms of space or in terms of time. We could see previously how this translation won´t affect to the output of the POMF, but now it´s time to see how the POMF locates those objects that the inputs have in common and how the filter discriminates between similar objects with similar shape and movement with other objects without that similarity.

We will see this point in the next examples where the Phase-Only filter will have to identify similar objects moving in different movies.

4.3.1 First example: one pattern in a movie with two objects

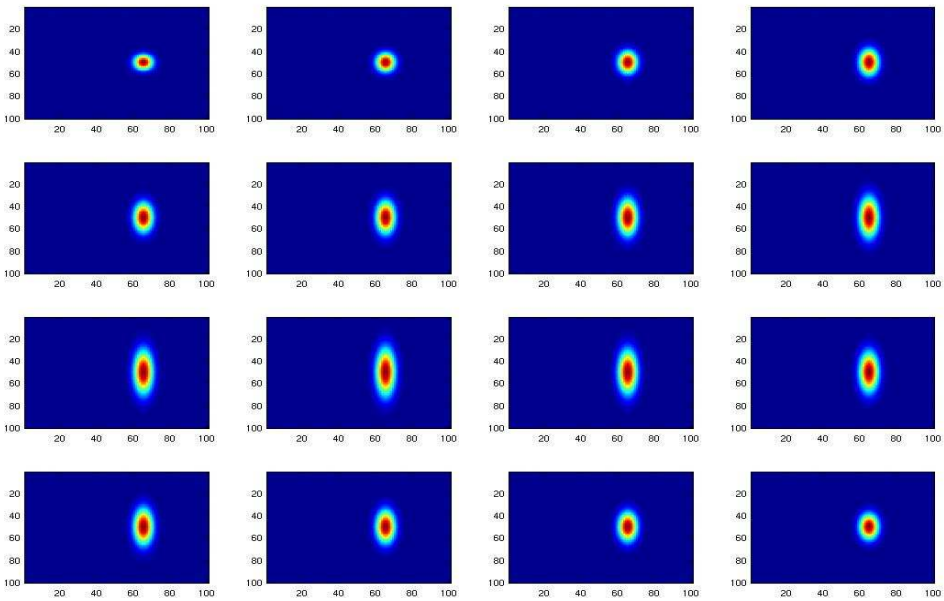

Figure 39. Pattern to recognize

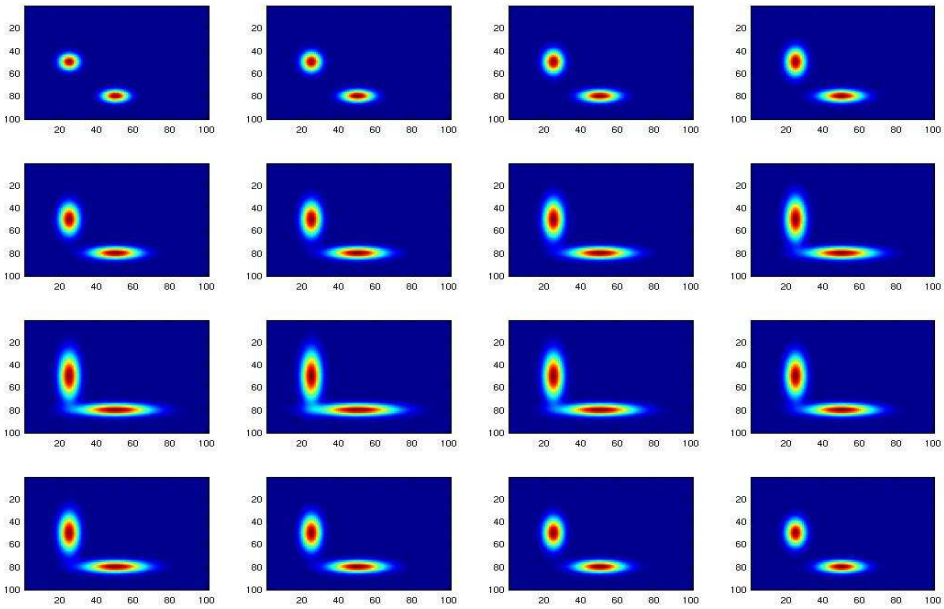

Figure 40. Movie $M_2(x,y,t)$

Given the two movies $M_1(x,y,t)$ and $M_2(x,y,t)$ illustrated in Figs. 39 and 40, with M_1 the pattern to recognize in M_2, we will see how the Phase-Only filter recognize the Gaussian of M_1 in M_2.

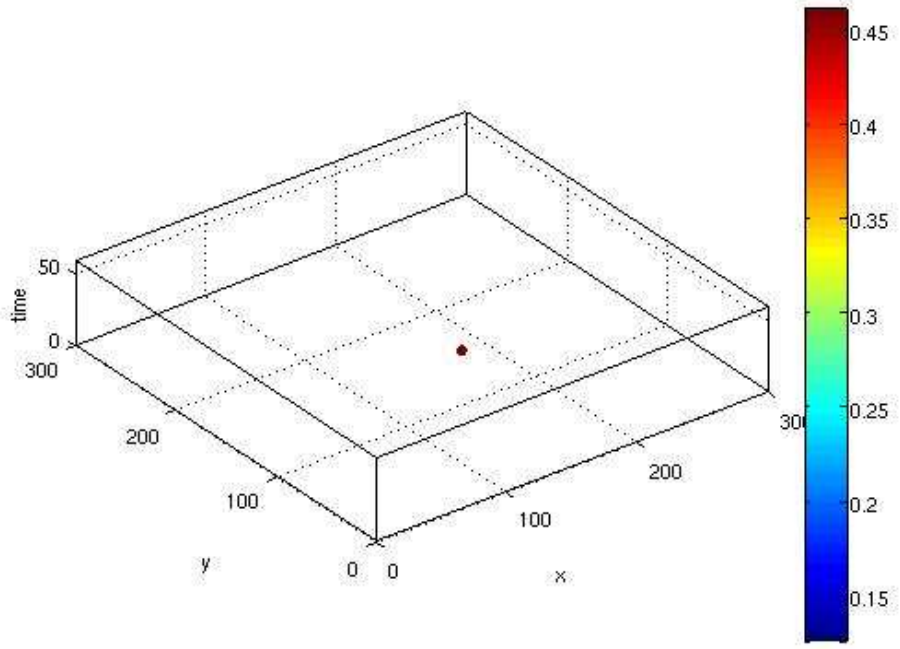

Figure 41. Output of the Phase-Only filter.

When we don't have any shift in time, maybe this visualization could be a little bit confusing. All the peaks will locate at zero shift in time which means that if the output has 59 frames, it will be in frame 30. Let's take a look at this frame to understand better what is happening.

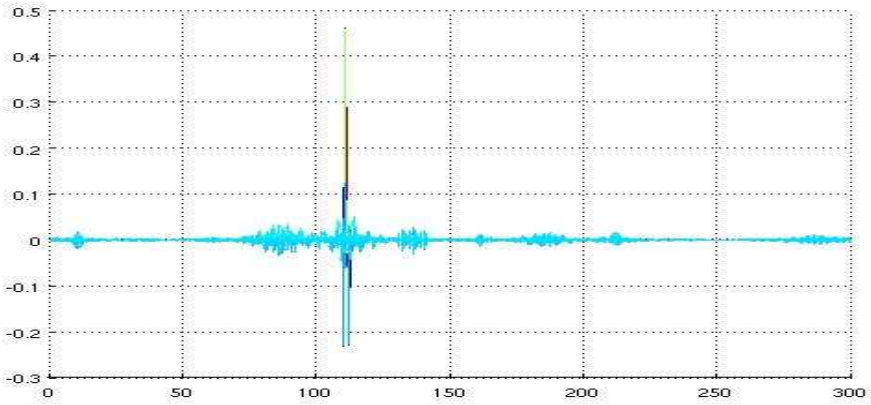

Fig 42. 1-D visualization of the zero shift frame (amplitude in y-axis)

We see how the Phase-Only filter perfectly locate the pattern in the movie M_2. And it is also able to tell us the shift between the pattern and the same object in the movie. So this filter works.

4.3.2 Second example: one pattern in a movie with three objects

The pattern to recognize is the same as the first example, but this time in the movie where we have to recognize the pattern there will be three objects instead of two.

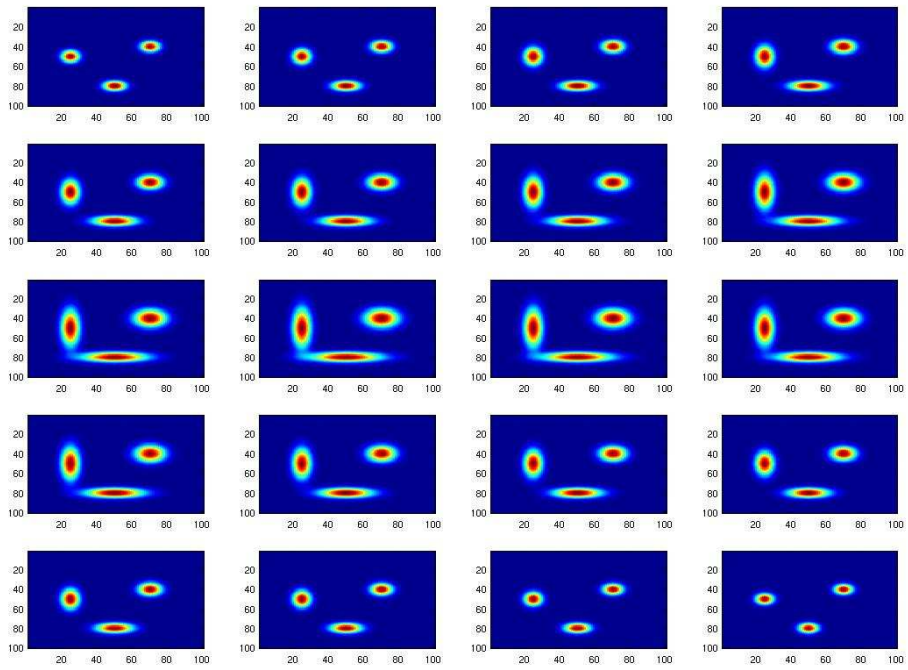

Figure 43. Movie $M_3(x, y, t)$

In this case, we have three Gaussians, which grow and shrink, where the three Gaussians are in different location and their shapes are different.

We will see on the next page how the Phase-Only filter is also able to find the pattern $I_1(x, y, t)$ when the filter has to discriminate between more than 3 objects. Again, as there is no shift in time we don't need to see all the frames, so we can fix our attention on the frame where all the information is.

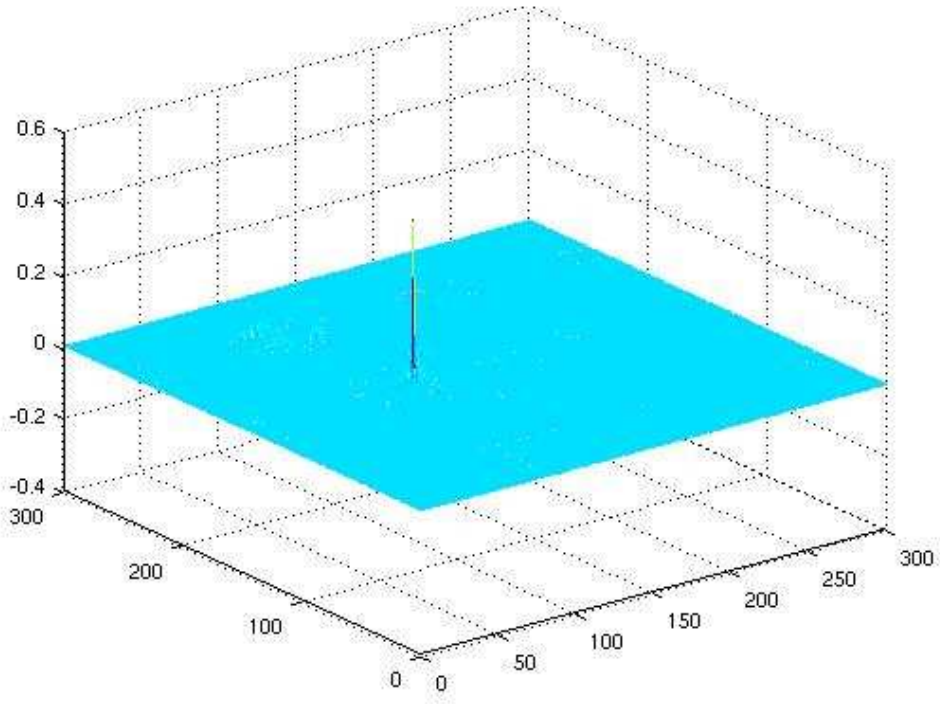

Figure 44. Output of the Phase-Only filter

We see how the narrow peak locates perfectly thee pattern shown before, since the shape of the pattern is so different from the shapes of the other objects present in M_3 there are no peaks from the cross-correlation between the pattern and the rest of the objects.

4.3.3 Third example: two patterns in a movie with 4 objects

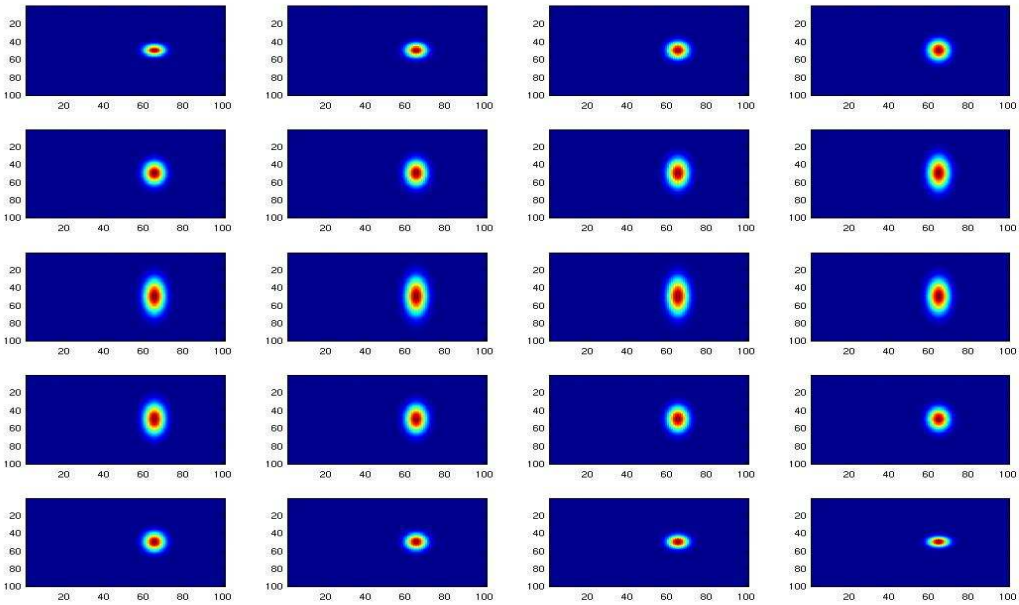

Figure 45. Pattern to recognize

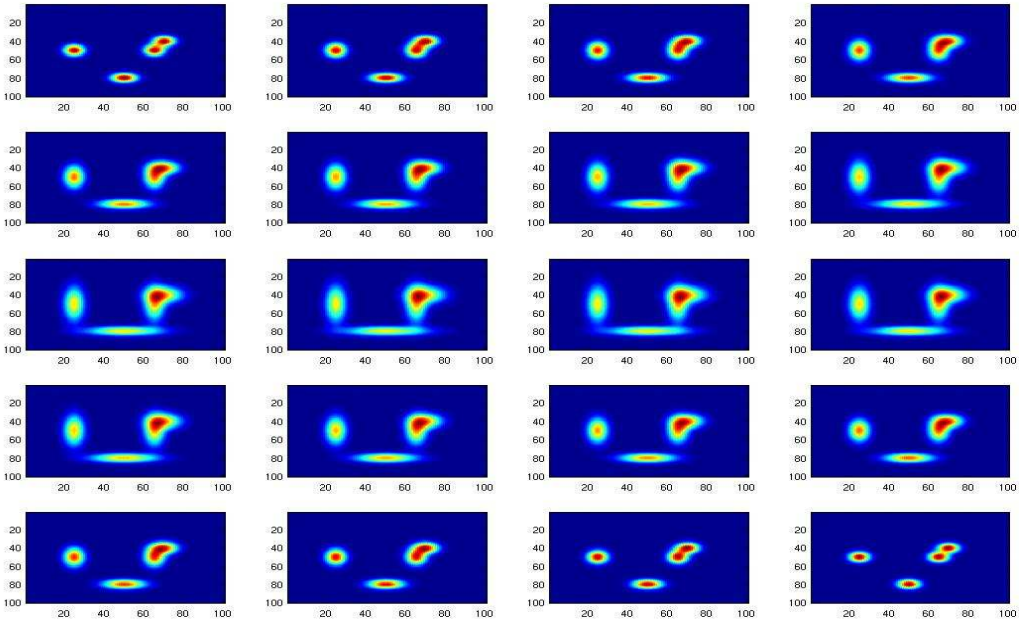

Figure 46. Movie where the Phase-Only filter has to find the pattern

This example could seem more complex than the other two previously mentioned, in this case the pattern is present in the movie M_4 in two places, we can see one of them in the left part of the movie, and the other one is mixed with another signal, in this case another Gaussian, will be the Phase-Only filter able to find the two locations of the pattern?. The answer is yes.

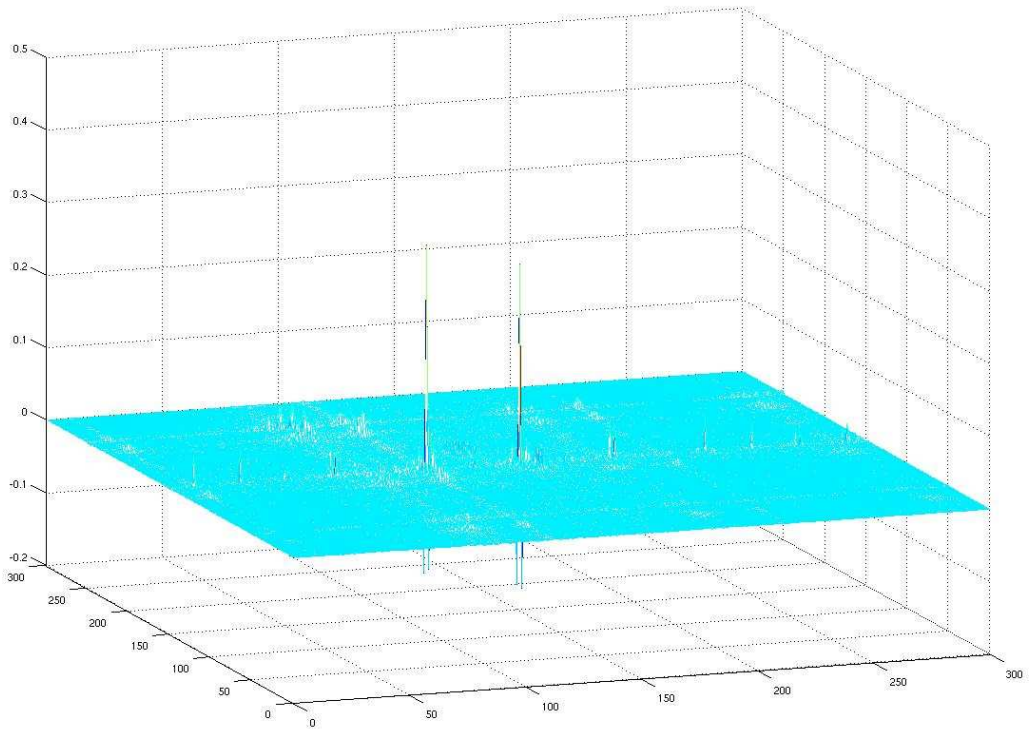

Figure 47. Output of the Phase-Only filter finding the patterns and their location

We see the two narrow peaks, one of them is clearer than the other one, this is due to the Gaussian hidden under the other Gaussian. Since the shape is not the same, the filter locates the pattern but is contaminated with other signal, which alters the filter output.

In all these examples the pattern is moving at the same time in the two movies, but now I am going to show how the Phase-Only filter is able to find the pattern even when it doesn't start at the same point in the two movies.

4.3.4 Fourth example: one pattern shifted in time in a movie with two objects

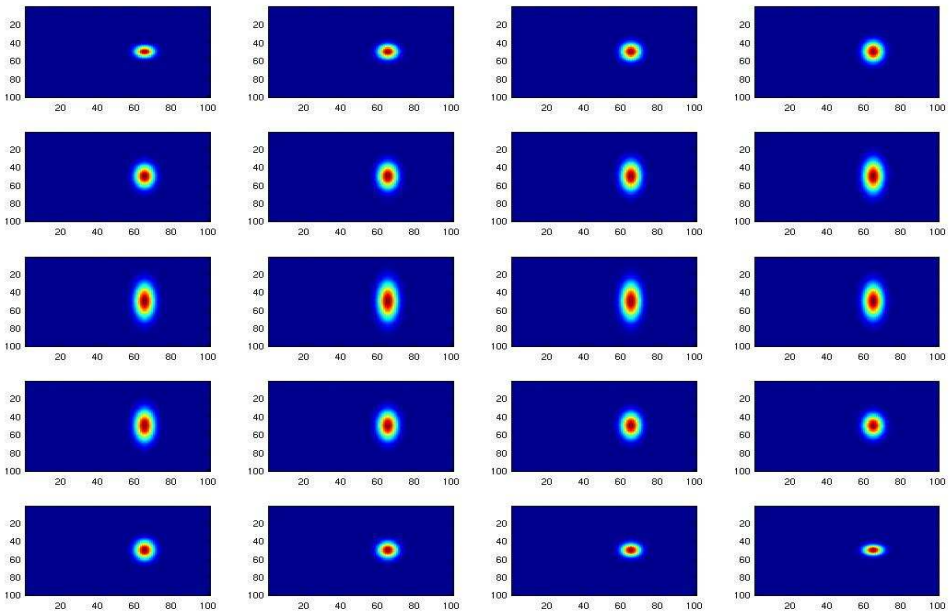

Figure 48. Pattern to recognize

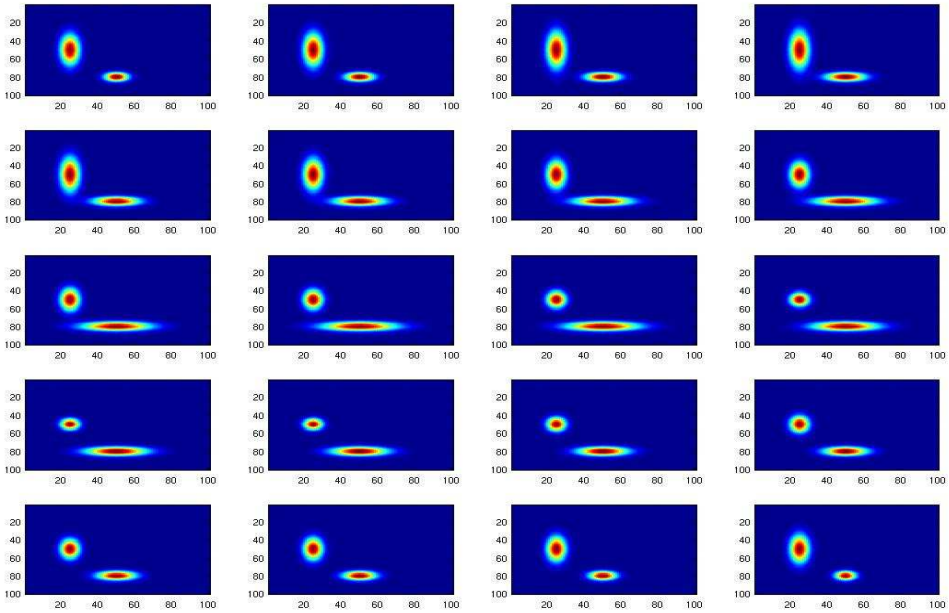

Figure 49. Movie M_1 where the filter has to find the pattern

This example illustrates how the Phase-Only filter performs when the goal is to locate a pattern. We note that this kind of temporal shift relationship may not be readily apparent visually, especially for a sequence with a large number of frames.

The goal is to determine whether there is a match, and if so, what the shifts in time and space are.

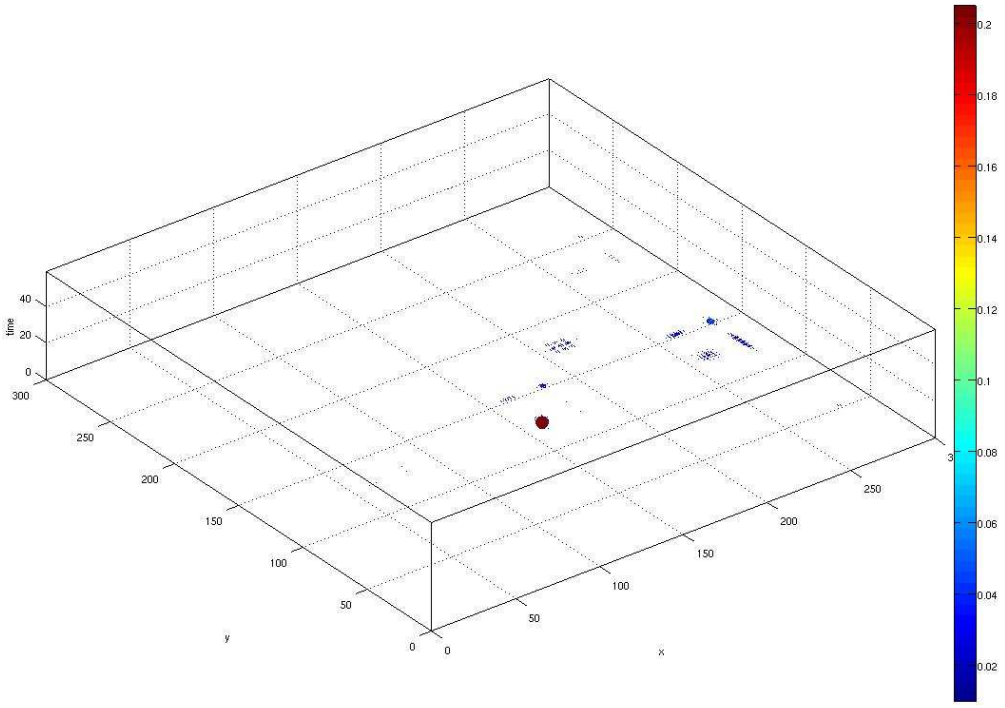

Figure 50. 3-D visualization of the output of the Phase-Only filter

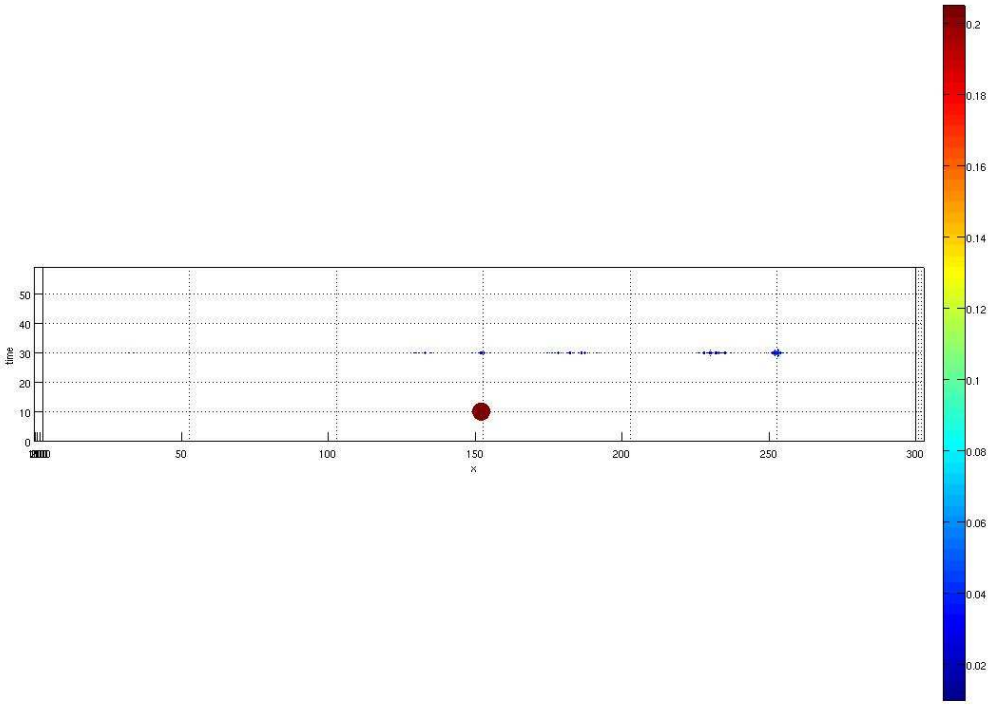

Figure 51.2-D (x,t) visualization of the crossocorrelation peak between the pattern and the movie M_1

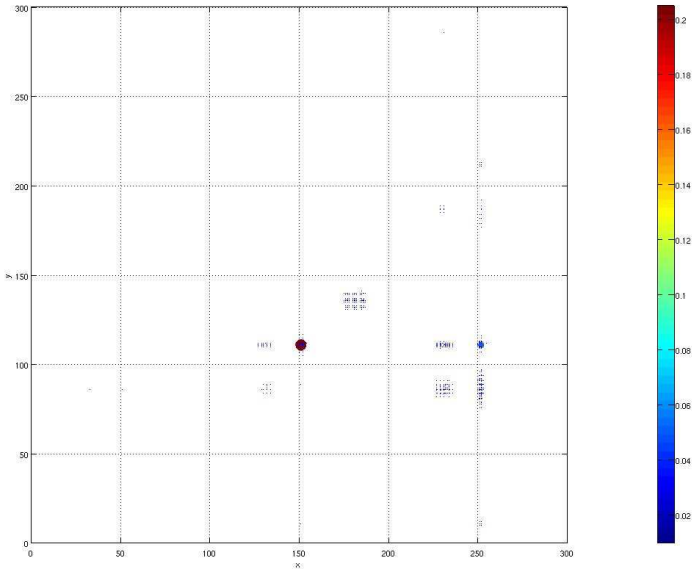

Figure 52. 2-D (x,y) visualization of the autocorrelation peak between the pattern and the movie M_1.

We see in the Figure 52 the shift of the pattern in M_1 in space, and in the Figure 51 that the Phase-Only filter locates perfectly the shift in time, showing us that now the autocorrelation peak is not on at zero lag but rather at lag 20.

This is a very important novelty in the study of matched filters applied to Spatio-temporal movies. The Phase-Only filter is able to find an object in a movie, what means locate the shape and its movement in it.

4.3.5 Fifth example: two patterns shifted in time in a movie with four objects

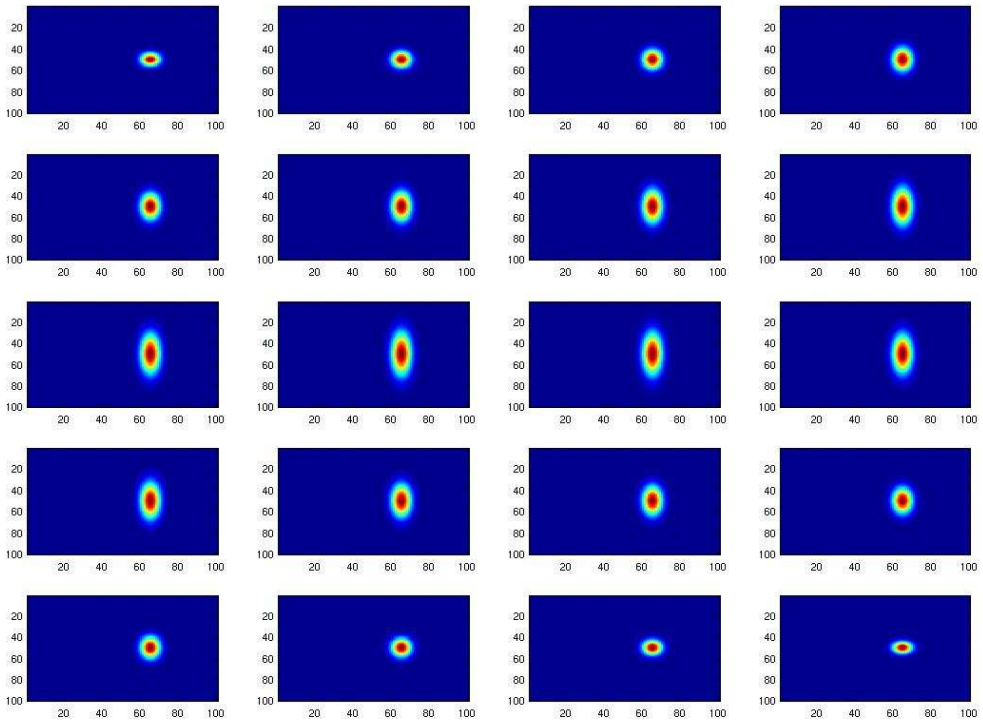

Figure 53. Pattern to recognize

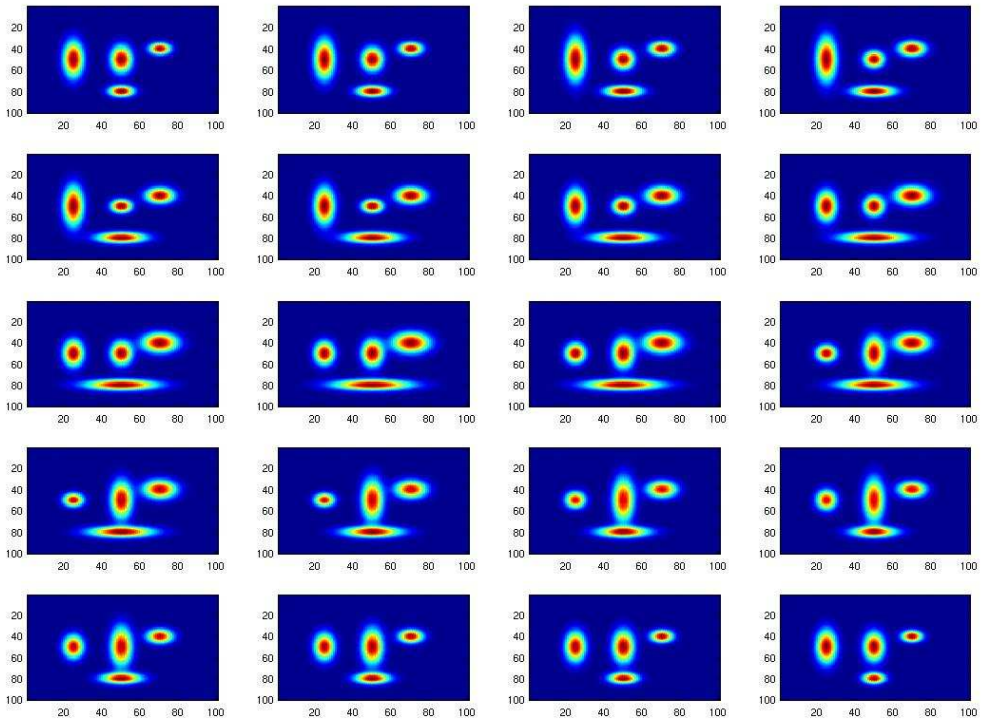

Figure 54. Movie M_1 where the filter has to find the pattern

This is the last example of this chapter and the example that shows all the properties of the Phase-Only filter in a more complete way.. This example is a small example, where we just have four objects in M_1 to recognize, and with a limited number of frames, in this example 59 frames.

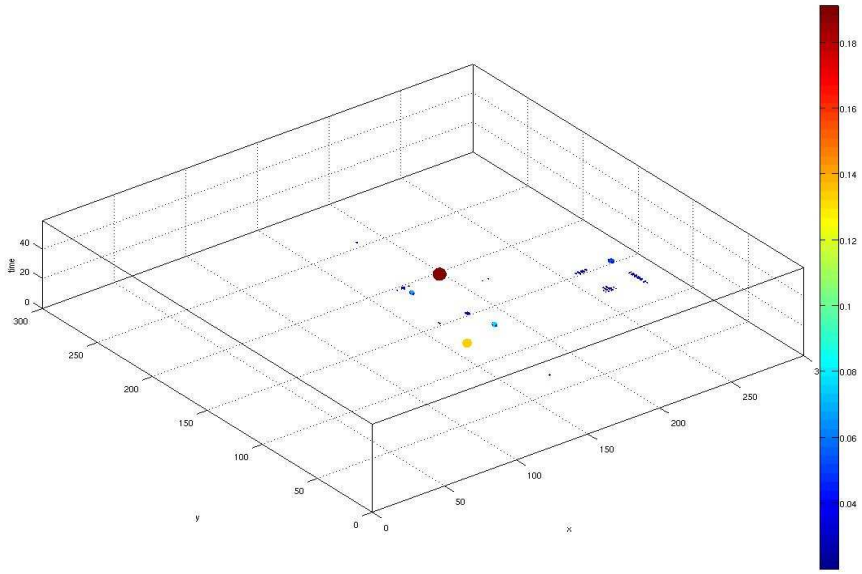

Figure 55. 3-D visualization of the output of the Phase-Only filter

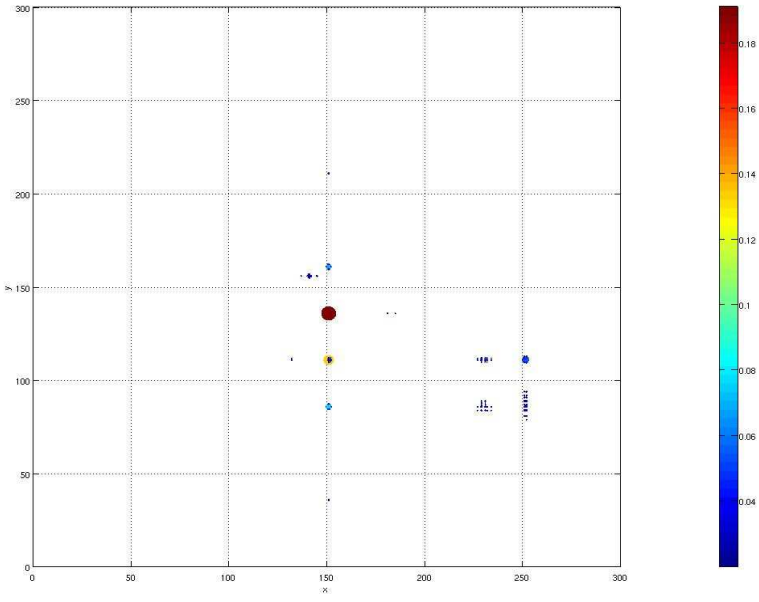

Figure 56. Location of the pattern in M_1 in a space visualization

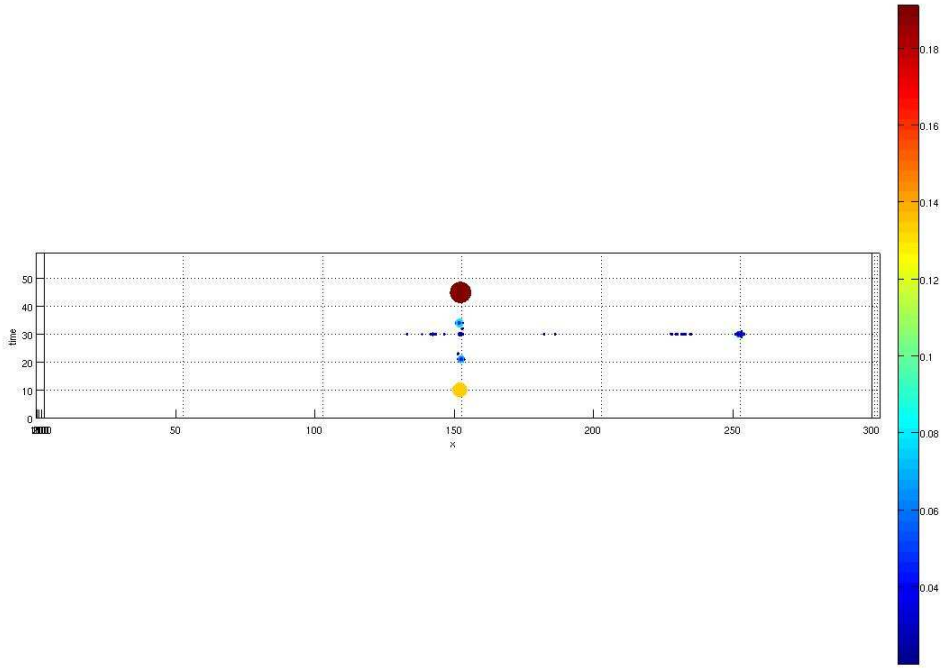

Figure 57. Location of the pattern in M_1 in a temporal visualization

We can see in the output the presence of two big peaks; the larger one has an amplitude around 0.18 and the smaller an amplitude of 0.13, and then we see more peaks due to the cross-correlation peaks between the pattern and the rest of objects in M_1.

These two peak peaks show us that the possibility that the pattern is located twice in the movie M_1 is very high, and we can also see where the pattern is placed in the movie M_1. We see in the Figure 56 the shift in space of the pattern as well, as, in the figure 57 where we can see the shift in time of the pattern.

The output tells us that there is an object in M_1 very similar to the pattern which starts 20 frames later than the pattern and another similar object that starts 15 frames before the pattern.

To summarize, I have explained and shown in this chapter the use of the Phase-Only filter to recognize patterns that have any kind of movement in these simple examples.

5. NEUROIMAGING

5.1 Introduction

Brain mapping refers to a set of neuroscience techniques predicated on the mapping of (biological) quantities or properties onto spatial representations of the (human or non-human) brain. All neuroimaging can be considered part of brain mapping. Brain mapping can be conceived as a more general form of neuroimaging, producing brain images supplemented by the result of additional (imaging or non-imaging) data processing or analysis, such as maps projecting (measures of) behavior onto brain regions.

Brain Mapping techniques are constantly evolving, and rely on the development and refinement of image acquisition, representation, analysis, visualization and interpretation techniques. Functional and structural neuroimaging are at the core of the mapping aspect of Brain Mapping.

The idea of localization of function within the brain has only been accepted for the last century and a half. In the early 19th century Gall and Spurzheim, were ostracized by the scientific community for their so-called science of phrenology [32]. They suggested that there were twenty-seven separate organs in the brain, governing various moral, sexual and intellectual traits. The importance of each to the individual was determined by feeling the bumps on their skull. The science behind this may have been flawed, but it first introduced the idea of functional localization within the brain, which was subsequently developed from the mid 1800's onwards by clinicians such as Jackson [33] and Broca. Most of the information available on the human brain came from subjects who had sustained major head wounds, or who suffered from various mental disorders [35]. By determining the extent of brain damage, and the nature of the loss of function, it was possible to infer which regions of the brain were responsible for which function.

Patients with severe neurological disorders were sometimes treated by removing regions of their brain. For example, an effective treatment for a severe form of epilepsy involved severing the corpus callosum, the bundle of nerve fibres which connect left and right cerebral hemispheres. Following the surgery patients were tested, using stimuli presented only to the left hemisphere or to the right hemisphere [36]. If the object was in the right visual field, therefore stimulating the left hemisphere, then the subject was able to say what they saw. However if the object was in the left visual field, stimulating the right hemisphere, then the subject could not say what they saw but they could select an appropriate object to associate with that image. This suggested that only the left hemisphere was capable of speech.

With the development of the imaging techniques of computerized tomography (CT) and magnetic resonance imaging (MRI) it was possible to be more specific as to the location of

damage in brain injured patients. The measurement of the electrical signals on the scalp, arising either from oscillatory background brain activity or from the synchronous firing of the neurons in response to a stimulus, known as electroencephalography (EEG), opened up new possibilities in studying brain function in normal subjects. However it was the advent of the functional imaging modalities of positron emission tomography (PET), single photon emission computed tomography (SPECT), functional magnetic resonance imaging (fMRI), and magnetoencephalography (MEG) that collectively have led to a new era in the study of brain function.

In this chapter the mechanisms of the techniques mentioned above are briefly outlined, together with an assessment of their strengths and weaknesses.

5.1.1 SPECT and PET

The imaging modalities of single photon emission computed tomography (SPECT) and positron emission tomography (PET) both involve the use of radioactive nuclides either from natural or synthetic sources. Their strength is in the fact that, since the radioactivity is introduced, they can be used in tracer studies where a radiopharmaceutical is selectively absorbed in a region of the brain.

The main aim of SPECT as used in brain imaging is to measure the regional cerebral blood flow (rCBF). The earliest experiments to measure cerebral blood flow were performed in 1948 by Kety and Schmidt [37]. They used nitrous oxide as an indicator in the blood, measuring the differences between the arterial input and venous outflow, from which the cellular uptake could be determined. This could only be used to measure the global cerebral blood flow, and so in 1963 Glass and Harper [38], building on the work of Ingvar and Lassen [39], used the radioisotope Xe-133, which emits gamma rays, to measure the regional cerebral blood flow. The development of computed tomography in the 1970's allowed mapping of the distribution of the radioisotopes in the brain, and led to the technique now called SPECT [40].

The radiotracer (or radiopharmaceutical) used in SPECT emits gamma rays. There are a range of radiotracers that can be used, depending on what is to be measured. For example I-123-3-quinuclidinyl 4-isodobenzilate is a neurotransmitter agonist which can be used for imaging receptors. For rCBF measurements Xe-133 can be introduced into the blood stream by inhalation.

Detection is carried out using a gamma camera - a scintillation detector consisting of a collimator, a NaI crystal, and a set of photomultiplier tubes as shown in Figure 58.

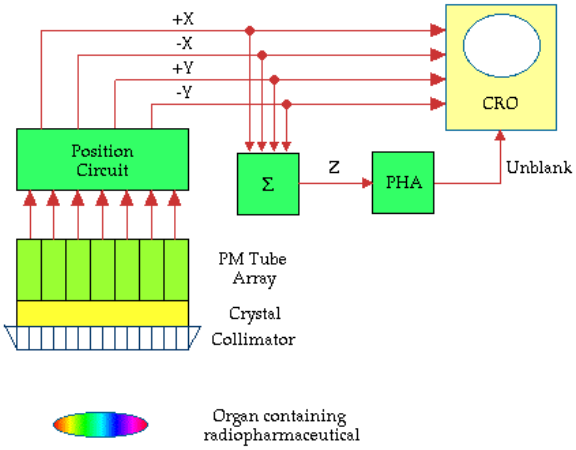

Figure 58. Schematic diagram of a gamma camera used in SPECT imaging. Image obtained from http://en.wikibooks.org/wiki/Basic_Physics_of_Nuclear_Medicine/Print_version

By rotating the gamma camera around the head, a three dimensional image of the distribution of the radiotracer can be obtained by employing appropriate filtered backprojection algorithms. The radioisotopes used in SPECT have relatively long half lives (a few hours to a few days) making them easy to produce and relatively cheap. This represents the major advantage of SPECT as a brain imaging technique, since it is significantly cheaper than either PET or fMRI. However it lacks good spatial or temporal resolution, and there are safety aspects concerning the administration of radioisotopes to the subject, especially for serial studies.

Positron emission tomography [41] has two major advantages over SPECT, namely better spatial resolution and greater sensitivity. This comes from using positron emitters such as O-15 and F-18 as the radionuclide. When such nuclei decay they emit a positron, that is a particle with the same rest mass as an electron but with charge +1. Once the positron is emitted it travels a short distance before colliding with an electron. The annihilation of the two particles creates two photons each with energy 511 keV. In order to conserve momentum, the two photons are emitted at virtually 180 degrees to each other, and it is these photons that are detected in a ring of scintillators and photomultiplier tubes surrounding the head (Figure 59).

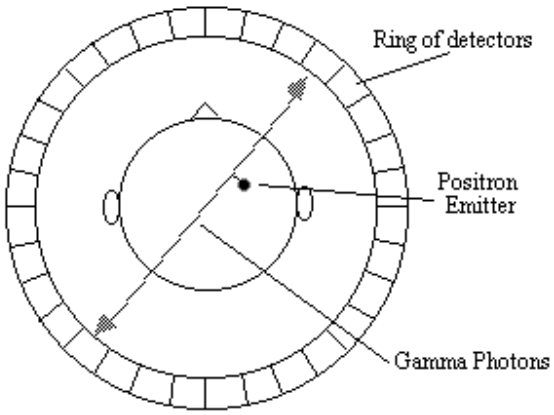

Figure 59. Schematic diagram of a PET scanner. A positron is emitted from a radioisotope in the brain. The positron annihilates with an electron, producing two photons emitted at 180 degrees to each other

Opposite pairs of detectors are linked so as to register only temporally coincident photons, thus defining a set of coincidence lines. Reconstruction of these lines by filtered back projection gives an image of the source of the annihilation. Since the detectors only record the site of the annihilation, resolution in a PET scanner is limited by the distance travelled by the positron through the tissue before it meets an electron. This fundamentally restricts the resolution of the scanner to 2 - 3 mm at best.

The positron emitters used in PET have short half lives, of the order of 2 - 100 minutes. This means that the isotopes must usually be made at the site of the scanner, using an expensive cyclotron. However, this short half life means that dynamic studies of brain function can be carried out using the technique.

Functional imaging studies using PET first appeared in 1984 with a study using C15O2. Usually two cognitive states are imaged, one active and one resting, and by subtracting these two states a map of the regions of the brain responsible for that task is made. PET is widely used as a tool for cognitive function, and much of the literature on brain function published in the last 10 years has used the technique. Positron emitting neurotransmitters, such as F-18 labelled DOPA, mean that dopamine function can be followed in patients with Parkinson's disease. The main drawback of PET is its use of radioisotopes, and its very high cost; however its neurotransmitter mapping ability means that it will retain a role even in the face of the less invasive, and more available fMRI, described below.

5.1.2 EEG and MEG

Measuring the electrical signals from the brain has been carried out for many decades [42], but it is only more recently that attempts have been made to map electrical and magnetic

activity. The electroencephalogram (EEG) is recorded using electrodes, usually silver coated with silver chloride, attached to the scalp and kept in good electrical contact using conductive electrode jelly. One or more active sites may be monitored relative to a reference electrode placed on an area of low response activity such as the earlobe.

The signals are of the order of 50 microvolts, and so care must be taken to reduce interference from external sources, eye movement and muscle activity. Several characteristic frequencies are detected in the normal background human EEG. For example, when the subject is relaxed the EEG consists mainly of frequencies in the range 8 to 13 Hz, called alpha waves, but when the subject is more alert the frequencies detected in the signal rise above 13Hz, called beta waves.

Measurements of the EEG during sleep have revealed periods of higher frequency waves, known as rapid eye movement (REM) sleep which has been associated with dreaming.

The EEG can also be measured in response to some regularly repeated stimulus such as the pattern reversal of a projected checkerboard, or more complicated task such as number memorising and recall. The signal from each electrode for an interval of time corresponding to before and during response to the stimulus is recorded and averaged together over a number of trials. The response is characterized by several factors, perhaps most importantly the delay, or latency, of the peak of the signal from the presentation of the stimulus. This is on the order of milliseconds for brain stem responses and 100's of milliseconds for cortical responses. For example a commonly detected response to an oddball stimulus, the P300, has a latency of around 300 ms (hence the name P300). Having found an electrical signal of interest, the magnitude of the peak can be mapped across the scalp giving an idea of the location of the source.

The major limitation of studying brain function using EEG is that the signals measured are recorded on the scalp, which may not represent the activity in the underlying cortex but may be influenced or even dominated by signals from regions remote from the electrode. However since the technique is very cheap and safe, it has many uses and can be involved in studies where the scanning techniques could not, such as continuous monitoring during sleep.

Since the magnetic signals generated by the current resulting from the firing of the neurons do not need to be conducted to the scalp, they are less affected by the electrical properties of the intervening tissue, and thus measuring them may give much greater signal localization than measuring the scalp currents themselves. This is the basis of the much newer technique of magnetoencephalography (MEG).

The first successful measurements of these magnetic fields were made by Cohen in 1972 [43]. The magnitude of the magnetic signals resulting from the electrical firing of the neurons is of the order of 10-13 Tesla, for 1 million synchronously active synapses. Such small signals are

picked up using a superconducting quantum interference device (SQUID) magnetometer (Figure 63).

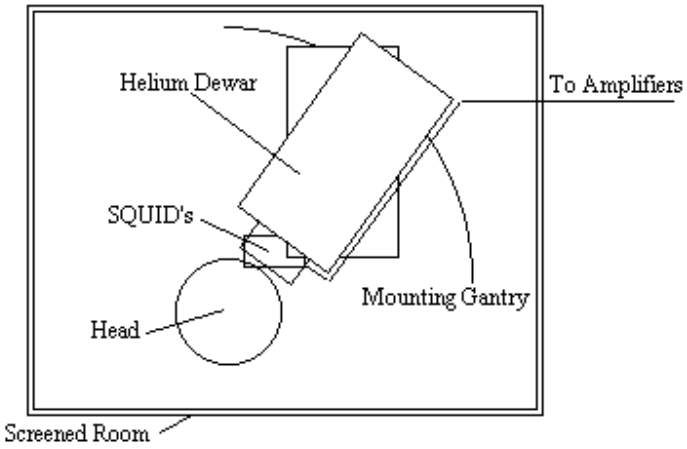

Figure 60. Schematic diagram of a magnetometer for measuring MEG's

Interference from external sources is a major problem with MEG, and the magnetometer must be sited in a magnetically shielded room. Current magnetometers have as many as 120 or more SQUIDS covering the scalp.

MEG experiments are carried out in much the same way as their EEG counterpart. Having identified the peak of interest, the signals from all the detectors are analyzed to obtain a field map. From this map an attempt can be made to ascertain the source of the signal by solving the inverse problem. Since the inverse problem has no unique solution, assumptions need to be made, but providing there are only a few activated sites close to the scalp then relatively accurate localization is possible, giving a resolution of the order of a few millimetres.

MEG has the advantage over EEG that signal localization may be, to a greater extent, possible, and over PET and fMRI in that it has excellent temporal resolution of neuronal events. However MEG is costly and its ability to accurately detect events in deeper brain structures is limited.

5.1.3 Functional MRI and MRS

The purpose of this section is to compare fMRI to the other modalities already mentioned, and also to consider the related, but distinct technique of magnetic resonance spectroscopy (MRS).

During an fMRI experiment, the brain of the subject is scanned repeatedly, usually using the fast imaging technique of echo planar imaging (EPI). The subject is required to carry out some task consisting of periods of activity and periods of rest, as with the other stimulus-

response imaging paradigms described above. During the activity, the MR signal from the region of the brain involved in the task normally decreases due to the flow of oxygenated blood into that region, which reduces the effective concentration of deoxygenated hemoglobin, the source of the so-called Blood Oxygen Level Dependent (BOLD) MR signal. Signal processing is then used to reveal these regions.

The main advantage of MRI over its closest counterpart, PET, is that it requires no contrast agent to be administered, and so is considerably safer. In addition, high quality anatomical images can be obtained in the same session as the functional studies, giving greater confidence, i.e. greater spatial resolution, as to the source of the activation. However, the function that is mapped is based on blood flow, and it is not yet possible to directly map neuroreceptors as PET can, nor the underlying neuronal activity as MEG and EEG can. The technique is relatively expensive, although comparable with PET; however since many hospitals now have an MRI scanner the availability of the technique is more widespread.

fMRI is limited to activation studies, which it performs with good spatial resolution. If the resolution is reduced somewhat then it is also possible to carry out functional magnetic resonance spectroscopy (fMRS), which is chemically specific, and can follow many metabolic processes. Since fMRS can give the rate of glucose utilization, it provides useful additional information to the blood flow and oxygenation measurements from fMRI in the study of brain metabolism.

5.1.4 Comparison of the Functional Brain Imaging Modalities

The brain imaging techniques that have been presented in this chapter all measure slightly different properties of the brain as it carries out cognitive tasks. Because of this the techniques should be seen as complementary rather than competitive. All of them have the potential to reveal much about the function of the brain and they will no doubt develop increasing clinical usefulness as more about the underlying mechanisms of each are understood, and the hardware becomes more available. A summary of the strengths and weaknesses of the techniques is presented in the figure 61.

Technique	Resolution	Advantages	Disadvantages
SPECT	10 mm	Low cost Available	Invasive Limited resolution
PET	5 mm	Sensitive Good resolution Metabolic studies Receptor mapping	Invasive Very expensive

EEG	poor	Very low cost Sleep and operation monitoring	Not an imaging technique
MEG	5 mm	High temporal resolution	Very Expensive Limited resolution for deep structures
fMRI	3 mm	Excellent resolution Non-invasive	Expensive Limited to activation studies
MRS	low	Non-invasive metabolic studies	Expensive Low resolution

Figure 61. Table comparison of modalities for studying brain function

5.2 Magnetoencephalography (MEG)

Since all the movies I have used in all the tests by using Phase-Only filter came from this technique, I think it should be useful to study in depth this imaging technique.

5.2.1 The basis of the MEG signal

Synchronized neuronal currents induce very weak magnetic fields that can be measured as MEG. However, the magnetic field of the brain is considerably smaller, at 10 fT (femtotesla) for cortical activity and 10^3 fT for the human alpha rhythm, than the ambient magnetic noise in an urban environment, which is on the order of 10^8 fT. Two essential problems of biomagnetism thus arise: weakness of the signal and strength of the competing environmental noise. The development of extremely sensitive measurement devices, SQUIDs, facilitates analysis of the brain's magnetic field and confronts the aforementioned problems.

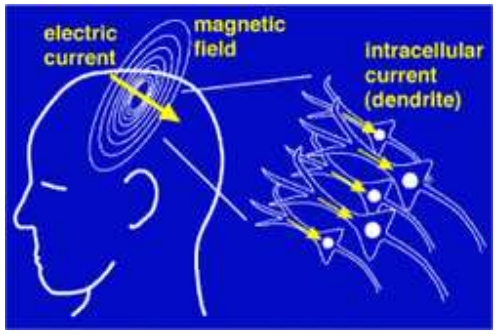

Figure 62. Origin of the brain's magnetic fiels. Image obtained from http://www.answers.com/topic/magnetoencephalography

The MEG (and EEG) signals derive from the net effect of ionic currents flowing in the dendrites of neurons during synaptic transmission. In accordance with Maxwell's equations, any electrical current will produce an orthogonally oriented magnetic field. It is this field which is measured with MEG. The net currents can be thought of as current dipoles which are current sources defined to have an associated position, orientation, and magnitude, but no spatial extent. According to the right-hand rule, a current dipole gives rise to a magnetic field that flows around the axis of its vector component.

In order to generate a signal that is detectable, approximately 50,000 active neurons are needed [44]. Since current dipoles must have similar orientations to generate magnetic fields that reinforce each other, it is often the layer of pyramidal cells in the cortex, which are generally perpendicular to its surface, that give rise to measurable magnetic fields. Furthermore, it is often bundles of these neurons located in the sulci of the cortex with orientations parallel to the surface of the head that project measurable portions of their magnetic fields outside of the head.

Researchers are experimenting with various signal processing methods to try to find methods that will allow deep brain (i.e., non-cortical) signal to be detected, but as of yet there is no clinically useful method available.

It is worth noting that action potentials do not usually produce an observable field, mainly because the currents associated with action potentials flow in opposite directions and the magnetic fields cancel out. However, action potential magnetic fields have been measured from peripheral nerves.

5.2.2 Source localization

Inverse problem

In order to determine the location of the activity within the brain, advanced signal processing techniques is used to determine from the magnetic fields measured outside the head

an estimate of the location of that activity's source. This is referred to as the inverse problem. (The forward problem is the situation where we know where the source(s) is (are) and we are estimating the field at a given distance from the source(s).) The primary technical difficulty is that the inverse problem does not have a unique solution (i.e., there are infinite possible "correct" answers), and the problem of finding the best solution is itself the subject of intensive research. [51],[52],[53] Adequate solutions can be derived using models involving prior knowledge of brain activity.

The source models can be either overdetermined or underdetermined. An overdetermined model may consist of a few point-like sources, whose locations are then estimated from the data. The underdetermined models may be used in cases where many different distributed areas are activated; there are several possible current distributions explaining the measurement results, but the most likely is selected. It is believed by some researchers in the field that more complex source models increase the quality of a solution. However this may decrease the robustness of the estimation and increasing the effects of forward model errors.

Many experiments use simple models, reducing possible sources of error and decreasing the computation time to find a solution. Localization algorithms make use of the given source and head models to find a likely location for an underlying focal field generator. An alternative methodology involves performing independent component analysis first in order to segregate sources without using a forward model, and then localizing the separated sources individually [54]. This method has been shown to improve the signal-to-noise ratio of the data by correctly separating non-neuronal noise sources from neuronal sources, and has shown promise in segregating focal neuronal sources.

Localization algorithms using overdetermined models operate by successive refinement. The system is initialized with a first guess. Then a loop is entered, in which a forward model is used to generate the magnetic field that would result from the current guess, and the guess then adjusted to reduce the difference between this estimated field and the measured field. This process is iterated until convergence.

Another approach is to ignore the ill-posed inverse problem and estimate the current at a fixed location. This method makes use of beamforming techniques. One such approach is the second-order technique known as Synthetic Aperture Magnetometry (SAM), which uses a linear weighting of the sensor channels to focus the array on a given target location. Whereas SAM uses the temporal domain, and a non linear fitting of the dipole, other approaches use the Fourier transform of the signals and a linear dipole fit. The so-approximated sources can be used to compute to estimate the synchronisation of large brain networks [45].

Magnetic source imaging

The estimated source locations can be combined with magnetic resonance imaging (MRI) images to create magnetic source images (MSI). The two sets of data are combined by measuring the location of a common set of fiducial points marked during MRI with lipid markers and marked during MEG with electrified coils of wire that give off magnetic fields. The locations of the fiducial points in each data set are then used to define a common coordinate system so that superimposing ("coregistering") the functional MEG data onto the structural MRI data is possible.

A criticism of the use of this technique in clinical practice is that it produces colored areas with definite boundaries superimposed upon an MRI scan: the untrained viewer may not realize that the colors do not represent a physiological certainty, because of the relatively low spatial resolution of MEG, but rather a probability cloud derived from statistical processes. However, when the magnetic source image corroborates other data, it can be of clinical utility.

Dipole model source localization

A widely accepted source-modeling technique for MEG involves calculating a set of Equivalent Current Dipoles (ECDs), which assumes the underlying neuronal sources are focal. This dipole fitting procedure is non-linear and over-determined, as the number of unknown dipole parameters is less than the number of MEG measurements [46]. Automated multiple dipole model algorithms such as Multiple Signal Classification (Multiple Signal Classification) and MSST (Multistart spatial and temporal) modeling are applied to analysis of MEG responses. The use of dipole models to characterize neuronal responses has three main drawbacks: (1) significant difficulties in localizing extended sources with ECDs, (2) problems with accurately estimating the total number of dipoles in advance, and (3) the sensitivity of dipole location, especially with respect to depth in the brain.

5.3 Evoked potentials

In neurophysiology, an **evoked potential** (or "evoked response") is an electrical potential recorded from a human or animal following presentation of a stimulus, as distinct from spontaneous potentials as detected by electroencephalograms or electromyograms. Evoked potential amplitudes tend to be low, ranging from less than a microvolt to several microvolts, compared to tens of microvolts for EEG, millivolts for EMG, and often close to a volt for EKG. To resolve these low-amplitude potentials against the background of ongoing EEG, EKG, EMG and other biological signals and ambient noise, signal averaging is usually required. The signal is

time-locked to the stimulus and most of the noise occurs randomly, allowing the noise to be averaged out with averaging of repeated responses [47]

Signals can be recorded from cerebral cortex, brain stem, spinal cord and peripheral nerves. Usually the term "evoked potential" is reserved for responses involving either recording from, or stimulation of, central nervous system structures. Thus evoked CMAP (compound motor action potentials) or SNAP (sensory nerve action potentials) as used in NCV (nerve conduction studies) are generally not thought of as evoked potentials, though they do meet the above definition.

5.3.1 Evoked Potentials Procedure

Electrodes need to be attached to various points on the scalp. The head is measured using a standardized EEG measurement technique to determine the right spots (each spot corresponding to a type of EP that will be measured - e.g. the two locations on the back of the skull for the visual cortex, etc.), which are marked with a writing implement akin to a very thick pencil. Each of these spots is rubbed with an oil-removing scrub to get rid of the skin oil, and then an electrode dipped in a liberal quantity of conductive gel (approximately the consistency of soft butter) is applied and pressed to each spot, and affixed with a strip of adhesive tape.

For visual evoked potential (VEP), you are placed in front of a computer screen, which shows a pattern of white and black squares like a chessboard, and a red dot in the middle that you are supposed to focus your eyes on with minimal movement. The procedure is done one eye at a time, with the eye that is not being tested blocked off with an eye patch. During the actual procedure, these squares alternate (white ones become black, black ones become white) at a rate of several times a second, which produces responses in the visual cortex, which is picked up by your skull electrodes. Since the computer controls the exact timing of the changes of the square colors, and receives the exact timing of the electric response in the corresponding electrodes, it is able to determine precisely the amount of time it takes for the visual stimulus to reach the visual cortex. For the somatosensory evoked potentials (SEP), additional electrodes are applied, in the same manner as described earlier.

For the upper SEP (arms), two stimulus electrodes are attached on the inside wrist, closer to the thumb. These electrodes will receive timed electric pulses that will produce an involuntary twitch of the thumb. An additional sensor electrode is applied on the back of your shoulder, close to the attachment point of the clavicle. Similar to the VEP, the computer times the electric pulses (which come at a rate of several times a second) and gets the responses from the appropriate skull electrode, thus determining the exact time it takes for the stimulus to reach the intermediate point on your shoulder, and then the brain. The same is then repeated on the other arm. For the lower SEP (legs), two stimulus electrodes are attached to the inside of your ankle, in such a way

as to produce an involuntary twitch of the big toe. Additional sensor electrodes are placed at the back of the knee (closer to the outside), on the spine of the lower back, and on the spine of the upper back. Electric pulses are then sent at a rate of several times a second, and the responses are recorded in the same manner as above.

For the brain auditory evoked potential (BAEP), the stimulus is supplied through headphones. The ear that is being tested receives a clicking sound, at a rate of several times a second, while the other ear receives static. Additional sensor electrodes are placed on the backs of your earlobes. The timing is determined as above.

5.3.2 Evoked potential signal determination

There are many things going on at once in the brain, so it is difficult to determine when the evoked potential from a particular stimulus arrives from just one stimulus. The technique used to amplify the signal is called signal averaging. The stimulus in each evoked potential test is applied many times (anywhere from tens to thousands of times, depending on the nature of the stimulus and the source of the signal of interest within the brain), and everything else besides the evoked potential is assumed to not be correlated to the stimulus, whereas the potential that is evoked by the stimulus is assumed to always occur at the same time relative to the stimulus. This allows the computer to pick out and amplify the one consistent peak or series of peaks that are caused by the applied stimulus by averaging across stimuli.

As an aside, in the work presented here zero-padding was applied in space but not in time, because due to the periodicity of the stimulus, the signal can be treated as periodic in time. Thus the circular convolution in time doesn't affect the result because the time is wrapped.

5.3.3 Brainstem Auditory Evoked Responses (BAER or ABR)

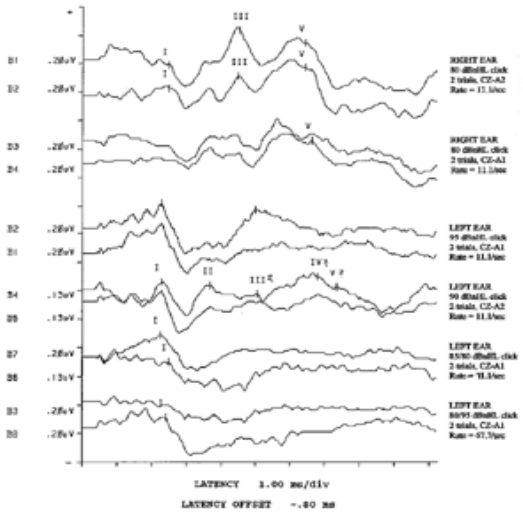

Figure 62. Brainstem auditory evoked response. Right ear responses are shown on top and left ear on the bottom half.

Brainstem auditory evoked responses (BAER), also known as auditory brainstem evoked response (ABR), test both the ear and the brain. They measure the timing of electrical waves from the brainstem in response to clicks or tone bursts in the ear. Computer averaging over time to filters background noise to generate an averaged response of the auditory pathway to an auditory stimulus three waves (1, 3 and 5) are plotted for each ear.

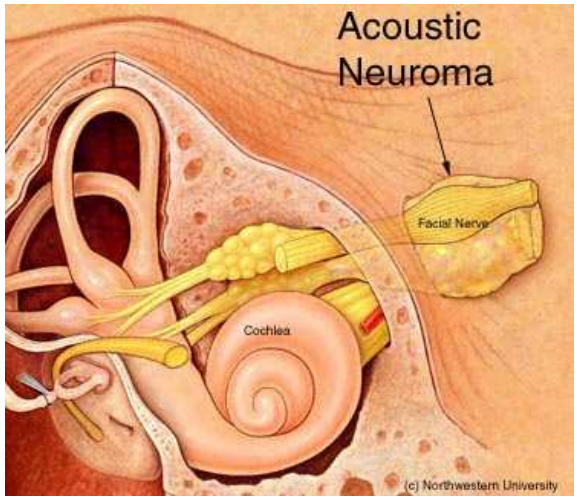

Figure 63. Ear

The main indication for BAER is when an acoustic neuroma is suspected. This generally comes about when there is an asymmetrical sensorineural hearing loss.

- BAER testing may also be useful in situations where an auditory neuropathy is suspected. In this case, it may be combined with otoacoustic emission testing.
- BAER's are commonly abnormal in brainstem disorders such as multiple sclerosis, brainstem stroke, or brainstem degenerative disorders. These are much less common than inner ear disorders, but also are intrinsically much more dangerous.
- BAER testing requires reasonable high-frequency hearing. This means that it is often not worth doing in persons over the age of 70. It is generally recommended that either an audiogram or at least a screening test for high frequency hearing be done prior to BAER testing.

I focused on this evoked response because in all the tests made in the next chapter, the movies I used as input of the Phase-Only filter come from this specific test. All the movies are made by using MEG and reproduce the response of an auditory evoked response test.

5.4 Cortical Surface transformations

The surface of the human cerebral cortex is a highly folded sheet with the majority of its surface area buried within folds. As such, it is a difficult domain for computational as well as visualization purposes. Several people from the ***nmr center*** (Nuclear Magnetic Resonance Center, Massachusetts General Hosp/Harvard Medical School) have therefore designed a set of procedures for modifying the representation of the cortical surface to (i) inflate it so that activity buried inside sulci may be visualized, (ii) cut and flatten an entire hemisphere, and (iii) transform a hemisphere into a simple parameterizable surface such as a sphere for the purpose of establishing a surface-based coordinate system.

Currently, the most widely used method of analyzing functional brain imaging data is to project the functional data from a sequence of slices onto a standardized anatomical 3-D space.

In order to facilitate the use of surface-based techniques for both display and analysis of structural and functional properties of the cerebral cortex, our collaborators have developed a unified procedure which begins with a previously reconstructed cortex (Dale and Sereno, 1993; Dale et al., 1998) and modifies it in order to achieve three separate but related goals:

(1) The ‘‘inflation’’ of the cortical surface so that activity occurring inside sulci may be easily visualized.

(2) The flattening of an entire hemisphere so that the activity across the hemisphere may be seen from a single view, and so that computational procedures which are not tractable on arbitrary manifolds may be employed in the analysis of the cerebral cortex.

(3) The ‘‘morphing’’ of a hemisphere into a surface, which maintains the topological structure of the original surface, but has a natural (i.e., closed-form) coordinate system.

All this can be studied in depth in the work *“Cortical Surface-Based Analysis: II: Inflation, Flattening, and a Surface-Based Coordinate System”* by Bruce Fischl, Martin I. Sereno, and Anders M. Dale [55] but since this work employs movies where the brain appears as a sphere we include a little bit more information about the transformation of surfaces of the brain. We believe that presenting a couple of examples of what is a flattered brain or a spherical brain could be useful to understand what is happening in the movies presented in the next chapter.

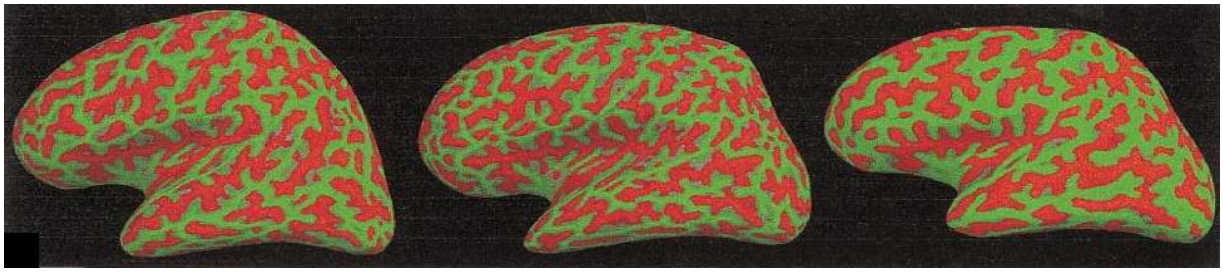

Figure 64. Inflated representations of the three cortical surfaces (sulci are red and green are light) [55].

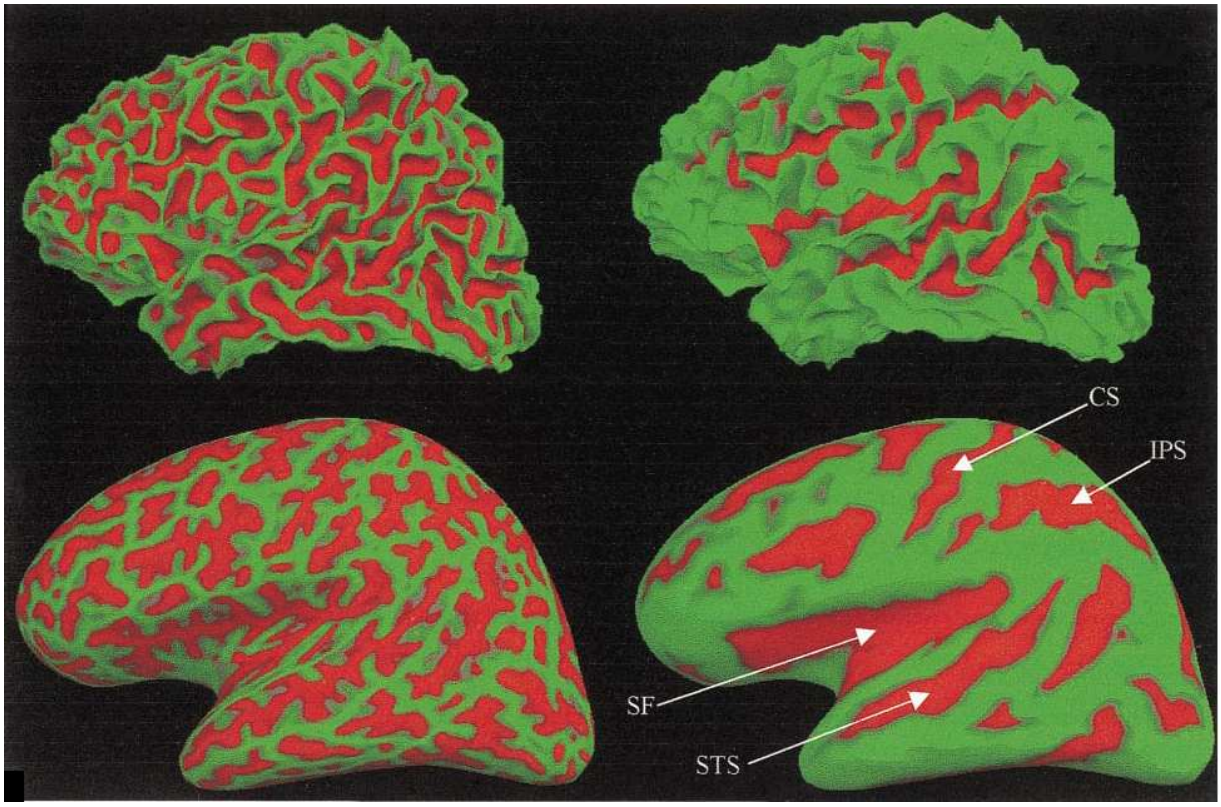

Figure 65. Mean curvature (left) and average convexity (right) painted onto folded (top) and inflated (bottom) representations of an individual subject's cortical surface.[55]

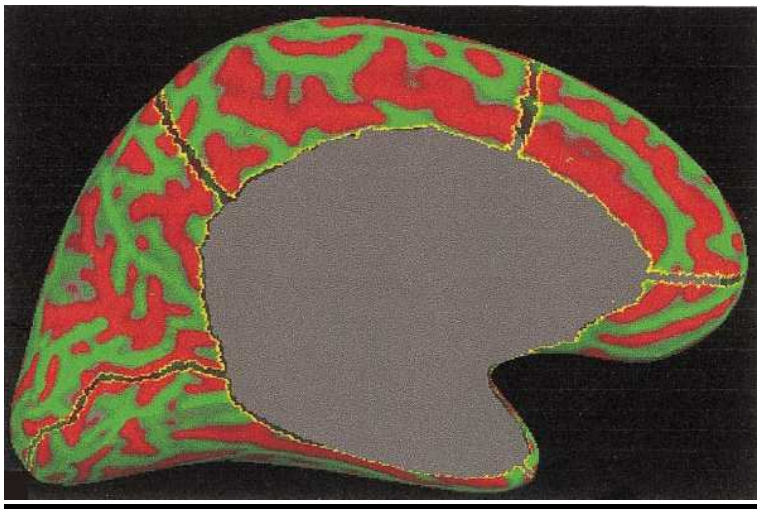

Figure 66. Medial view of an inflated surface after the introduction of cuts. Yellow regions indicate the borders of the cut surface.[55]

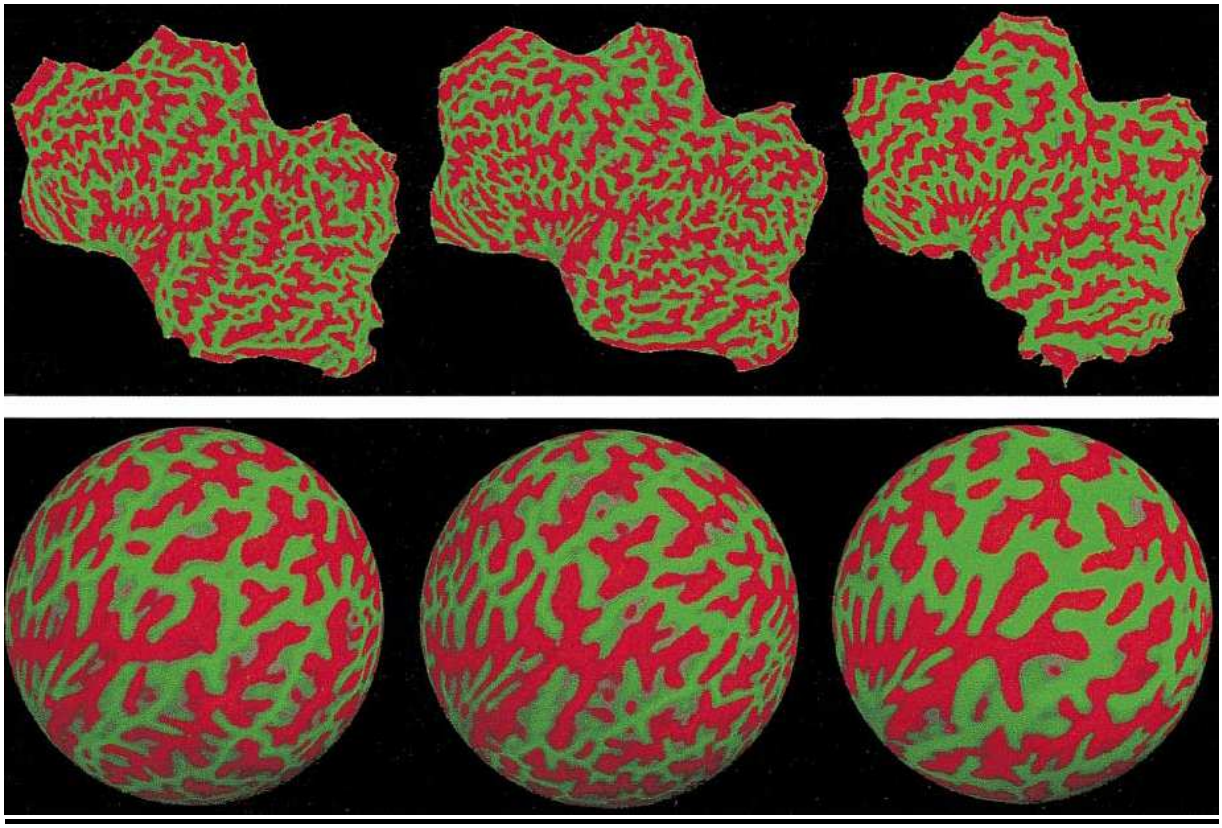

Figure 67. Three flattened left hemispheres (sulci are red and green are light) and lateral view of three left hemispheres after spherical transformation.[55]

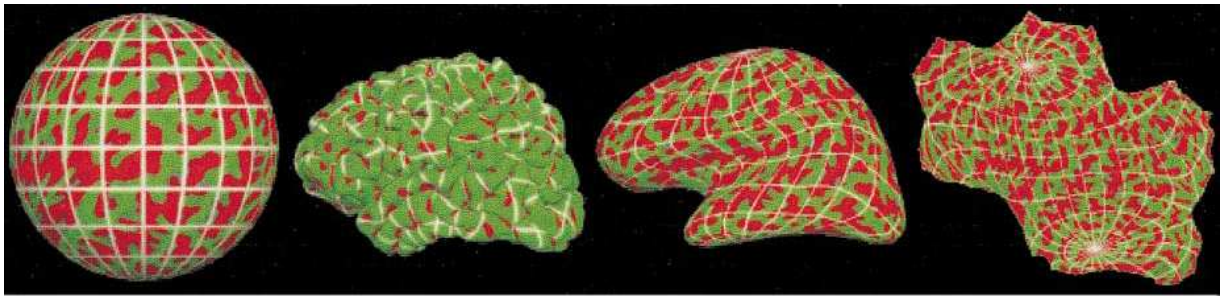

Figure 68. Spherical coordinate system painted onto a variety of surface representations.[55]

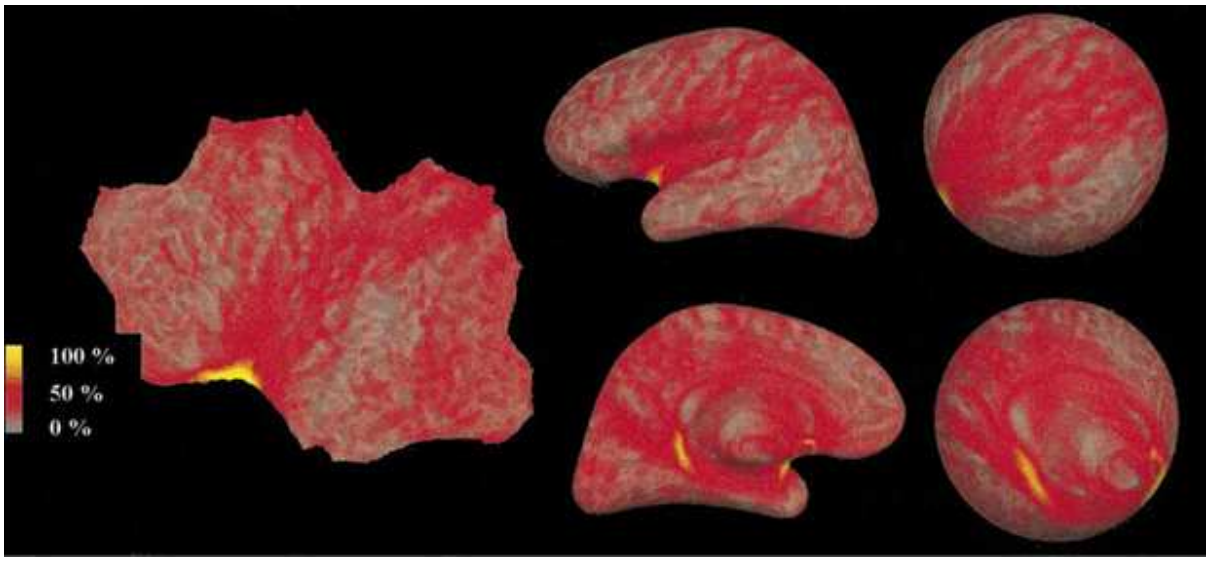

Figure 69. Spatial distribution of metric distortion introduced by the spherical transformation, painted onto flattened (left), inflated (center), and spherical (right) representations of the same surface. Lateral and medial views are shown in the top and bottom rows, respectively.[55]

The authors (Bruce Fischl, Martin I. Sereno, and Anders M. Dale), presented in [55] a unified set of procedures for transforming a previously reconstructed cortical surface. These transformations achieve two primary goals. First, they facilitate visualization of cortical activation patterns, including the detailed topographic organization of cortical areas, as well as distributed activity occurring across an entire hemisphere. In addition, such transformations enable two-dimensional analysis techniques to be applied to the functional and structural properties of the cortical surface.

The mapping procedures I have presented have the advantage of being optimal with respect to a well-defined energy functional that measures the amount of metric distortion and degree of folding of the transformed surface. In conjunction with segmentation methods, these procedures allow the routine use of surface-based visualization and analysis of functional and structural properties of the human cortex.

6. EXPERIMENTS WITH REAL DATA

6.1. Introduction

The aim of this project has always been the implementation of a filter which was able to automatically compare two spatio-temporal neuroimaging movies in order to quantify the grade of similarity between them. We will examine the performance of the Phase-Only filter in a setting in which we have *a priori* knowledge of the similarity between all the movies, so that we can judge whether the Phase-Only filter reports similarity in the same way that it is perceived visually. In order to quantify the POMF performance, we first define four metrics in order to quantify the resemblance between movies.

6.1.1 Amplitude of the main peak

The amplitude of the main peak is one of the four factors we are going to study in the output of the phase only filter. The main peak amplitude depends directly on the degree of similarity between inputs.

The ideal output as we have seen for the autocorrelation is a peak with amplitude equal to 1. In the examples reported above, the difference between good match and poor match was on the order of a difference of 0.8. However when we are dealing with measured neuroimaging movies, that difference decreases a lot, so that 0.01 becomes a reasonable metric in terms of amplitude between good match and poor match.

6.1.2 Relation of the main to the secondary peak

This relation is another of the four factors we will study in the output of the Phase-Only filter. We are going to look for the peaks in the output to try to understand and analyze what happens with the inputs. When we are working with real images of the brain, what we only want is a peak. Since every stimulus has a different region of activation in the brain, the presence of two high peaks would show us that the activation in the inputs comes from a different stimulus and therefore the region of the brain that show us the activation is different.

Since we are trying to compare whole movies the presence of two big peaks in different location will drive us to a wrong conclusion, because the movies don't come from the same stimulus, as we will illustrate in the next example .

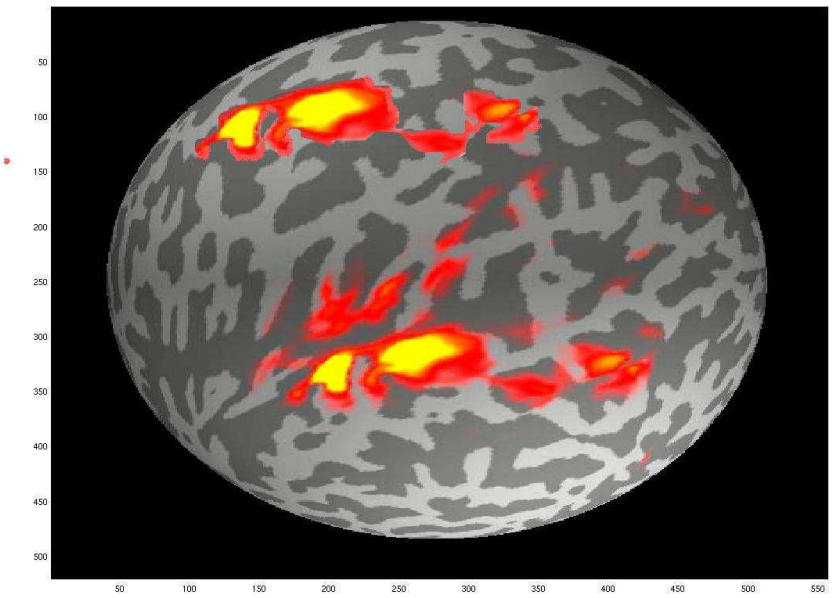

Figure 70. Frame of a real movie M_1

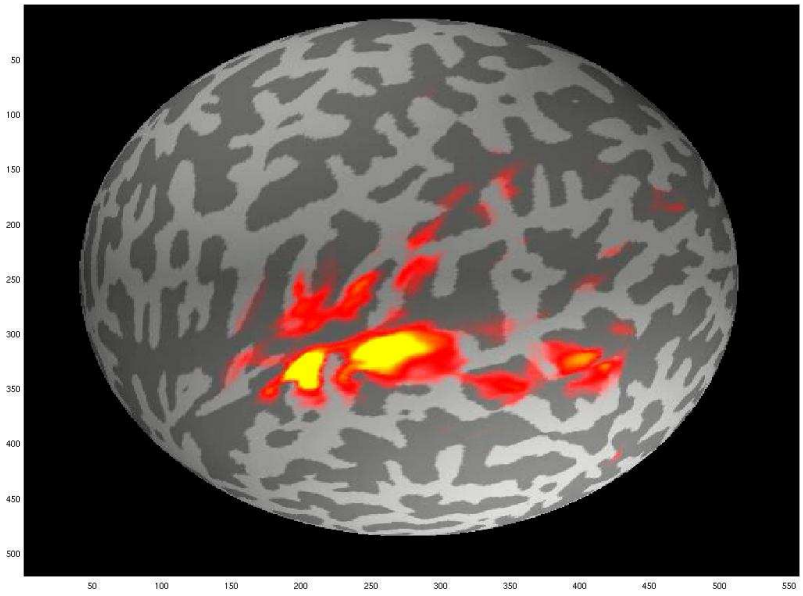

Figure 71. Frame of a real movie M_2

The output of the Phase-Only filter when the inputs are M_1 and M_2 would show us two high autocorrelation peaks due to the presence of a common shape and energy in the two inputs. We would obtain a peak at zero shift and another peak that would tell us the shift in space of these two similar shapes. This is totally wrong, because the movies are TOTALLY different, due to the presence of this shape in that part of the brain.

The relation of the main to the secondary peak (which we will refer of as main—secondary peak) is calculated as a simple division between the value of the maximum amplitude and the value of the second maximum peak in the frame where the main peak is located in the output of the phase-only filter. The best ratio possible would be infinite, if we just have a main peak, and no noise in the output, and the worst possible scenario is a relation equal to 1, that would mean that there two equal peaks in the same frame, as we will see later this is possible when we just obtain noise.

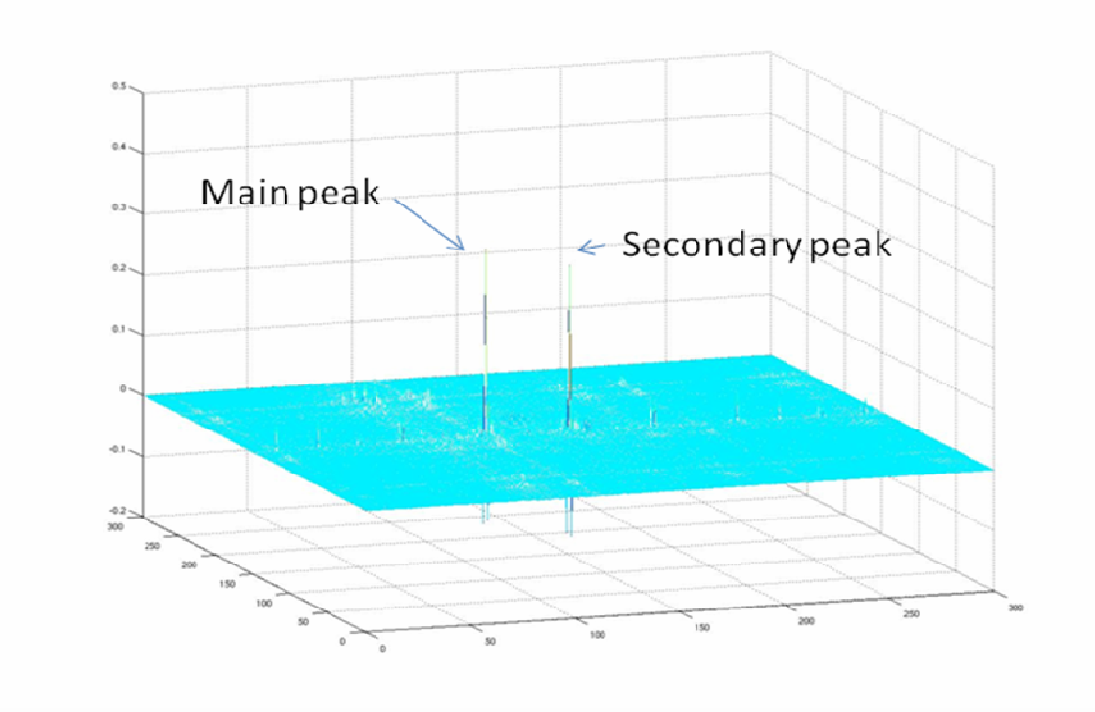

Figure 72. Frame to study the main-secondary peak

$$main\text{-}secondary\ relation = \frac{Main\ peak}{secondary\ peak}$$

6.1.3 Location of the main peak

The location of the main peak is very important in order to avoid false positives. For the same reason mentioned before, if the output of the Phase-Only filter was a very narrow and clear peak by only seeing the first two metrics we could assure that is the same movie, but if the location of the correlation peak is not at zero shift, that would mean that we have a similar shape with similar energy in another part of the brain. As we know, if the activation appears in a different part, this is a result of a different stimulus; it is not the same activation in the temporal lobe than in the frontal lobe. So if we expect to obtain a good match between movies we will look for the main peak at the spatial zero shift.

6.1.4 *Local Signal* Noise Ratio (*Local* SNR)

The SNR will be the last of the factors we will study in the output of the phase only filter. This ratio will show us the relation between the main peak and its surroundings. It is defined as a *local* SNR, which is meant to mimic the human visual interpretation of whether the peak is "clear" or not. We define local SNR in this project as follows:

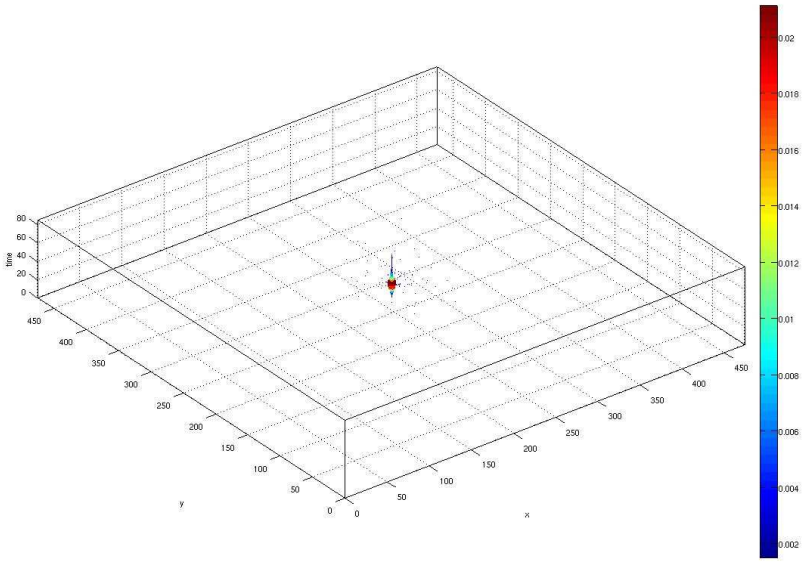

Figure 73. Example of output of the Phase-Only Filter

First we locate in which frame the main peak appears. Once this is determined we look the surrounding region to obtain the local SNR

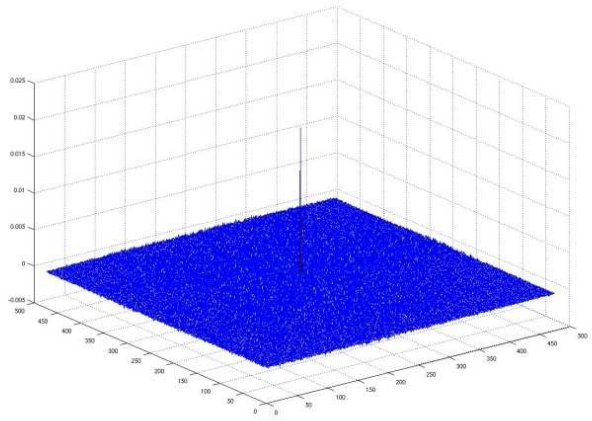

Figure 74. Frame of the example before shown where the main peak is located

In this example, the frame where the main peak is located is the frame 43. So we have this frame which size is 474x475. To calculate the local SNR, we surround the main peak with a square of size depending on how precise we want our SNR to be, centered on the main peak. In all the examples of this thesis, the size of the square is 41x41. We chose this value because we wanted the square to be between 5% and 10% of the total size of the output, to present a good relation between the human visual interpretation previously commented and the data calculated. .

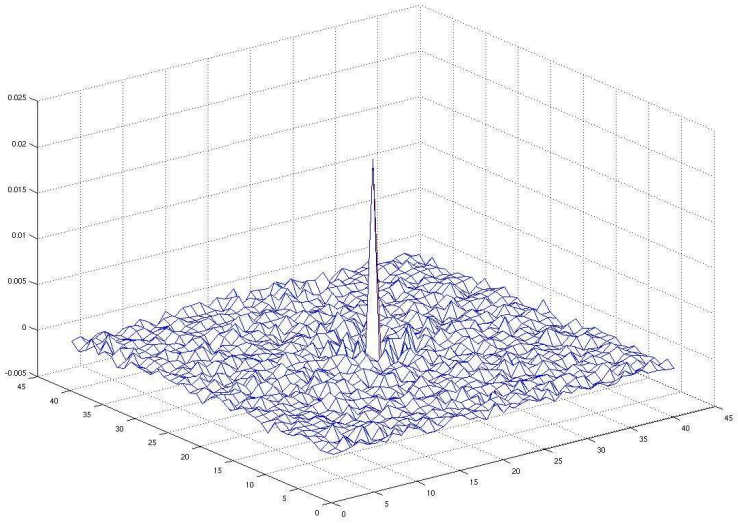

Figure 75. local frame where the maximum is located.

Then the SNR is defined as

$$SNR = 10 * \log_{10} \frac{(Max)^2}{Var(\text{local frame} - Max)}$$

Figure 76. Formula to calculate the local SNR

being max the value of the maximum peak at the output and the expression (local frame - max) the result of the frame once we remove the main peak from the local frame (Figure 75). We do this by making the value of the pixel where the maximum is located equal to 0.

To calculate the variance of the local frame once the main peak has been removed we reshape the local frame [41x41] into a vector [1x1681], and we calculate the variance of this vector.

6.2 Real Movies

All the movies used in this part of the thesis were taken as MEG movies, I explained in the section 5.2 how these movies are taken, and the movies are the result of a Brainstem Auditory Evoked Responses test, which mechanism I explained in the section 5.3.3

I obtained 4 movies, depending on which ear was the source and which hemisphere was studied in the test, so the movies I will use as inputs in the Phase only filter are:

- Left Ear Left Hemisphere
- Left Ear Right Hemisphere
- Right Ear Left Hemisphere
- Right Ear Right Hemisphere

There will be six possible scenarios with these 4 inputs, so the aim of this test is to find which inputs have a good match or a poor match in order to see which is more important, the source or the hemisphere under study. We will see the relation between these movies and how the brain acts in this auditory evoked potentials test.

First of all, I will comment on the way I prepared the movies to be able to work with them and Matlab. The movies were given to me as MPEG movies. I had to convert the MPEG movies into AVI "uncompressed" movies because Matlab only inputs movies as this file type.

Once the movies have been introduced to Matlab, the size of the movie becomes **520x556x151**, We have to keep in mind that after the zero-padding transformation the movie

will become **1560x1668x151,** which means that the we need a very powerful computer to be able to work with them, because just the operation fftn could take days or even could be impossible if we don't have enough RAM memory.

Matlab automatically saves the movie as a structure, where we have 3 matrices for every frame (RGB). The transformation I applied to convert the RGB to gray scale is the classical formula of the pixel luminance, **Y = 0.3*R + 0.59*G + 0.11*B**. The weights are based on studies of the human eye which have shown that the sensitivity to red, green, and blue differs, therefore the luminance has different scaling factors for each color channel [56]. Once I have the matrix, I remove all the information I don't need in the movie, for example the zeros surrounding the brain and the background which is the same for all the frames.

One example movie that was supplied by our collaborators is shown below in Fig. 77 Left Ear Left Hemisphere.avi. The following figure shows the same frame once I have removed the background of the brain and all the information not needed.

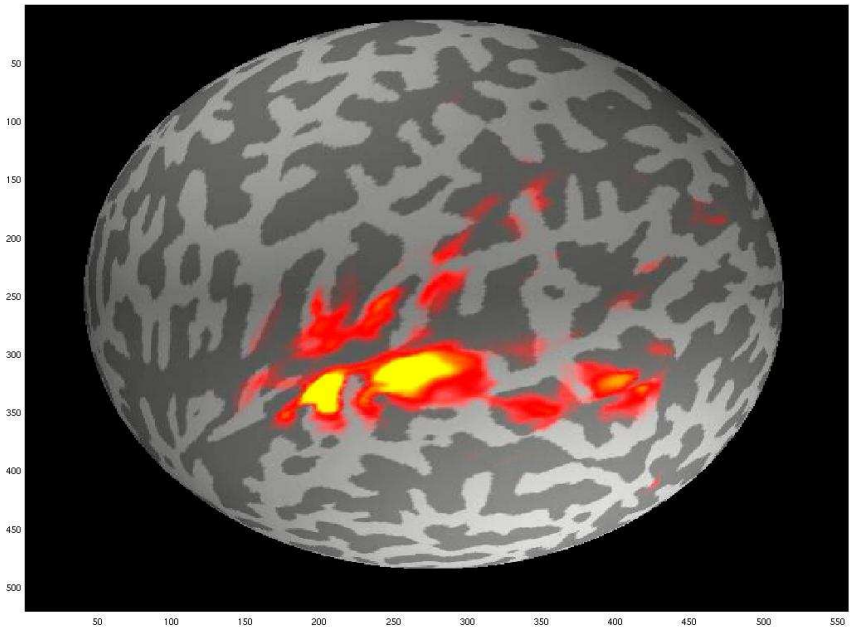

Figure 77. Real frame for and auditory evoked potential test

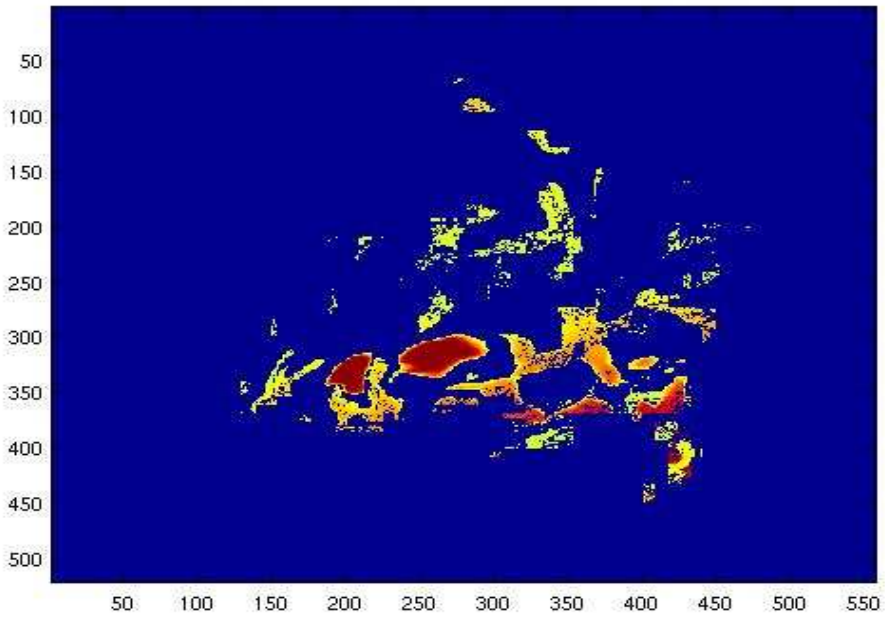

Figure 78. The same frame after the transformation explained before

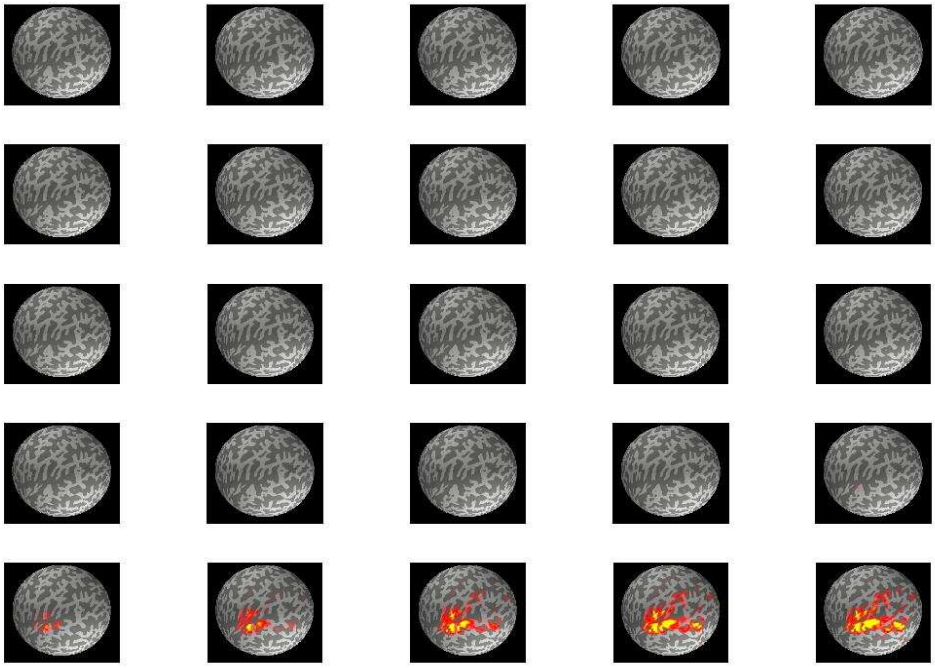

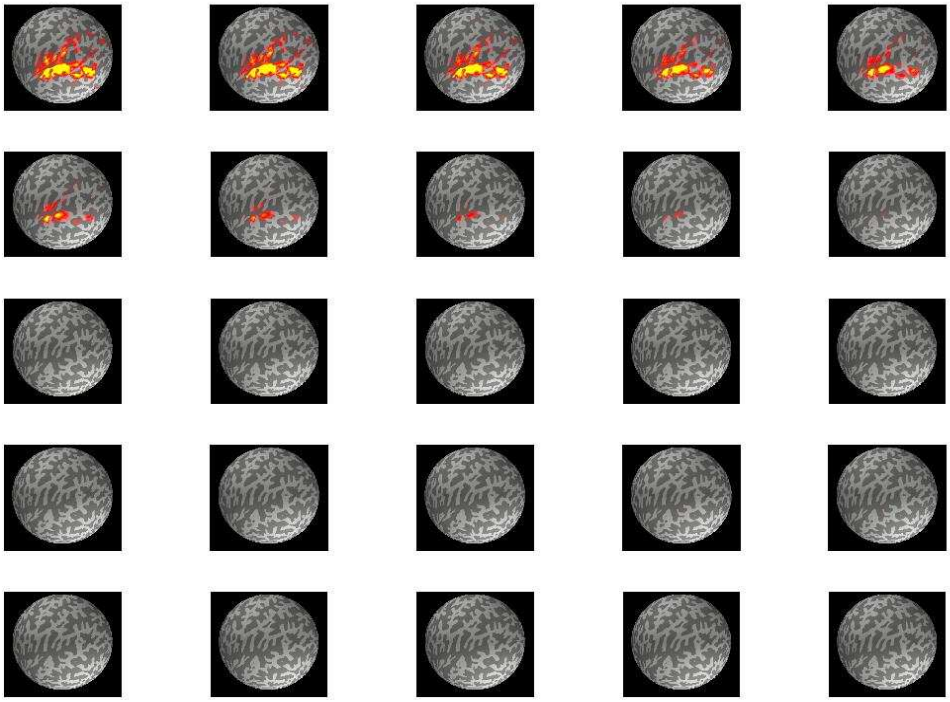

Fig 79. Example of original movie before transformation

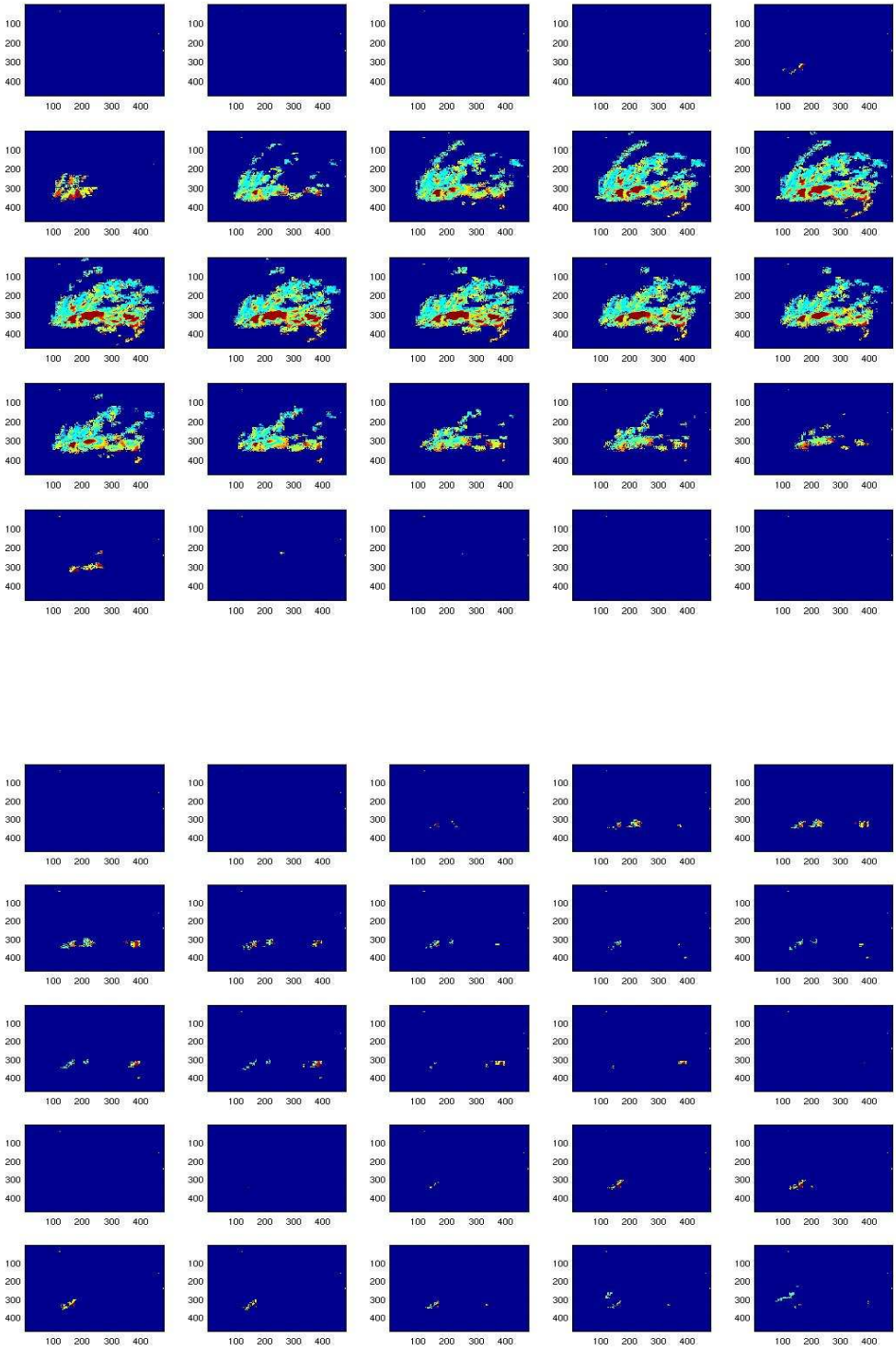

Fig 80. Example of final movie after transformation

The concept of removing all the information not needed could seem confusing, what that means is that if we have an acknowledge *a priori* of the grade of similarity between the movies under study we can try to thresholded the values in each frame in order to improve the data obtained.

By thresholding the values of the original movies what we wanted to obtain was a value of the threshold which improve the amplitude of the main peak at the output of the Phase-Only filter while increasing the relation main-secondary peak for a possible good match between movies and while decreasing the relation main-secondary peak for a poor match between movies.

To obtain that acknowledge *a priori* we ran the filter with the original movies and by looking at the results we set the differences between the grades of similarity obtained.

Once we had that discrimination between possible good match and poor match we started to try different values for the threshold. Those values were all the multiples of 10, from 10 to 230.

Movie values between:

-Left Ear Left = [0 - 235]

-Right Ear Left = [0 - 237]

-Left Ear Right = [0 - 235]

-Right Ear Right = [0 - 233]

The threshold applied was 130. All the values under this number were made equal to 0.

By doing this, I obtained this improvement in the outputs of the Phase-Only filter.

Inputs of the POMF	**Maxim amplitude of the POMF**	**Acknowledge *a priori***	**Relation main-secondary peak**
Left Left Right Left	+38.8%	Possible good match	+35%
Left Right Right Right	+24%	Possible good match	+41.7%

Left Left Left Right	+18.2%	Poor match	-1.2%
Left Left Right Right	+17.6%	Poor match	-10%

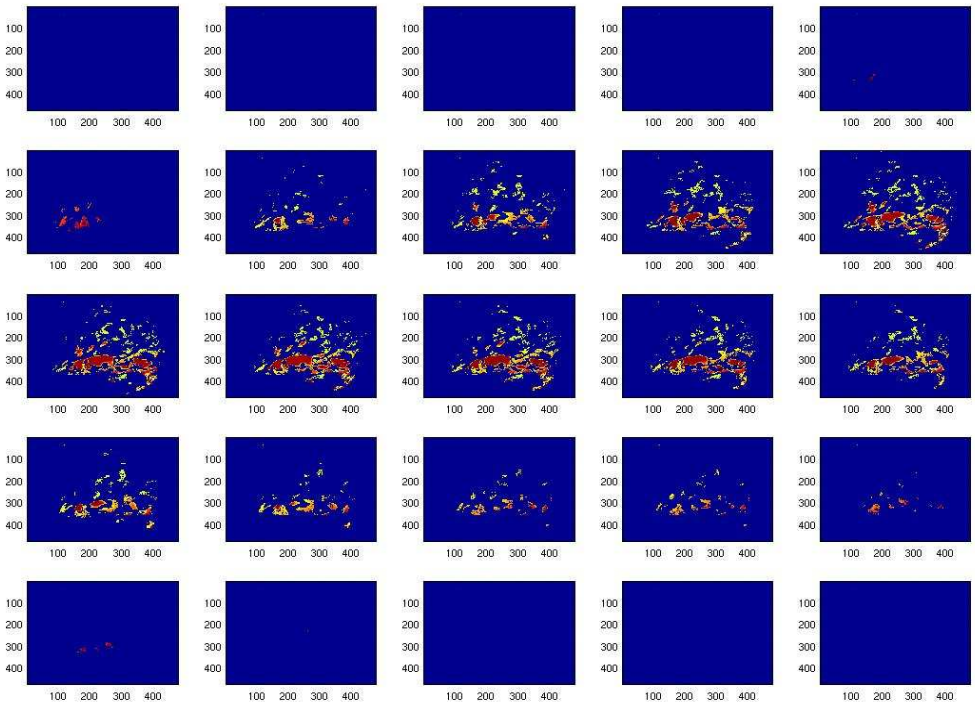

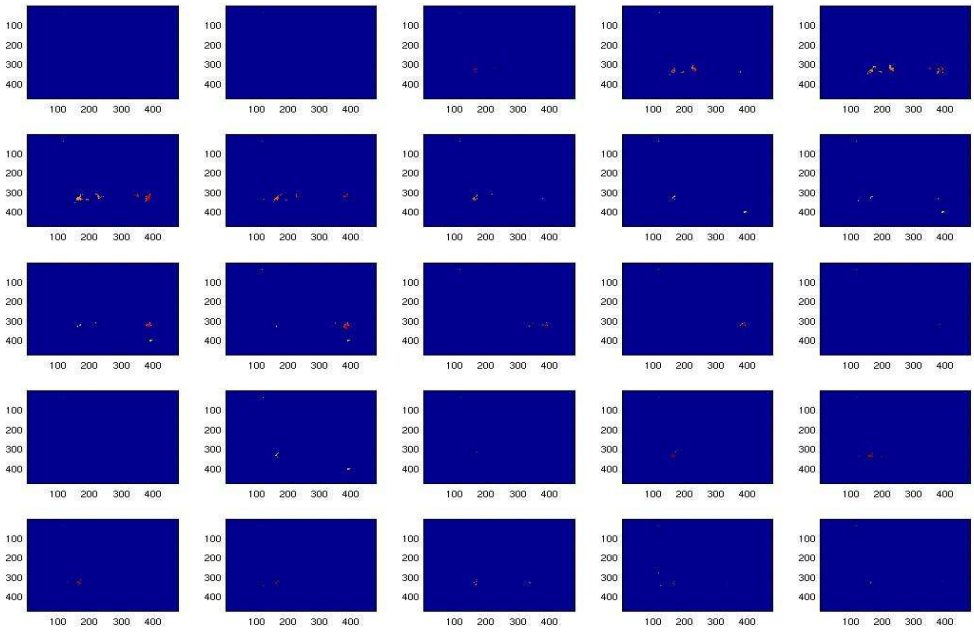

Fig 81. Example of final movie after transformation and thresholding

The figure 81 was the original movie after removing the background and the borders and after applying the threshold.

Once I have explained the metrics to take in consideration in the study of the output of the phase only filter, it is important to talk about one big limitation I faced when it was time to work with real movies.

Since I used Matlab for all the test done, memory is a important concept when we work with this kind of tool. A real movie after the transformation has this size [1422 x 1425 x 122], what means that to do the Fast Fourier Transformation of them, the memory required to save in memory the two inputs and the output after zero-padding, if they are saved as *double*, is at least 6 Gb of RAM memory, and we have to add all the intermediate operation that also require memory. Since the machine I used for doing these tests wasn't that powerful I had to do the tests with a limited number of frames per image.

The next figure shows the energy of the all the frames in the movies.

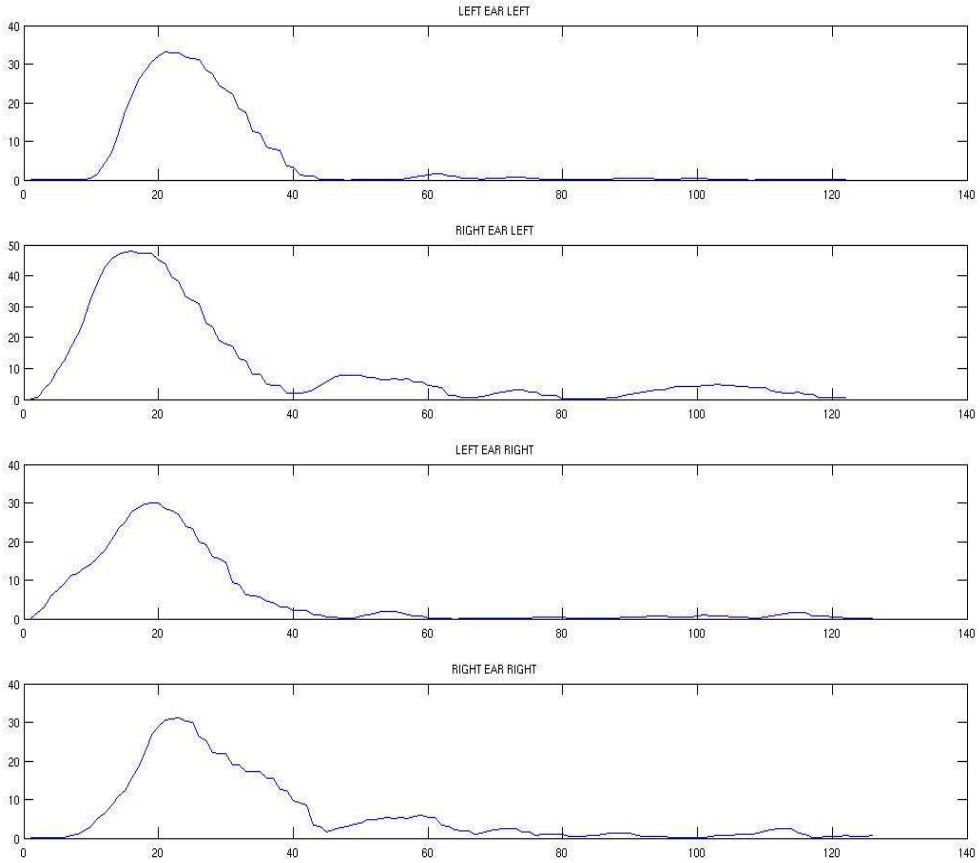

Fig 82. Distribution of the energy by frame in the original movies

We can see how all the energy in the movies is concentrated in the first frames of the movies, so I did all the test for the 85 first frames of the movies. It is a good approximation of the whole energy. Indeed below we report on the percentage of the total energy that these 85 frames represent.

- Left Ear Left Hemisphere - 99 % of the total energy
- Left Ear Right Hemisphere - 96.48 % of the total energy
- Right Ear Left Hemisphere - 91.97 % of the total energy
- Right Ear Right Hemisphere - 95.54 % of the total energy

I will show now the four movies under study; the movies will be shown as originally supplied, without any transformation.

Left Ear Left Hemisphere

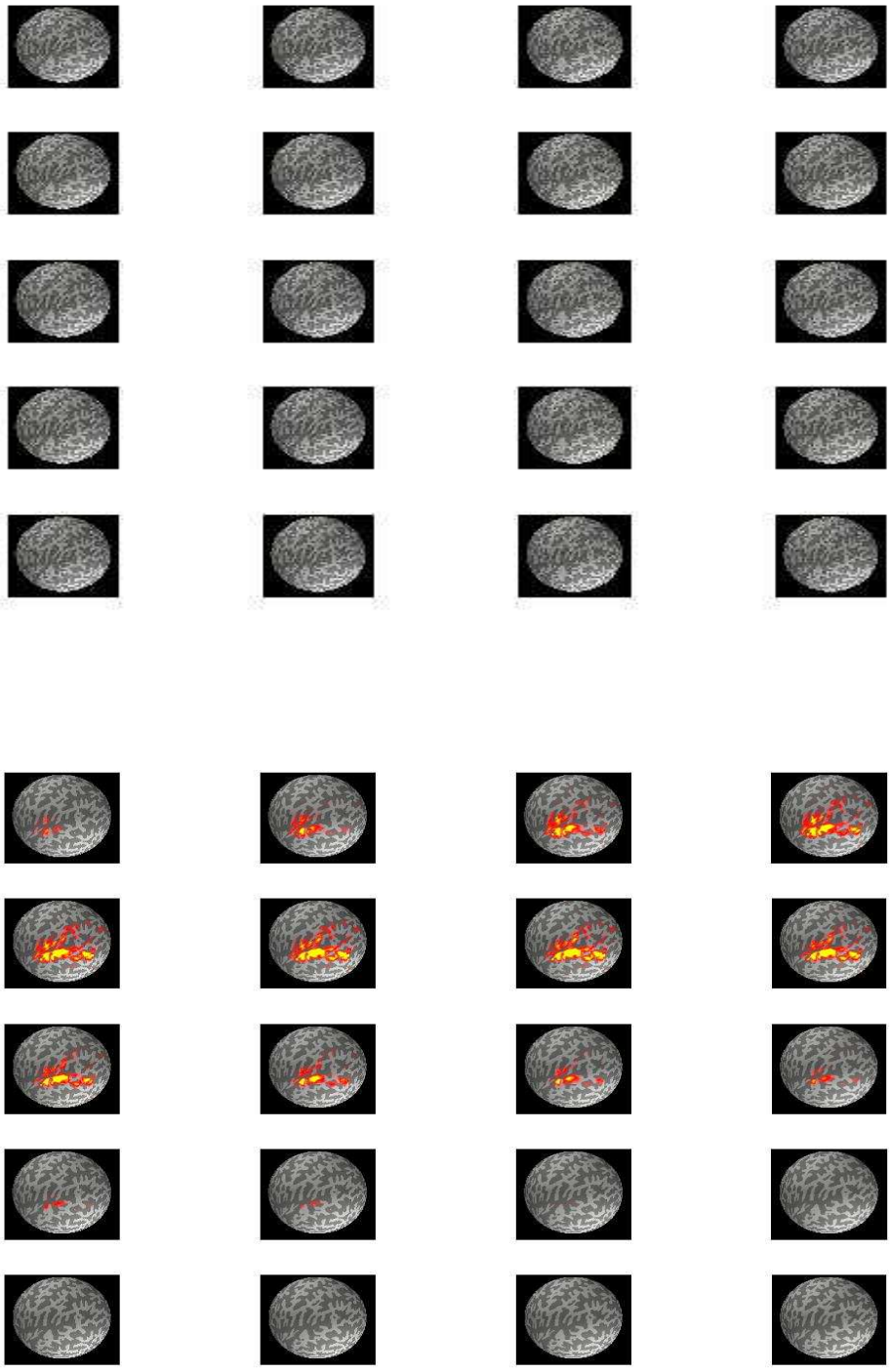

Fig 83. Sequence of even frames of Left Ear Left Hemisphere from frames 4 to 80

Left Ear Right Hemisphere

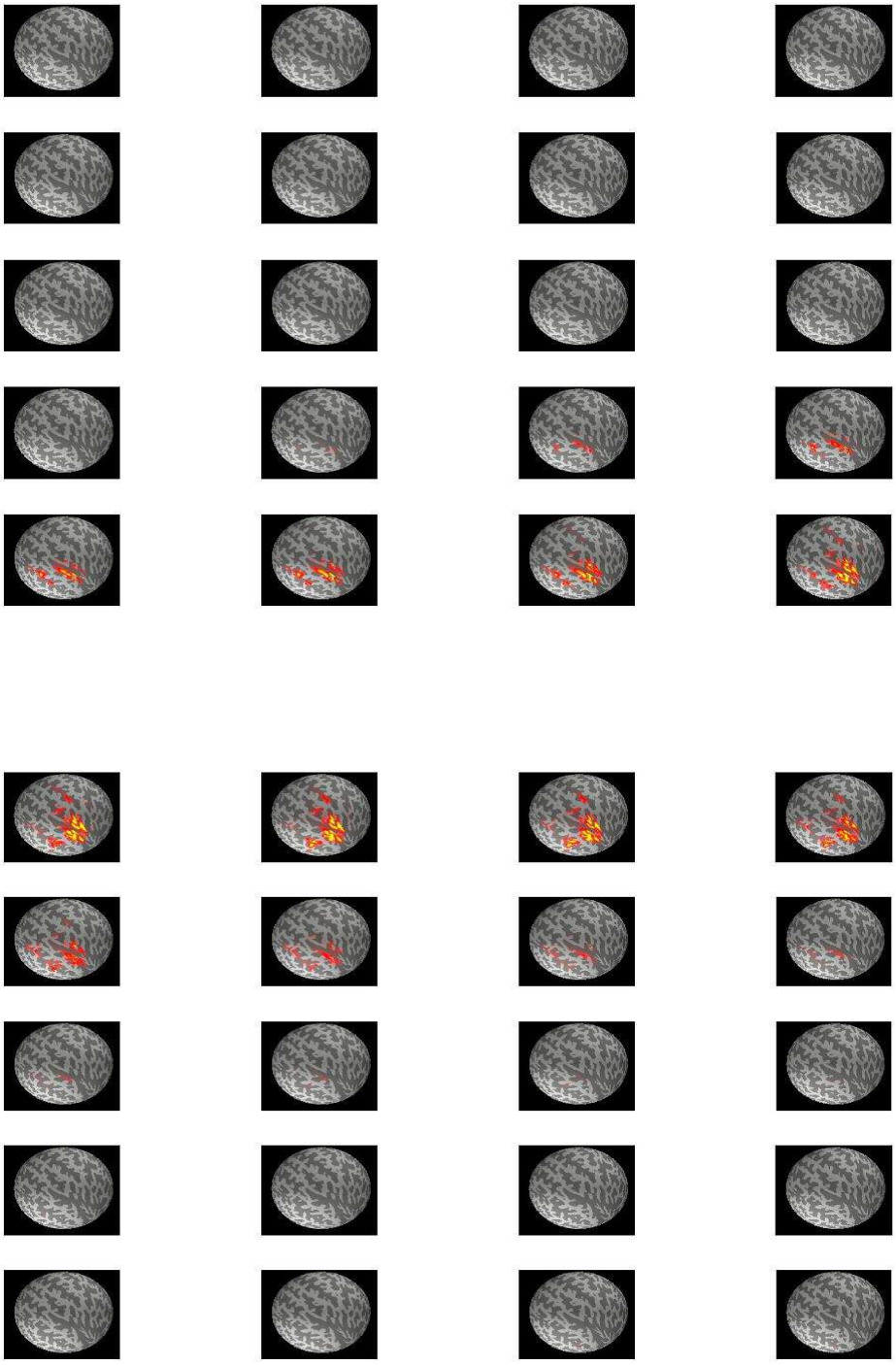

Fig 84. Sequence of even frames of Left Ear Right Hemisphere from frames 4 to 80

Right Ear Left Hemisphere

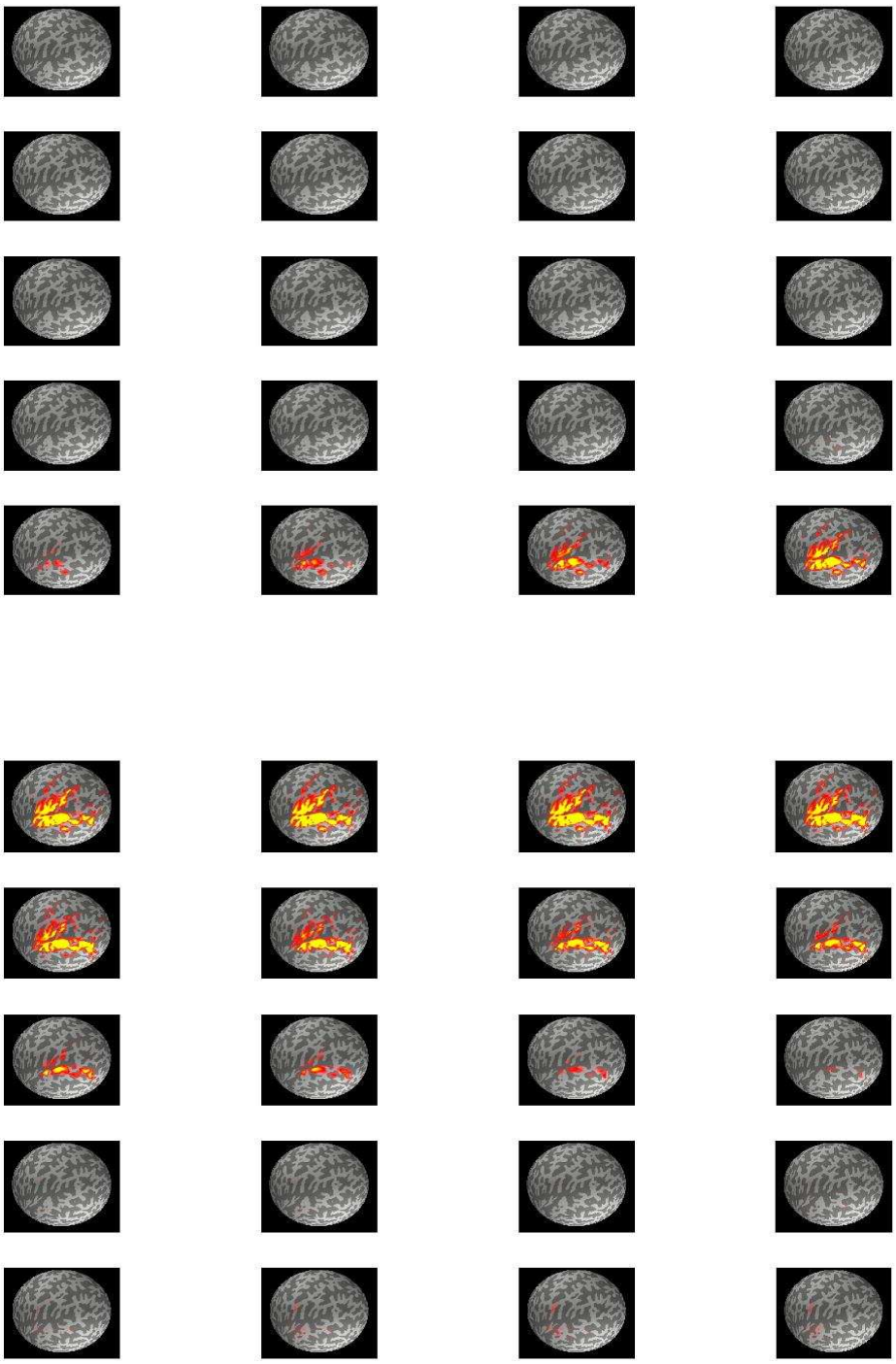

Fig 85. Sequence of even frames of Right Ear Left Hemisphere from frames 4 to 80

Right Ear Right Hemisphere

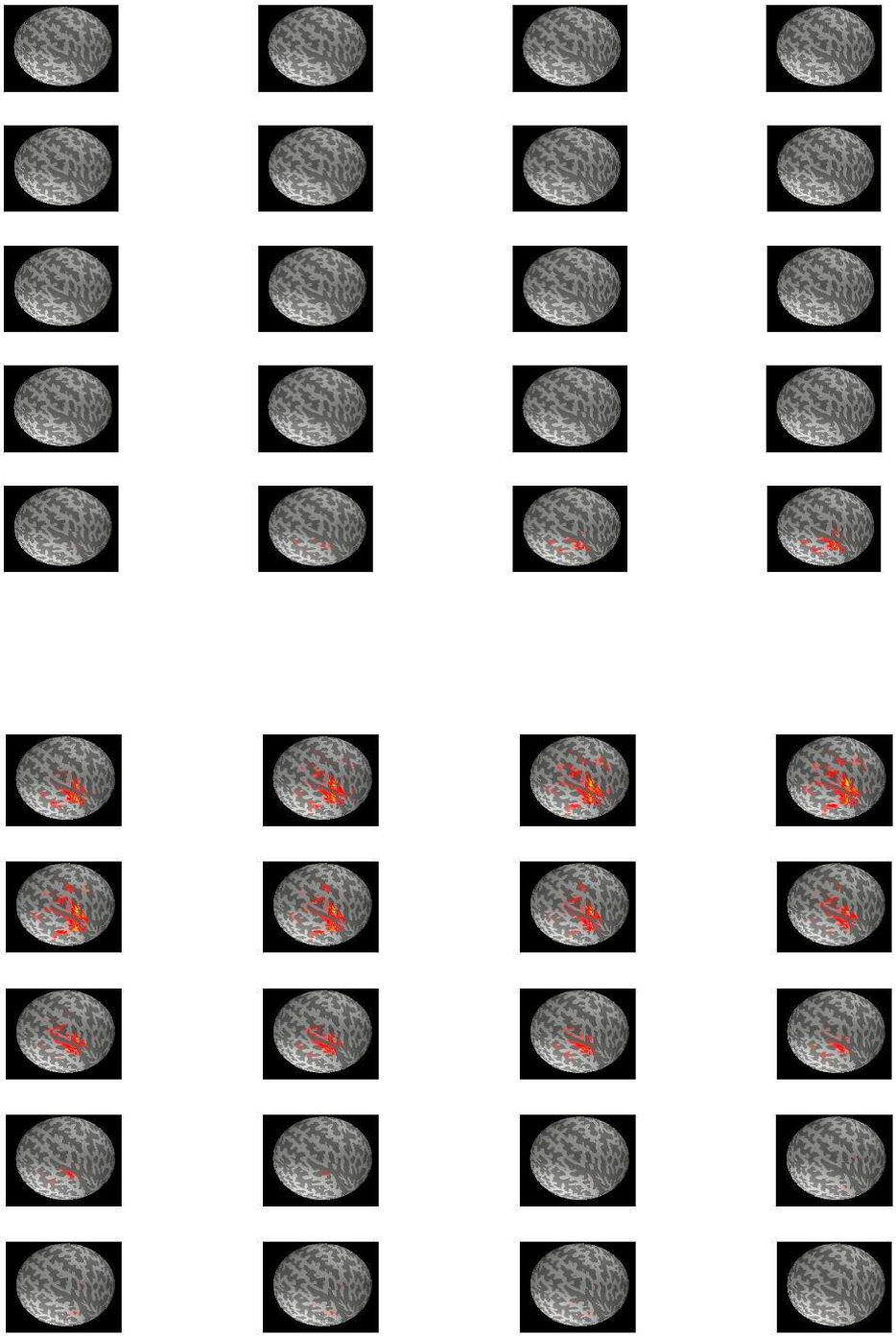

Fig 86. Sequence of even frames of Right Ear Right Hemisphere from frames 4 to 80

The table below shows us two examples of a possible good match and two example of a poor match. In order to test all the possible combination depending on the source and the hemisphere in a visual way we have omitted in this thesis the visualization of the output of the Phase-Only filter for the combination Right Left – Right Right and Left Right – Right Left due to the similarity with the other 2 combination with a poor match even though the results of these test are presented later in the table 100.

Left Left Right Left	Different source **Same** hemisphere
Left Right Right Right	Different source **Same** hemisphere
Left Left Left Right	**Same** source Different hemisphere
Left Left Right Right	Different source Different hemisphere

Table 87.

As we can see in the movies before shown the background of the brain is different depending on if it is the left hemisphere or the right hemisphere. In order to obtain coherent results in the test, we perform a left-right flip of the right hemisphere to be able to compare them with the left hemisphere movies. Since I remove the background this won't give us any wrong information, because I will only look at the activation in the brain. Once I have the left-right flip of the right hemisphere, the activation will appear in the same temporal lobe and we will be able to compare the movies in a more accurate way.

To see if there is a good match or a poor match, after hundreds of test, I obtained a value for the metrics that could give us an approximate idea if there is a good match or a poor match between the movies. To arrive at this value I tested different possibilities and then once I had the value of the parameters I checked the similarity of the movies with my own eyes to determine if there was a good match or not. This value cannot be taken as a real threshold to make decisions

because it is so subjective, but is a first approximate value. After these tests we will see that we can make other conclusions about this threshold

For real movies with a size of **474 x 475 x 85**, we consider that we have a good match if:

- *The maximum amplitude of the output of the Phase-Only filter* **> *0.01***
- *The relation main-secondary peak* **> *2.5***

6.2.1 Left Ear Left Hemisphere vs. Right Ear Left Hemisphere

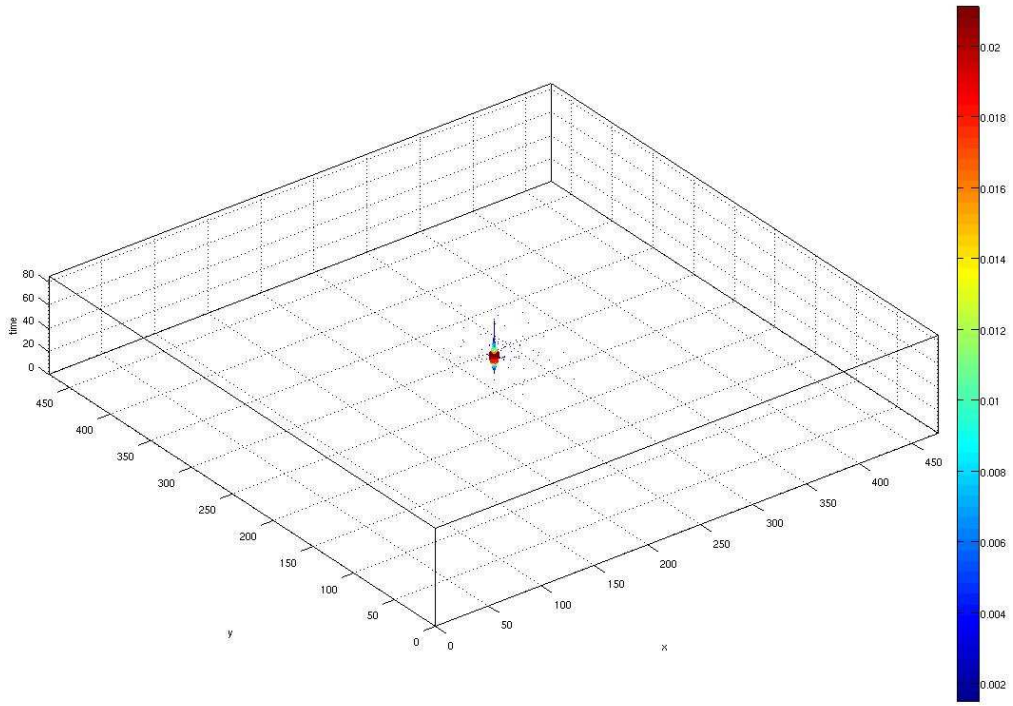

Figure 88. 3D visualization of the Output for this test

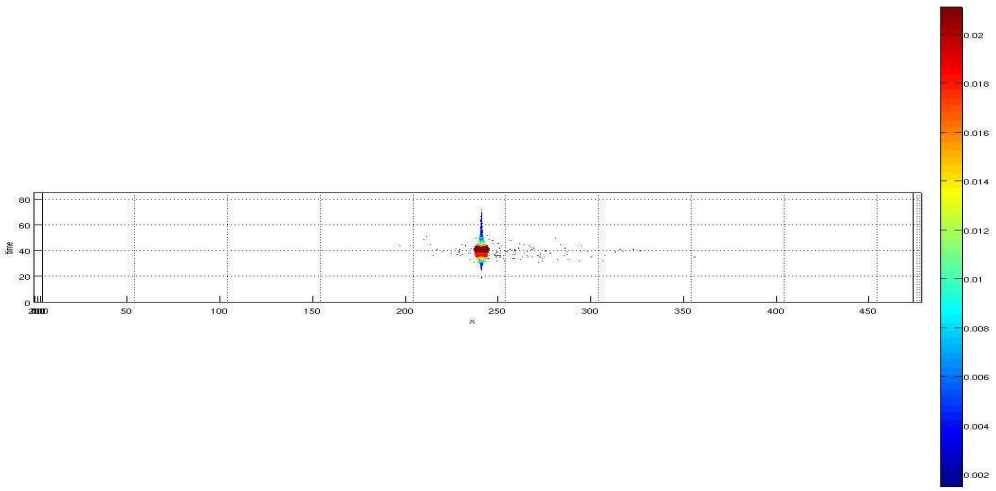

Figure 89. Temporal visualization of the Output for this test

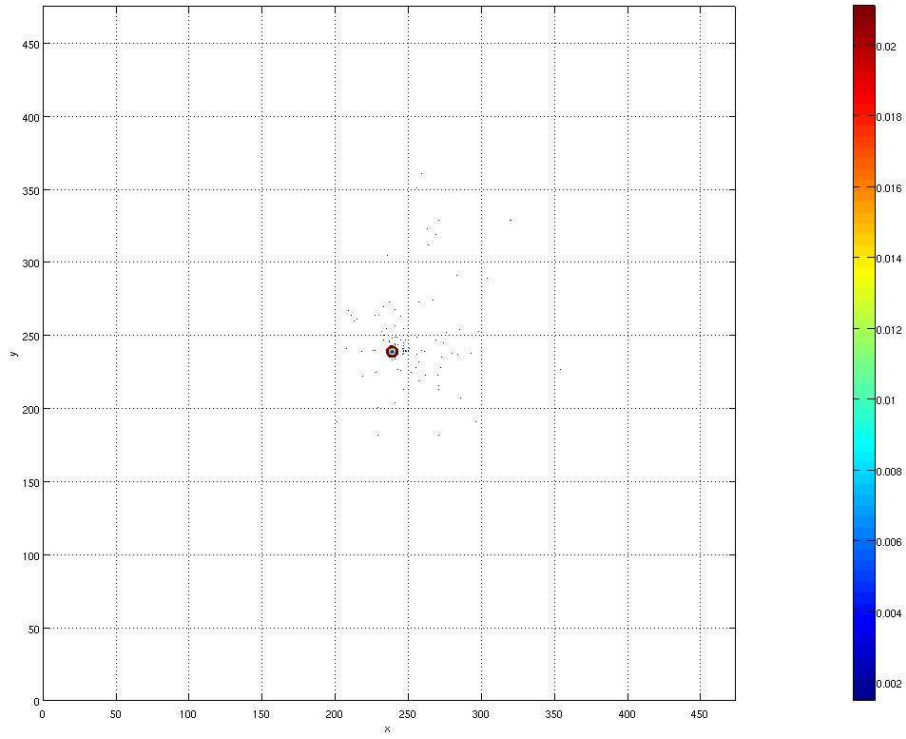

Figure 90. Space visualization of the output for this test

- **Maximum amplitude** **0.0211** *> 0.01*
- **Relation main-secondary** **11.08** *> 2.5*
- **Local SNR** **32.22**

We can see how the main peaks are all placed in the center of the image in terms of space, which means there are no shifts in space. According with the experimental threshold, the output of the Phase-Only filter tells us that these two movies have a **good match.**

6.2.2 Left Ear Left Hemisphere vs. Right Ear Right Hemisphere

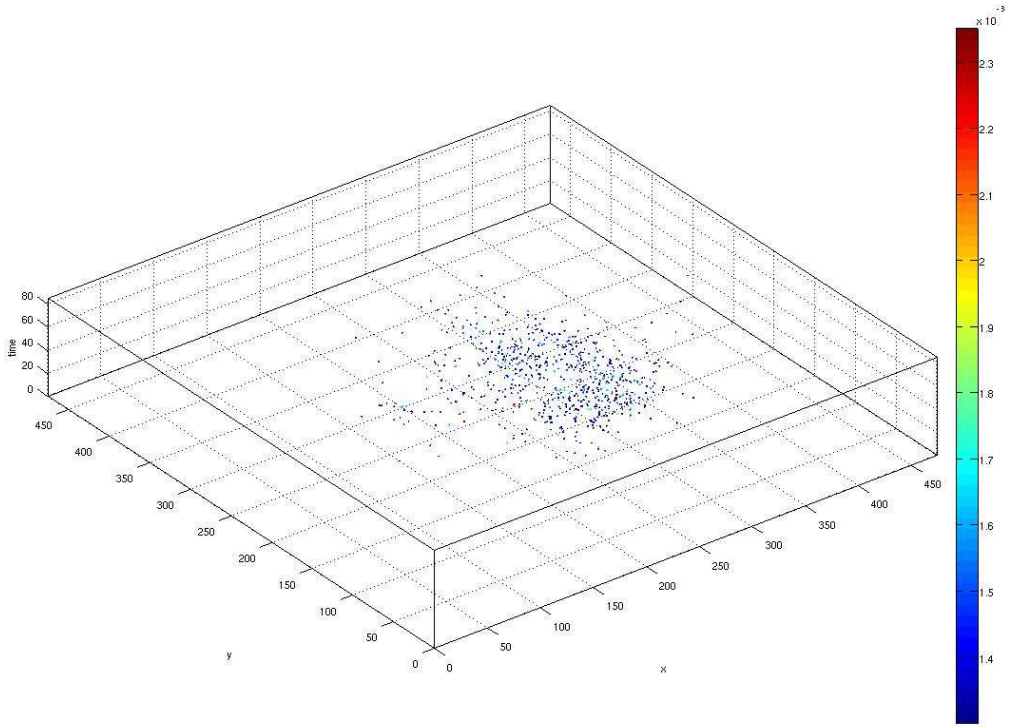

Fig 91. 3D visualization of the output for this test

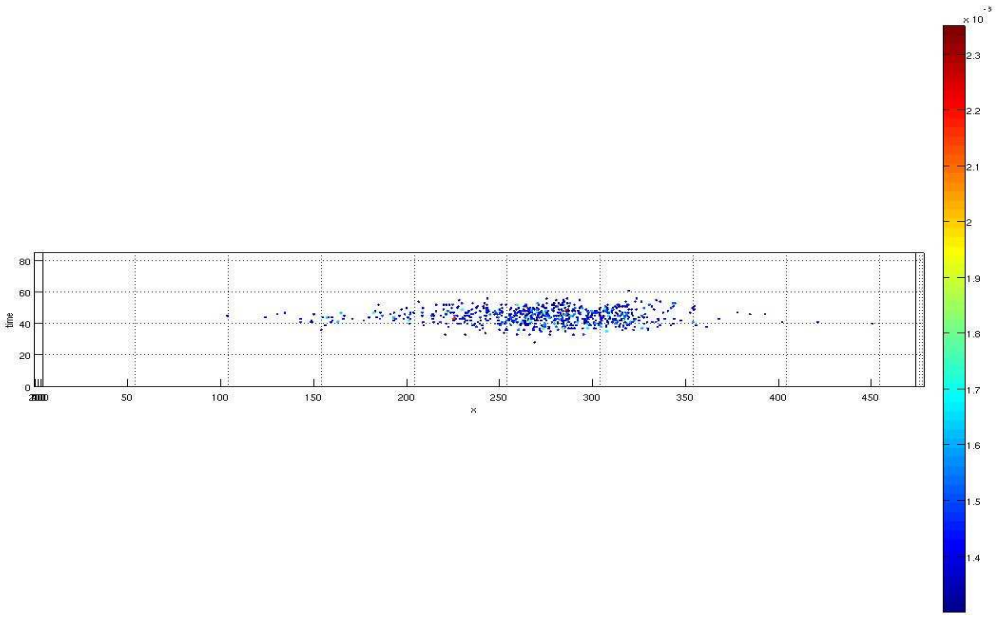

Figure 92. Temporal visualization of the Output for this test

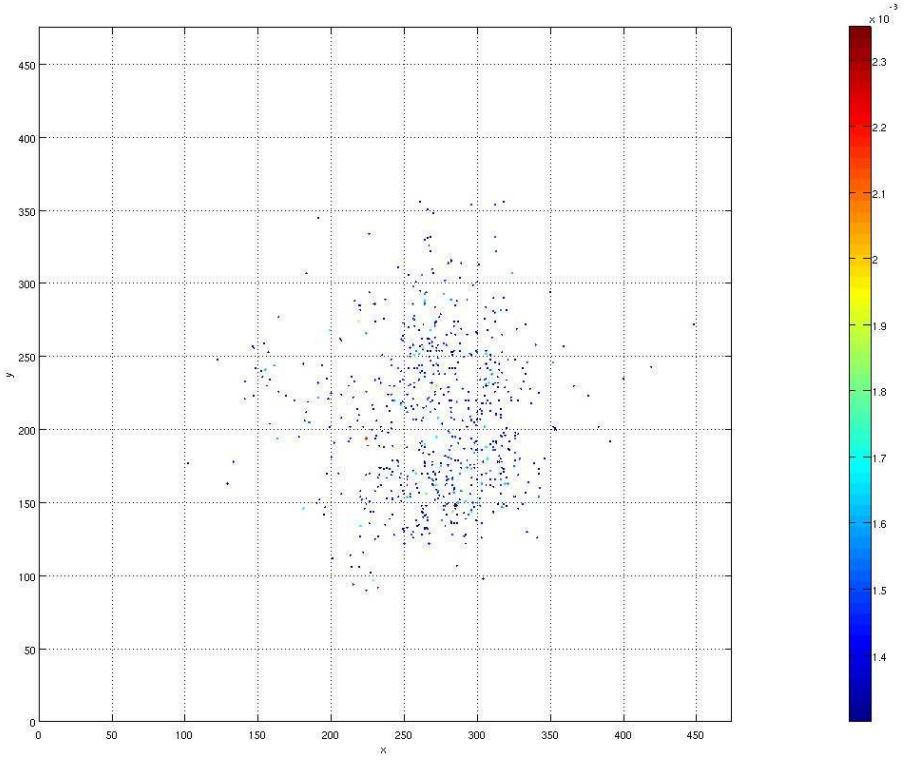

Figure 93. Space visualization of the Output for this test

- **Maximum amplitude** **0.0024** *< 0.01*
- **Relation main-secondary** **1.3974** < 2.5
- **Local SNR** **14.7526**

We can see the presence of a lot of noise in the output of the Phase-Only filter, there are no clear peaks in the center of the image, and both the relation main-secondary peak and the local SNR are very low. The Phase-Only filter is showing us that between these two moves there is a **poor match**

6.2.3 Left Ear Right Hemisphere vs. Right Ear Right Hemisphere

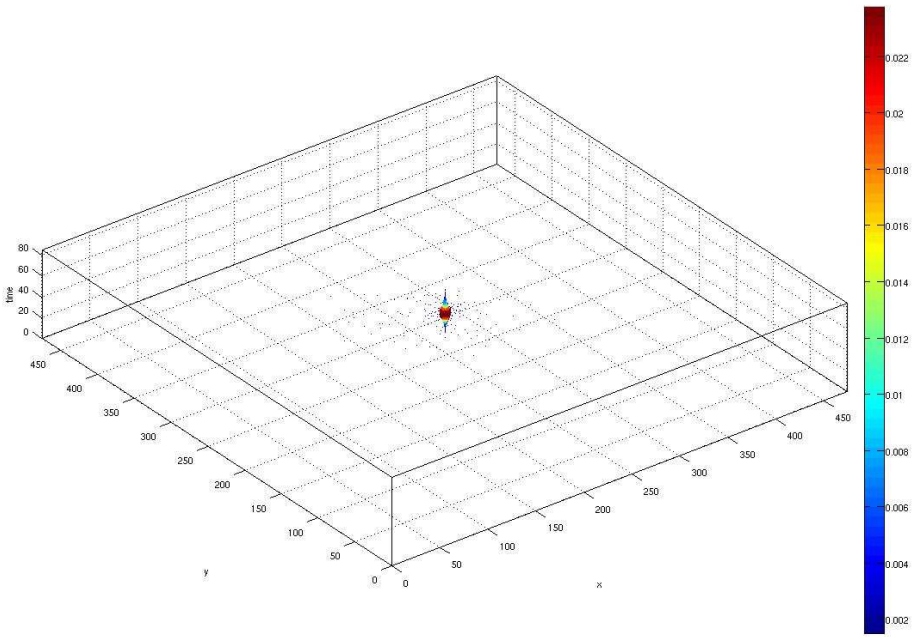

Figure 94. 3D visualization of the Output for this test

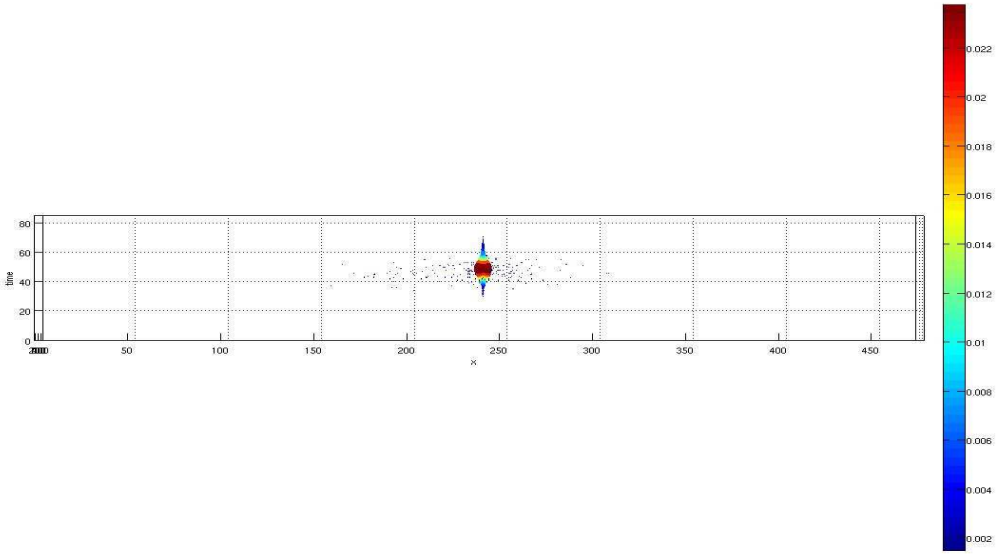

Figure 95. Temporal visualization of the Output for this test

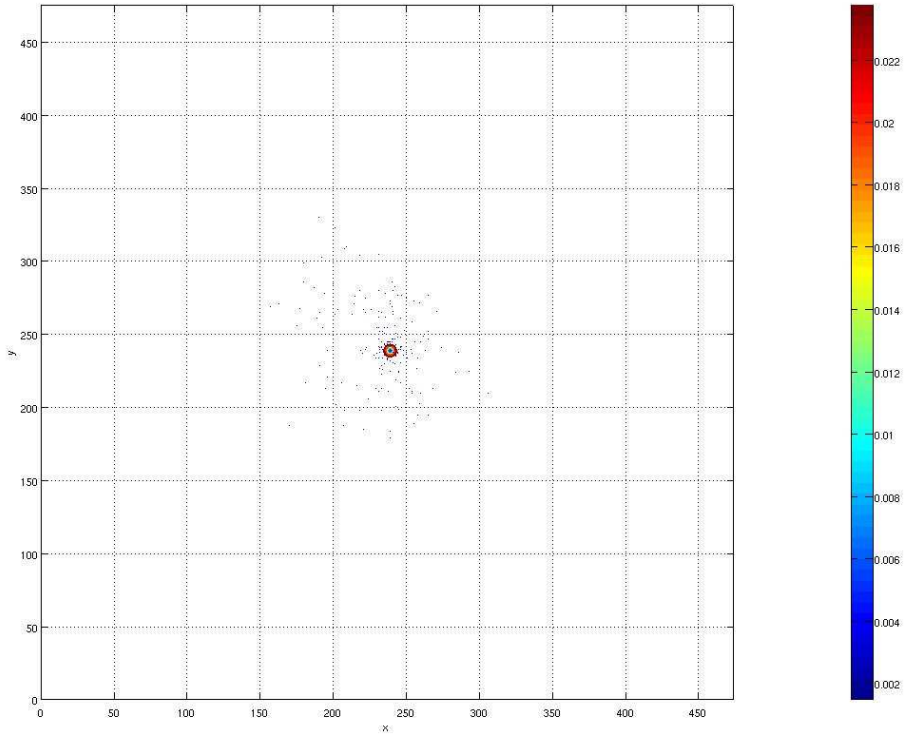

Figure 96. Space visualization of the Output for this test

- **Maximum amplitude** **0.0211** *> 0.01*
- **Relation main-secondary** **11.5** *> 2.5*
- **Local SNR** **31.92**

We can see, like in the first test, how the main peaks are all placed in the center of the image in terms of space, which means there are no shifts in space. According with the experimental threshold, the output of the Phase-Only filter tells us that these two movies have a **good match.**

6.2.4 Left Ear Left Hemisphere vs. Left Ear Right Hemisphere

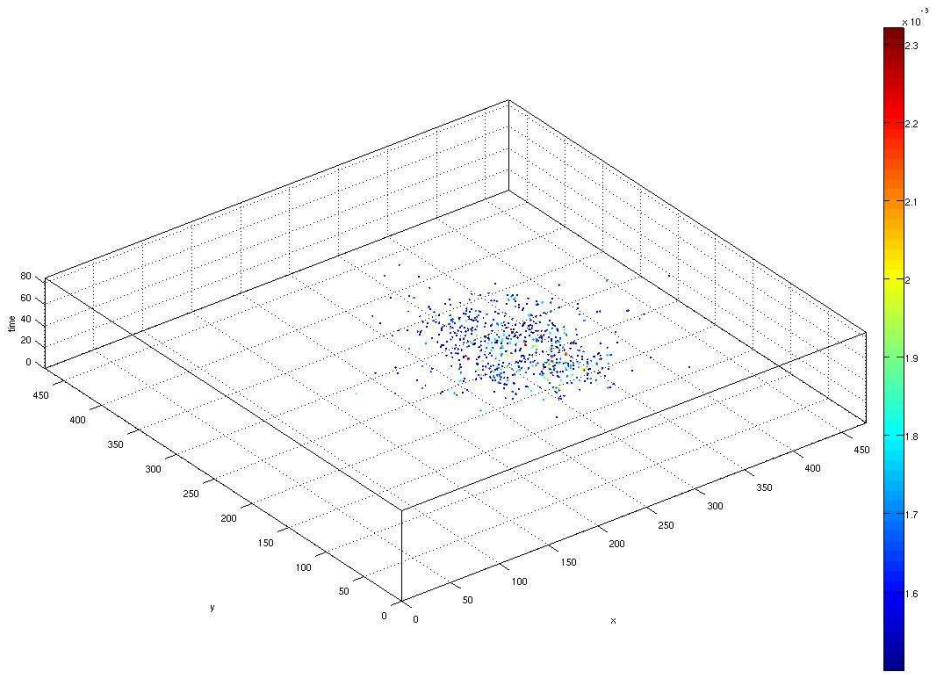

Figure 97. 3D visualization of the Output for this test

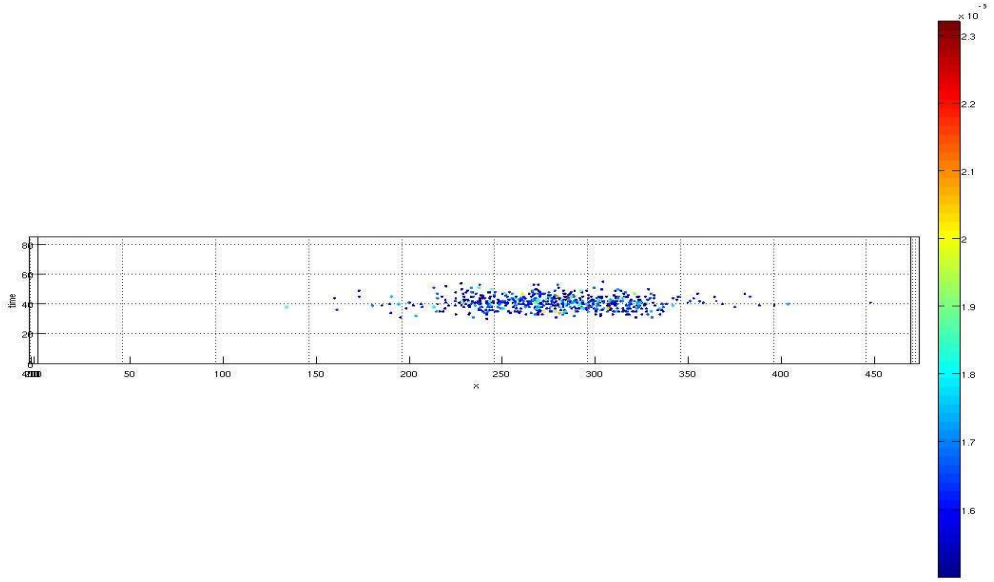

Figure 98. Temporal visualization of the Output for this test

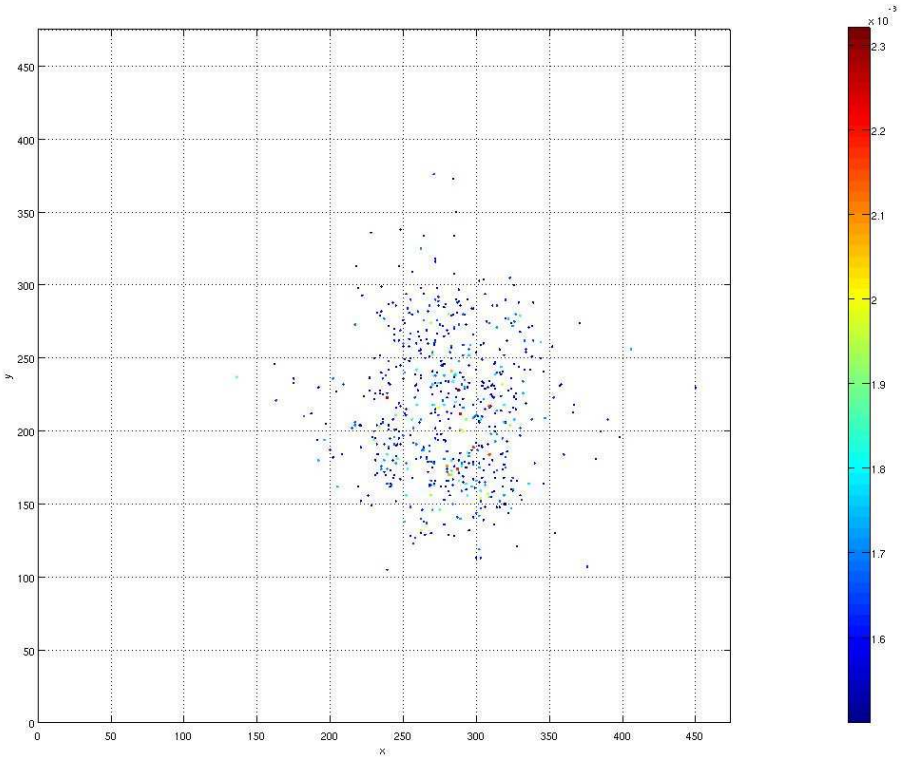

Figure 99. Space visualization of the Output for this test

- **Maximum amplitude** **0.0023** *< 0.01*
- **Relation main-secondary** **1.3762** < 2.5
- **Local SNR** **13.6267**

We can see the presence of a lot of noise in the output of the Phase-Only filter, there are no clear peaks in the center of the image, and both the relation main-secondary peak and the local SNR are very low. The Phase-Only filter is showing us that between these two moves there is a **poor match**

6.2.5 Comparison of the results of this test made with the Phase-Only filter and real auditory evoked responses movies

inputs	Maximum amplitude	Relation main-secondary	Local SNR
Left Ear Left Hem. Right Ear Left Hem.	0.0211	11.0804	32.22
Left Ear Right Hem. Right Ear Right Hem.	0.0211	11.5034	31.92
Left Ear Left Hem. Right Ear Right Hem.	0.0024	1.3972	14.7526
Left Ear Left Hem. Left Ear Right Hem.	0.0023	1.3762	13.6267
Right Ear Left Hem. Right Ear Right Hem.	0.0016	1.0563	13.1737
Left Ear Right Hem. Right Ear Left Hem.	0.0017	1.1198	12.8177

Table 100. Results of all the test done with the 4 inputs given

We can see in the table 100 the comparative of the results in green when there is a **possible good match** and in black where there is a **poor match.** As hypothesized, the Phase-Only filter is able to find a degree of matching between movies by using the metrics we have defined. We can see clearly the difference between good match and poor match.

- Maximum amplitude ten times bigger for good matches
- Relation main-secondary peak more than ten times bigger for possible good matches
- Local SNR at least 15 dB bigger in good matches than in poor matches

Once we have analyzed the result of this test we can see that the condition *a priori* to make the decision of possible good match or poor match was correct, because the differences between them are very clear. By using the 3-D visualization we can see the shift undergone between the movies in space and time. The shift in time tells us how the energy of the movies are shifted in time, so it is not a delay between movies but how the common shape and the common energy between them are shifted in time.

Analyzing the results we can take a very clear conclusion in the comparison of movies (MEG) obtained with the auditory evoked responses test.

- **Same Source and different hemisphere** **POOR MATCH**
- **Different sources and different hemisphere** **POOR MATCH**
- **Different sources and same hemisphere** **GOOD MATCH**

The Phase-Only filter has determined four different parameters to check if the relation between these kind of movies is good or not. Now by using these parameters the Phase-Only filter is able to determine by itself the match of these inputs, being the presence of the human being totally unnecessarily.

6.2.6 Real movies: comparison of POMF vs. Traditional Cross-correlation filter

I have demonstrated in this thesis the application of the Phase-Only filter as one way of comparison of Functional Neuroimaging Time Sequences. I have demonstrated the advantages and disadvantages of the use of a Phase-Only filter over the traditional Cross-correlation filter, but to reinforce all I have claimed before we compare how the traditional cross-correlation filter acts when the inputs are two movies with a good match and two movies with a poor match. We are going to see how the determination of the match between movies is totally impossible, making this kind of filter totally ineffective.

The next page will show us a good match and the next page will show us a poor match, illustrating that it would be very difficult to draw conclusions about the match between movies as the Phase-Only filter is able to do.

Left Ear Left Hemisphere vs. Right Ear Left Hemisphere – GOOD MATCH

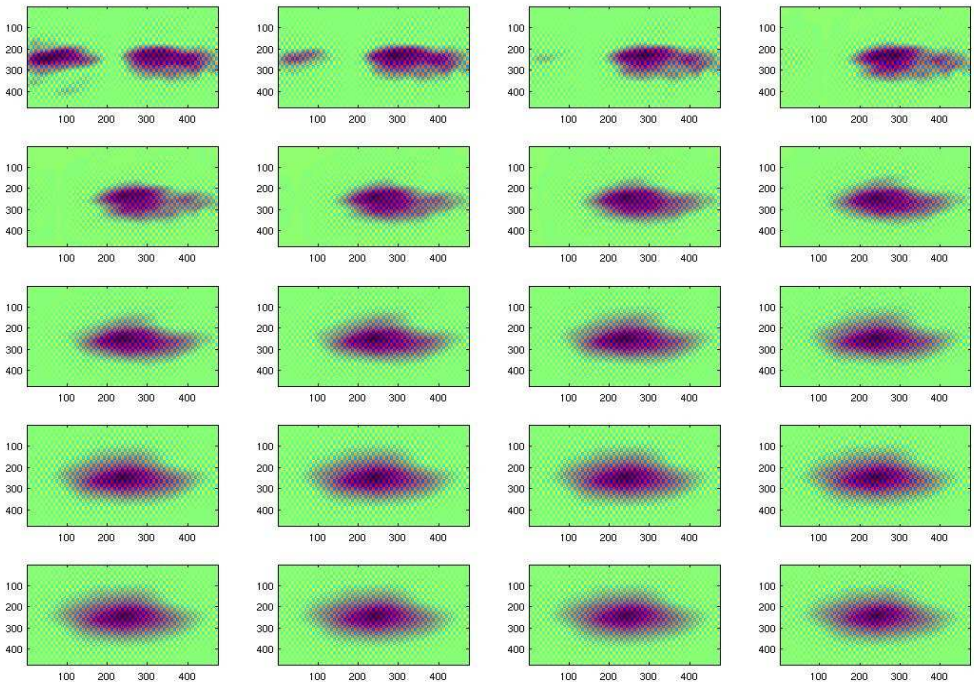

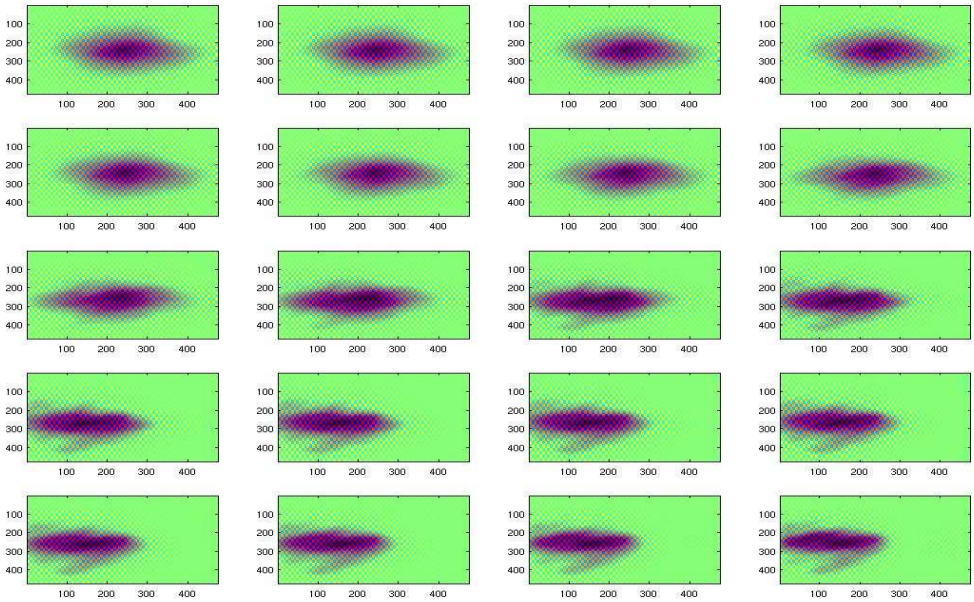

Figure 101. 2D visualization of the Output for this test (traditional cross-correlation filter)

Left Ear Left Hemisphere vs. Right Ear Right Hemisphere – POOR MATCH

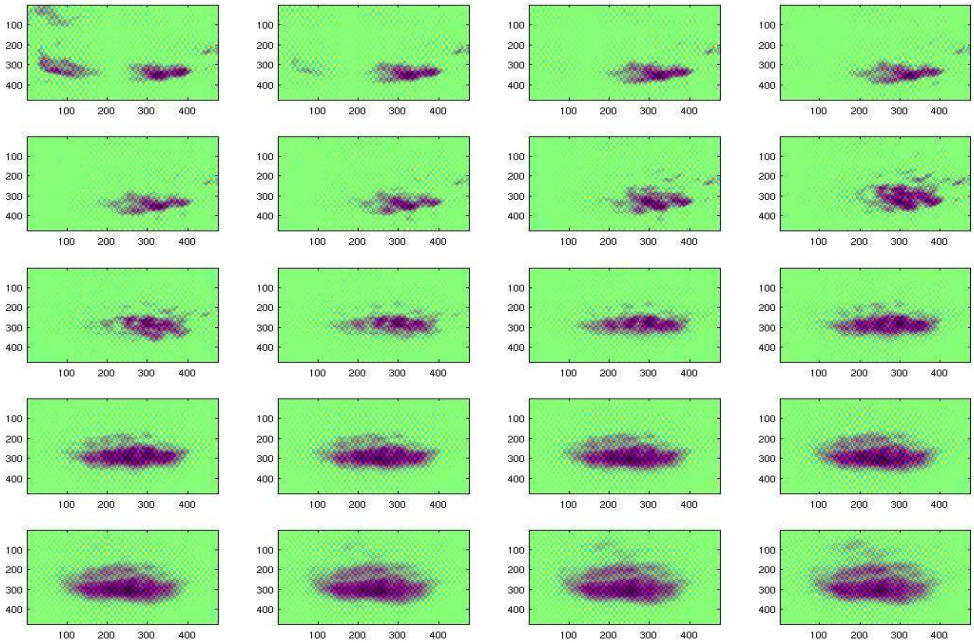

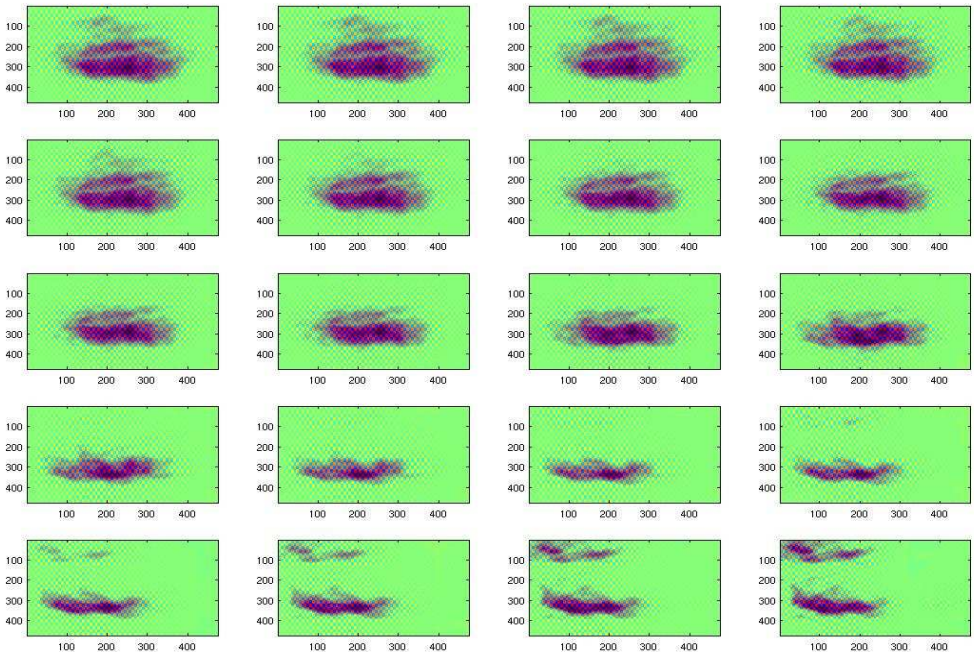

Figure 102. 2D visualization of the Output for this test (traditional cross-correlation filter)

7. CONCLUSIONS and FUTURE WORK

First of all, We have studied and demonstrated all of the properties of the Phase-Only filter when we worked with both 2-D images and spatio-temporal movies. The main characteristics and the reason why to use this filter (which only preserves the phase of the signals) are appropriate to think about when comparing the similarity between images and movies.

We studied the behavior of the Phase-Only filter when the input underwent a shift in space (in relation with the other input) while working with a 2-F image.

We also studied the behavior of the Phase-Only filter when one of the inputs underwent a shift in space, and how the filter can perfectly pinpoint the peak of the correlation between the movies.

The application of the Phase-Only filter in the field of the pattern recognition has been demonstrated before in many studies, but the application of this type of filter when needing to find an object in movement has been demonstrated here in section 4, opening a new path inside the pattern recognition field in spatio-temporal movies.

Finally, We have shown the application of the properties of the Phase-Only filter inside the world of neuroimaging. The professionals of the neuroimaging world have to make, prepare, and compare thousands of spatio-temporal movies every day, and this approach could be very useful in the future for those who have to compare spatio-temporal movies or even have to make new improvements in the preparation of new movies. By using this filter, we can set parameters which can identify the perfection or imperfection of the technique used in the representation of the real movie.

In the future this filter could be used to determine the authenticity of the spikes presents in brains of people who suffer from epilepsy, for example to check the correlation between these spikes, to try to find if it there exists any similarity between them.

By using this filter, We have set a couple of important metrics in order to give a grade of similarity between spatio-temporal movies. This new study shows that these factors are directly related to the grade of match between two movies. In the future the study of these factors may give us the key to “teach” the filter how to make the decision of if two movies are similar or not.

8. REFERENCES

[1] D.I. Barnea and H.F.Silverman,"A class of algorithms for fast image registration," IEEE Trans. Comput., vol. 21, no. 2, pp. 179-186, 1972

[2] G.J. Vanderburg and A. Rosenfeld, "Two-stage template matching," IEEE Trans. Comput., vol. 26, pp.384-393, 1977

[3] M. Svedlow, C. D. McGlem, and P.E. Anuta, "Image registration:Similarity measure and processing method comparisons," IEEE Trans. Aerosp. Electron. Syst., vol. 14, no. 1, pp. 141-149,1978.

[4] W. K. Pratt, Digital Image Processing. New york: John Wiley & Sons, 1978, pp. 526-566

[5] A. Goshtadby, "Template matching in rotated images," IEEE trans. Pattern Anal. Machine Intell., vol.7 no. 3, pp. 338-344, 1985

[6] E.Peli, R. A. Angliere, and G. T. Timberlake, "Feature-based registration of retinal images," IEEE Trans. Med. Imag., vol 6, no 3, pp 272-278, 1987

[7] S. Mitra, B. S. Nutter, T. F. Krile, and R. H. Brown, "Automatic method for fundus imageregistration and analysis," Applied Optics, vol. 27, no. 6, pp. 1107-1112, 1988

[8] J. Segman, "Fourier cross correlation and invariant transformations for an optimal recognition of functions deformed by affine groups," J. Opt. Soc. Am. A., vol. 9, no.6, pp 895-902, 1992

[9] A. Venot and V. Leclerc, "Automated correlation of patient motion and gray value prior to substraction in digitized angiography," IEEE Trans Med. Imag., vol. 3, no. 4, pp. 179-186, 1984

[10] A. Venot, J. C. Liehn, J. F. Lebruchec, and J. C. Roucayrol, "Automated comparison of scintigraphic images," J. Nucl. Med.,vol.27, pp. 1337-1342, 1986

[11] M.K.Hu, "Visual pattern recognition by moments invariants," IRE Trans. Information theory, vol. 8, pp. 179-187, 1962

[12] Y.S. Abu-Mostafa and D. Psaltis, "Recognition aspects of moment invariants," IEEE Trans. Pattern Anal. Machine Intell., vol. 6, no.6, pp. 698-706. 1984

[13] M. R. Teague, "Image analysis via the general theory of moments," J. Opt. Soc. Am., vol. 70, no.8, pp. 920-930, 1980

[14] C. H. Teh and R. T. Chin, "On image analysis by the methods of moments," IEEE Trans. Pattern Anal. Machine Intell., vol. 10, no. 4, pp. 496-513, 1988

[15] M. O. freeman and B. E. A. Salch, " Moments invariants in the space and frequency domains," J. Opt. Soc. Am. A., vol. 5, no. 7, pp. 1073-1084, 1988

[16] J. Altmann and H. J. P. Reitbock, "A fast correlation method for scale and translation-invariant pattern recognition," IEEE Trans. Pattern Anal. Machine Intell., vol. 6, no. 1, pp. 46-57, 1984.

[17] Z. Y. Sheng, C. Lejeune, and H. H. Arsenault, "Frequency-domain Fourier-Mellin descriptors for invariant pattern recognition," Optical Engineering, vol. 27, no. 5, pp. 354-357, 1988.

[18] S. S. Reddi, "Radial and angular moment invariants for image identification," IEEE Trans. Pattern Anal. Machine Intell., vol. 3, no. 2, pp. 240-242, 1981.

[19] M. Miller, T. Nguyen and C.Yang, "Symmetric Phase-Only Matched Filter (SPOMF) for Frequency-Domain Software GNSS Receivers," Position, Location, and navigation symposium, 2006 IEEE/ION, page 187-197.

[20] A.V. Oppenhein and J. S. Lim, "The importance of phase in signals," IEEE Proc., vol. 69, no. 5, pp. 529-541, 1981.

[21] J. L. Horner and P. D. Giantino, "Phase-only matched filtering," Appied Optcis, vol. 23, no. 6, pp. 812-816, 1984

[22] B. V. K. V. Kumar and Z. Bahri, "Efficient algorithm for designing a ternary valued filter yielding maximun signal to noise ratio," Applied Optics, vol. 28, no. 10, pp. 1919-1925, 1989.

[23] B. Javidi and J. Wang, "Binary nonlinear joint transform correlation with median and subset median thresholding," Applied Optics, vol. 30, no. 8, pp. 967-976, 1991.

[24] O. K. Ersoy and M. Zeng. "Nonlinear matched filtering," J. Opt. Soc. Am. A., vol. 6, no. 5, pp. 636-648, 1989.

[25] T. Kolzer, J. Rosen, and J. Shamir, "Phase extraction pattern recognition," Applied Optics, vol. 31, no. 8, pp. 1126-1137, 1992.

[26] B.V.K.V. Kumar and E. Pochapsky, "Signal-to-noise ratio consideration in modified matched spatial filters," J. Opt. Soc. Am. A., vol. 3, no. 6, pp. 777-786, 1986

[27] Symmetric Phase-Only Matched Filtering of Fourier-Mellin Transforms for Image Registration and Recognition, Qin-sheng Chen, Michel Defrise, and **F.** Deconinck, ***Member,*** *lEEE*. IEEE TRANSACTIONS ON PATTERN ANALYSIS AND MACHINE INTELLIGENCE, VOL. 16, NO. 12, DECEMBER 1994

[28] D. L. Flannery, J. S. Loomis, and M. E. Milkovich, "Transformatio ternary phase-amplitude filter formulation for improved correlation discrimination," Appl. Opt., vol. 27, no. 19, pp. 4079-4083, 1988.

[29] Z. Q. Wang, W. A. Gillepsie, C. M. CartWright, et al., "Optical pattern recognition using a synthetic discriminant amplitude-compensated matched filter," Appl. Opt., vol. 32, no. 2, pp. 184-189, 1993.

[30] J.H. Horver and P. D. Gianino, "Pattern recognition with binary phase-only filters," Appl. Opt., vol. 24, pp. 609-611, 1985

[31] David L. Flannery, member, IEE, and Joseph L. Horner. " Fourier Optcial Signal Processors", Proceeding of the IEEE, vol. 77, no. 10, october 1989

[32] Gall, F. J. and Spurzheim, J. C. (1810) `Anatomie und Physiologie des Nervensystems im Allgemeinen und des Gehirns insbesondere', F. Schoell, Paris.

[33] Jackson, J. H. (1931) `Selected Writings of John Hughlings Jackson', Hodder and Stoughton, London.

[35] Penfield, W. and Rasmussen, T. (1952) `The Cerebral Cortex of Man'. Macmillan, New York.

[36] Sperry, R. W. (1968) Hemisphere Deconnection and Unity in Conscious Awareness. American Psychologist **23,**723-733.

[37] Kety, S. S. and Schmidt, C. F. (1948) The Nitrous Oxide Method for the Quantitative Determination of Cerebral Blood Flow in Man: Theory, Procedure and Normal Values. J. Clin. Invest. **27,**476-483.

[38] Glass, H. I. and Harper, A. M. (1963) Measurement of Regional Blood Flow in Cerebral Cortex of Man through Intact Skull. Br. Med. J. **1,**593.

[39] Ingvar, D. H. and Lassen, N. A. (1961) Quantitative Determination of Regional Cerebral Blood-Flow. Lancet **2,**806-807.

[40] Kuhl, D. E. and Edwards R. Q. (1963) Image Separation Radioisotope Scanning. Radiology **80,**653-661.

[41] Fox, P. T., Mintun, M. A., Raichle, M. E. and Herscovitch, P. (1984) A Noninvasive Approach to Quantitative Functional Brain Mapping with $H_2{}^{15}O$ and Positron Emission Tomography. J. Cereb. Blood Flow Metab. **4,**329-333.

[42] Berger, H. (1929) Über das elektrenkephalogramm des menschen. Arch. Psychiatr Nervenkr **87,** 527-570.

[43] Cohen, D. (1972) Magnetoencephalography: Detection of the Brain's Electrical Activity with a Superconducting Magnetometer. Science **175,**664-666.

[44] Okada Y (1983): Neurogenesis of evoked magnetic fields. In: Williamson SH, Romani GL, Kaufman L, Modena I, editors. Biomagnetism: an Interdisciplinary Approach. New York: Plenum Press, pp 399-408

[45] Schnitzler, A. and Gross, J. Normal and pathological oscillatory communication in the brain. Nature Reviews Neuroscience, 2005;6:285–96.

[46] Huang, M; Dale, A M; Song, T; Halgren, E; Harrington, D L; Podgorny, I; Canive, J M; Lewis, S; Lee, R R. Vector-based spatial-temporal minimum L1-norm solution for MEG. NeuroImage, 2005; 31:1025-1037.

[47] Karl E. Misulis, Toufic Fakhoury (2001), Spehlmann's Evoked Potential Primer, Butterworth-heinemann,

[48] An Effective Approach for Iris Recognition Using Phase-Based Image Matching

Kazuyuki Miyazawa, Student Member, IEEE, Koichi Ito, Member, IEEE, Takafumi Aoki, Member, IEEE, Koji Kobayashi, and Hiroshi Nakajima

[49] Fingerprint Matching Using Phase-Only Correlation and Fourier-Mellin Transforms

Jianxin Zhang, Zongying Ou and Honglei Wei Key Laboratory for Precision and Non-traditional Machining Technology of Ministry of Education Dalian University of Technology Dalian, Liaoning Province, China

[50] "Face Recognition using Processed Histogram and Phase-Only Correlation (POC)"

Fazl-e-Basit*, Muhammad Younus Javed and Usman Qayyum$ Department of Computer Engineering, College of Electrical and Mechanical Engineering, National University of Sciences and Technology, Rawalpindi, Pakistan

[51] Solving the Electrocardiography Inverse Problem by Using an Optimal Algorithm Based on the Total Least Squares Theory Guofa Shou; Ling Xia; Mingfeng Jiang; Natural Computation, 2007. ICNC 2007. Third International Conference on Volume 5, 24-27 Aug. 2007 Page(s):115 – 119

[52] Dynamic medical imaging as a partial inverse problem Greensite, F.; Engineering in Medicine and Biology Society, 2004. IEMBS '04. 26th Annual International Conference of the IEEE Volume 1, 2004 Page(s):1014 - 1017 Vol.2

[53] The Use of Genetic Algorithms for Solving the Inverse Problem of Electrocardiography Mingfeng Jiang; Ling Xia; Guofa Shou; Engineering in Medicine and Biology Society, 2006. EMBS '06. 28th Annual International Conference of the IEEE Aug. 2006 Page(s):3907 – 3910

[54] The Forward model - the imaging process by Björn Gustavsson (2000)

[55] Cortical Surface-Based Analysis II: Inflation, Flattening, and a Surface-Based Coordinate System Bruce Fischl,* Martin I. Sereno,† and Anders M. Dale*,1 *Nuclear Magnetic Resonance Center, Massachusetts General Hosp/Harvard Medical School, Building 149, 13th Street, Charlestown, Massachusetts 02129; and †Department of Cognitive Science, University of California at San Diego,

[56] http://en.wikipedia.org/wiki/YUV#Formulas